GEORG-AUGUST-UNIVERSITÄT GÖTTINGEN

Nucleo-cytoplasmic shuttling of snoRNAs in

Saccharomyces cerevisiae

Dissertation

for the award of the degree
"Doctor rerum naturalium"
of the Georg-August-Universitat Gottingen

within the doctoral program "Biology"
of the Georg-August University School of Science (GAUSS)

submitted by

Gianluca Zaccagnini

From Rome, Italy

Göttingen, April 2022

Thesis Committee:

   Prof. Dr. Heike Krebber
      Department of Molecular Genetics
      Institute for Microbiology and Genetics

   PD Dr. Wilfried Kramer
      Department of Molecular Genetics
      Institute for Microbiology and Genetics

   Dr. Oliver Valerius
      Department of Molecular Microbiology and Genetics
      Institute for Microbiology and Genetics

Members of the Examination Board:

Referee: Prof. Dr. Heike Krebber
      Department of Molecular Genetics
      Institute for Microbiology and Genetics

2nd Referee: Dr. Oliver Valerius
      Department of Molecular Microbiology and Genetics
      Institute for Microbiology and Genetics

Further Members of the Examination Board:

   Prof. Dr. Jörg Stülke
      Department of General Microbiology
      Institute for Microbiology and Genetics

   Prof. Dr. Kai Heimel
      Department of Molecular Microbiology and Genetics
      Institute for Microbiology and Genetics

   Prof. Dr. Stefani Pöggeler
      Department of Genetics of Eukaryotic Microorganisms
      Institute for Microbiology and Genetics

   PD Dr. Wilfried Kramer
      Department of Molecular Genetics
      Institute for Microbiology and Genetics

Date of oral examination: 23th June 2022

Affidavit

I hereby declare that I prepared this doctoral thesis titled "Nucleo-cytoplasmic shuttling of snoRNAs in *Saccharomyces cerevisiae*" independently and with no other sources and aids than quoted.

Göttingen, April 2022

_____

Gianluca Zaccagnini

Table of Contents

3.   Material and methods

Table of figures

Table of tables

1. Abstract

Small nucleolar RNAs (snoRNAs) are a group of small non-coding RNAs involved in the post-transcriptional modification of RNAs, such as rRNA and tRNA. The importance of their role is evidenced by the rRNA regions subject to modification that are highly conserved throughout evolution. In *Saccharomyces cerevisiae*, snoRNAs are transcribed in the nucleus and processed by the activity of the nuclear ribonucleases Rnt1, Rrp6, and Rat1. Thus, it was always assumed that snoRNAs never leave the nucleus. However, recent work has revealed the binding between snoRNAs and proteins atypical for this group, including the Mex67 export factor. Therefore, in the present work, we investigated the possibility of a cytosolic phase of snoRNAs by *in vivo* RNA co-immunoprecipitation (RIP) and fluorescent *in situ* hybridization (FISH) experiments. We confirmed that snoRNAs bind the export factor Mex67 and that they use it to be exported from the nucleus. Furthermore, we showed that the Sm-like2-8 (Lsm2-8) complex, a heteroheptameric complex involved in the processing of different non-coding RNAs, is able to bind different snoRNAs and not just U3 snoRNA as reported in the literature. We found that the Lsm2-8 complex binds snoRNAs in the nucleus, with the exception of U3, which appears to bind the Lsm-ring in the cytosol, after export. Following export, the Lsm2-8 complex turned out to be crucial for the nuclear re-import of the snoRNAs via the karyopherins Mtr10 and Cse1. Indeed, cytoplasmic fractionation and FISH experiments revealed a cytosolic mislocalization of snoRNAs in the mutant strains of MTR10 and CSE1 that cooperate in the nuclear re-import of snoRNAs. Moreover, the same cytosolic mislocalization was observed in the mutant strain for LSM8, confirming the importance of the Lsm-ring for the snoRNA re-import, potentially by connecting the snoRNA with the importins Mtr10 and Cse1. Finally, we investigated the role of the snoRNA second transcription termination site (site II). Using the cytoplasmic fractionation experiment in the *trf4Δ* mutant, which is known in the literature to bypass the first termination site (site I), we showed that when snoRNAs terminate transcription at the second site, they are more inclined to be exported into the cytosol. Furthermore, through a FISH experiment, we reinforced this result by observing a higher cytosolic localization of a snoRNA (snR65) in a strain where we mutated the sequence of the

first transcription termination site, thus forcing termination at site II. Therefore, our data show the presence of a cytosolic pool of snoRNAs in *S. cerevisiae*, and we propose that snoRNAs are exported as a step of their maturation pathway. Moreover, we suggest that the cytosolic localization of snoRNAs may depend on the transcription termination site used.

2. Introduction

In all organisms, the protein-coding genes are transcribed into messenger RNAs (mRNAs) that are in turn translated into protein by a macromolecular complex known as the ribosome. The ribosome is composed of two ribonucleoprotein subunits, the small and the large subunit. In baker yeast, the small 40S subunit has one ribosomal (r)RNA (18S) and 33 distinct ribosomal proteins, whereas the large 60S subunit contains three rRNAs (5S, 5.8S, and 25S) and 46 ribosomal proteins **(Woolford Jr and Baserga 2013).** During the 35S pre-rRNA maturation pathway, endo- and exonucleases carry out a series of cutting and trimming steps in order to produce a complete and functional ribosome **(Turowski and Tollervey 2015)**. In addition to cleavage, during transcription of the 35S pre-rRNA, other modification steps occur in the nucleolus through the transient binding of 75 different small nucleolar RNAs (snoRNAs) to specific sections of the pre-rRNA. Many publications support a model in which snoRNA modification takes place post-transcriptionally, but it was shown that some of these modifications can occur co-transcriptionally, raising questions about when snoRNAs can modify the rRNA **(Kos and Tollervey 2010)**.

Most snoRNAs direct pre-rRNA modifications such as methylation of the 2'-hydroxyl group of the ribose (2'-O-methylation) **(Figure 1a)** and the isomerization of uridine to pseudouridine **(Figure 1b)**.
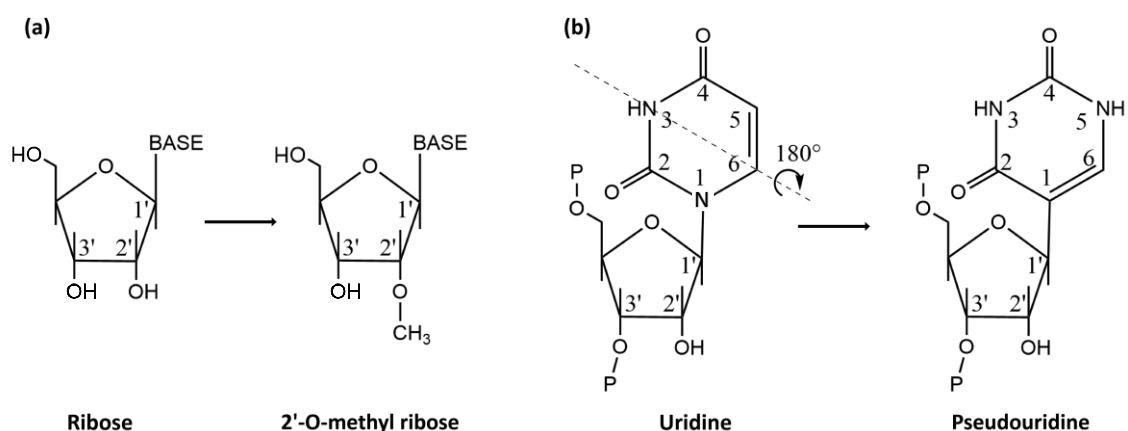
Figure 1: Chemical modifications carried out by snoRNAs. **(a)** Methylation of the 2'-hydroxyl group of the ribose carried out by the C/D snoRNA. **(b)** Pseudouridylation is a reaction carried out by H/ACA snoRNP that leads to the isomerization of a uridine to a pseudouridine.

However, some snoRNAs (U17, U14, and U3) are involved in a distinct function, the pre-rRNA cleavage **(Turowski and Tollervey 2015)**, while snR10 appears to be important in different activities. The loss of this snR10 makes cells more susceptible to osmotic and cold stresses. It also reduces the efficiency of pre-rRNA processing and leads to a decrease in translation efficiency **(King et al., 2003; Tollervey and Guthrie 1985; Tollervey 1987)**. All the activities related to snoRNA are carried out by specific proteins that bind to the snoRNA structure, forming a ribonucleoprotein complex known as snoRNP **(Turowski and Tollervey 2015)**.

In many cases, the functions of rRNA modifications carried out by snoRNAs remain enigmatic. However, the rRNA regions subject to modification, which are located in functional centers, are highly conserved throughout evolution, indicating the critical role played by snoRNAs. In the case of rRNA, these modifications can either stabilize interactions or provide rigidity, with the 2'-O-methylation that increases the hydrophobicity and the pseudouridylation that allows further hydrogen bonding. The importance of these modifications in yeast can be seen in severe phenotypes caused by global loss of either 2'-O-methylation or pseudouridylation, but also in mammalian, mutations of DKC1 (Cbf5 in yeast, the enzyme involved in the pseudouridylation) reduces translation rates and fidelity **(Ojha et al., 2020; Turowski and Tollervey 2015)**. Nevertheless, it was shown that, instead of acting individually, many of these modifications have a cumulative and synergistic effect on ribosome function. For example, Helix 69 of the 25S rRNA contains several modified nucleotides, and the removal of these modifications through the snoRNAs deletion impairs cell growth, disrupts ribosome structure, and alters translational efficiency **(Liang et al., 2007)**. Moreover, in humans, the importance of snoRNAs can be seen in diseases such as Prader-Willi syndrome or Creutzfeldt-Jakob disease **(Cohen et al., 2013; Duker et al., 2010)**.

2.1. snoRNAs classification

snoRNAs are a class of non-coding RNA that is mostly short (60–300 nt long), nucleoli-localised and present in all eukaryotic organisms. They are classified as box C/D or box H/ACA based on the presence of highly conserved sequences ('boxes').

The stable and catalytically active form of both classes consists of the RNA structure bound by a unique group of core proteins: Nop1, Nop56, Nop58, and Snu13 for the C/D class, and Cbf5, Nhp2, Nop10, and Gar1 for the H/ACA class **(Kufel and Grzechnik 2018)**. Even though there are high similitudes between archaeal and eukaryotic snoRNAs, it is important to remember that most of the information about snoRNA architecture came from high-resolution structures of archaeal snoRNAs **(Watkins and Bohnsack 2012)**.

2.1.1. C/D snoRNAs

C/D snoRNAs are usually shorter than H/ACA, with lengths ranging from 60 to 90 nucleotides, and near their 5' and 3' termini, they have two conserved sites, boxes C (consensus sequence RUGAUGA) and D (consensus sequence CUGA), respectively **(Figure 2a)**. Boxes C and D fold into a kink-turn secondary structure (k-turn), which functions as a binding site for C/D snoRNA core proteins, required for biogenesis and correct localization. In *S. cerevisiae*, it is possible to find additional motifs, the boxes C' and D', that generally form a stem-loop structure known as a K-loop. The boxes C' and D' have the same consensus sequences as the boxes C and D, respectively, but are often less well conserved and the sequences are more degenerated. The guide regions, which contain sequences that can create a base pair stretch with an RNA target, are directly upstream of the boxes D' and/or D **(Dupuis-Sandoval et al. 2015)**. The catalytic subunit of box C/D snoRNPs **(Figure 3a)** is Nop1 (fibrillarin in humans), which is involved in the 2'-O-methylation of the target **(Tollervey et al., 1991)**. Concerning the other snoRNP core proteins, Nop56 and Nop58 form a heterodimer structure on the snoRNP, interacting with the guide regions of the snoRNAs. Moreover, it has been shown that they crosslink with rRNA in vivo, implying that they play a direct role in substrate recognition **(van Nues et al., 2011)**. Finally, Snu13 shows a binding with the C/D motif (K-turn) *in vitro*, but not to the K-loop structures expected for the C'/D' motif. However, studies *in vivo* indicate that the C'/D' motif recruits Snu13 independently of the C/D motif. As a result, it is likely that Snu13 and Nop56 bind the C'/D' motif together **(Watkins and Bohnsack 2012).**
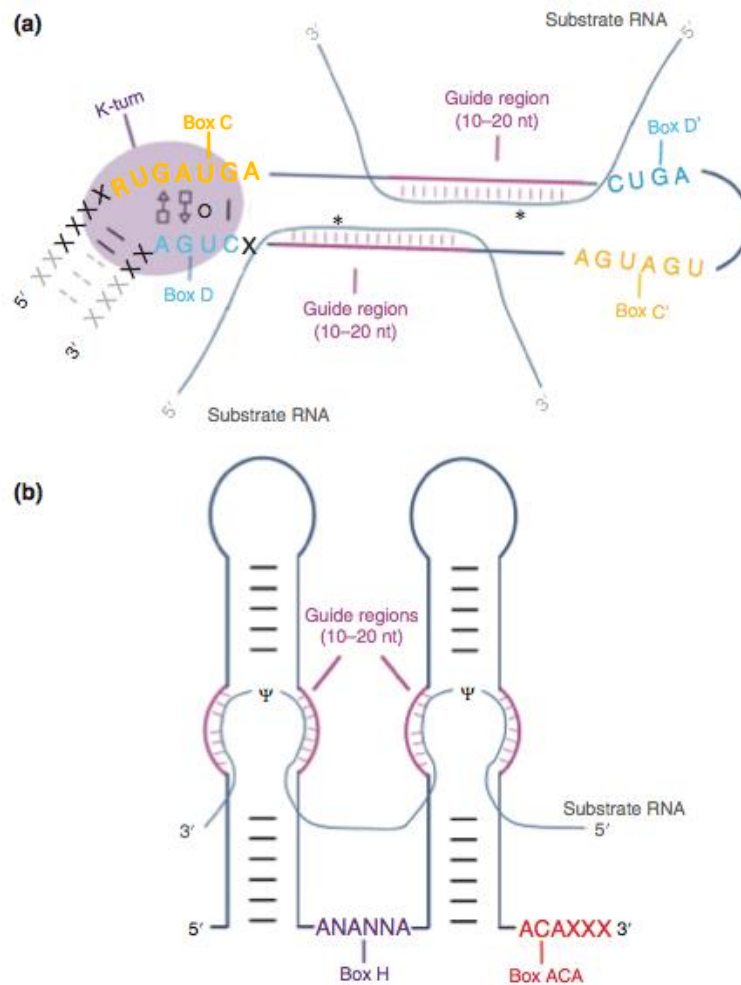
Figure 2: Features and structures of snoRNAs. (a) In C/D snoRNA, there are two conserved sequences called boxes C/C' and D/D', shown in orange and cyan, respectively. The k-turn, a secondary structure formed by the fold of the boxes C and D, is highlighted in purple. The guide regions are highlighted in pink and are located directly upstream of the boxes D and/or D'. An asterisk indicates the target nucleotide for 2'-O-methylation, which is located five nucleotides upstream of box D or D'. **(b)** The H/ACA class is formed by two hairpins connected by the hinge region, or box H (shown in purple). Three nucleotides upstream of the 3'-end, there is the ACA box (highlighted in red). The bulges present in the two hairpins contain the guide regions (shown in pink) that coordinate the pseudouridylation of the uridine target. The modification of the residue takes place 14–15 residues upstream from the box H or ACA. In the picture R: Guanine / Adenine (purine), N: Adenine / Guanine / Cytosine / Uracil, X: different nucleotides depending on the snoRNA. Modified from **(Dupuis-Sandoval et al. 2015)**.

2.1.2. H/ACA snoRNAs

H/ACA snoRNAs **(Figure 2b)** differ from the C/D class not only by their length, ranging between 120 and 140 nucleotides, but also by their typical secondary structure, which consists of a "hairpin-hinge-hairpin-tail" motif **(Dupuis-Sandoval et al., 2015).** The first conserved region is the H box, which is in the hinge that connects the two hairpins and is formed by the sequence ANANNA, where N can be any

nucleotide. The second conserved sequence is the ACA box, which is at the end of the second hairpin and located three nucleotides upstream of the 3'-end of the molecule **(Ganot et al., 1997)**. The H/ACA snoRNA hairpins have bulges in the middle of their structures that contain the guide regions where the binding to the target occurs. The uridine that needs to be modified is located 14–15 nucleotides upstream of the ACA or H region **(Torchet et al., 2005)**.
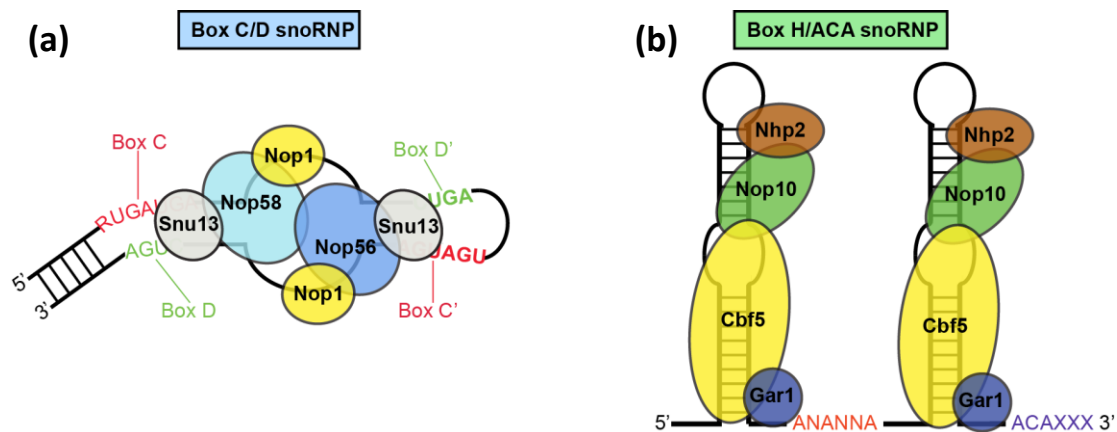
Figure 3: **Box C/D and box H/ACA snoRNP**. Both family are composed of four core proteins and the snoRNA structure. **(a)** For C/D snoRNP the core proteins are Snu13, Nop56, Nop58 and Nop1 as catalytic subunit. **(b)** For H/ACA the core proteins are Nhp2, Gar1, Nop10, and Cbf5 as catalytic subunit. In *S. cerevisiae*, the H/ACA RNA structure contains two hairpins, each of which binds to three of the four major protein factors. Gar1 is part of the snoRNP through interaction with Cbf5.

For the H/ACA snoRNP class, the four core proteins are Cbf5 (Dyskerin in human), Gar1, Nhp2, and Nop10 **(Figure 3b)**. Unlike in archaea, where there is only one stem, as mentioned above, in *S. cerevisiae* the H/ACA group shows two stems, and both are essential for the accumulation of snoRNA *in vivo* and for the RNP formation *in vitro*. The current model proposes that each stem is bound by a set of the four H/ACA core proteins. Unlike Cbf5, which covers the majority of the stem due to its bulk, Nhp2 and Nop10 proteins bind only the upper part of the stem, and the interaction between Cbf5 and Nop10 is required for Nhp2 to bind to the snoRNA. The lower stem creates an L-shaped structure with Cbf5 that identifies the two A, which are the two most conserved nucleotides in the ACA motif. Gar1 is the only protein that does not bind directly to RNA but instead associates with the complex via its interaction with the catalytic domain of Cbf5. It appears to be important but not necessary for snoRNP activity, and it plays a role in product release after the

reaction is complete **(Watkins and Bohnsack 2012; Watkins et al., 1998; Czekay and Kothe 2021)**.

2.2. The genomic organization of snoRNAs

The genomic organization of snoRNAs is dynamic, with different processing pathways. snoRNAs that are transcribed from genes can appear as independently transcribed, equipped with their own promoter elements, or as clusters transcribed as a single polycistronic transcript. Alternatively, snoRNA genes are found within intron coding units, lacking an independent promoter. The genomic organization of snoRNAs differs within species, but there is always at least a fraction that is driven by independent promoters **(Figure 4) (Lui and Lowe 2013)**. In *S. cerevisiae*, with the exception of snR52, which is under the control of RNAP III (RNA polymerase III) **(Moqtaderi and Struhl 2004)**, snoRNAs are transcribed by RNAP II (RNA polymerase II) and appear as monocistronic. In agreement with the deficiency of introns, there are only eight intron-encoded snoRNAs, and all intronic snoRNA units are individual. In *S. cerevisiae*, all clustered snoRNAs are transcribed from genes with their own promoter **(Dieci et al. 2009)**.

	Animals			Plants		Yeast		Protozoans		Archaea	
	H. sapiens	*C. elegans*	*D. melanogaster*	*O. sativa*	*A. thaliana*	*S. cerevisiae*	*S. pombe*	*G. lamblia*	*T. brucei*	*P. furiosis*	*S. solfataricus*
Independently transcribed snoRNA genes											
Individual	9.2% (42/456)	26.1% (42/161)	3.5% (8/227)	21.3% (76/357)	23.1% (57/246)	65.7% (50/76)	78.2% (43/55)	100% (20/20)	1.1% (1/93)	91.7% (5/60)	97.0% (31/33)
Clustered	0.5% (2/456)			48.7% (174/357)	59.3% (146/246)	22.4% (17/76)	14.5% (8/55)		97.8% (91/93)	6.7% (4/60)	3.0% (2/33)
Intron-encoded snoRNA genes											
Individual	90.3% (412/456)	73.9% (119/161)	59.5% (135/227)		9.3% (23/246)	10.5% (8/76)	7.3% (4/55)			1.6%[c] (1/60)	
Clustered			36.1% (82/227)	29.1% (104/357)	2.4% (6/246)						
RNA Polymerase III Dependent snoRNA genes		Yes[a]	0.9% (2/227)	0.8% (3/357)	5.7% (14/246)	1.3% (1/76)			1.1%[b] (1/93)		

Figure 4: The genomic organization of snoRNA genes and their distribution within species. snoRNA genes (colored block arrows) can be independently transcribed or are intron-encoded. All the independently transcribed snoRNAs shown in the picture are transcribed by RNAP II and can be transcribed as individual or clustered. In a few organisms, a low percentage of snoRNAs can be transcribed through RNAP III (1/76 in *S. cerevisiae*). Notably, dramatic changes can be observed in different organisms. For example, in *S. cerevisiae*, only 10.5% of snoRNAs are intron-encoded, while in *H. sapiens* the situation is the opposite, with 90.3% of snoRNAs being intron-encoded and only 9.2% independently transcribed **(Lui and Lowe 2013)**.

2.3. Maturation pathway in *Saccharomyces cerevisiae*

All independently transcribed snoRNAs, except the RNAP III-dependent snR52, are RNAP II transcribed with their transcription termination mediated by the combined action of the Nrd1-Nab3-Sen1 (NNS) complex and the cleavage and polyadenylation factor (CPF)-cleavage factor (CFI)-complex. To complete their maturation pathway, all pre-snoRNAs are trimmed by ribonucleases at the 3'-, or both the 5'- and 3'-ends. Depending on the snoRNA, the cap can be removed or retained and subsequently post-transcriptionally modified **(Kufel and Grzechnik 2018)**.

2.3.1. Transcription termination

In *S. cerevisiae*, independently transcribed snoRNAs terminate their transcription mostly through the NNS complex, which is formed by the RNA-binding proteins Nrd1 and Nab3 and the RNA:DNA helicase Sen1 **(Porrua and Libri 2015)**. The phosphorylation that occurs on the tandem repeats (consensus: Tyr1 - Ser2 - Pro3 - Thr4 - Ser5 - Pro6 - Ser7) present on the RNAP II C-terminal domain (CTD) is important for the selection of this specific transcription termination process. Ser2 phosphorylation accumulates during transcription and is preferentially bound by factors of the CPF-CFI complex (cleavage and polyadenylation factor - cleavage factor I) involved in mRNA transcription termination. On the contrary, during the early stages of transcription, the phosphorylation of Ser5 is predominant and is recognized by the NNS protein Nrd1. First, during the early phases of the transcription, the CTD-interacting domain of Nrd1 recognizes a properly phosphorylated RNAP II CTD, and, together with Nab3, forms a heterodimer Nrd1–Nab3. The nascent RNA is then bound by Nrd1 and Nab3 via their NNS-binding sites, which are GUA[A/G]/UGUA for Nrd1 and UCUU/CUUG for Nab3, with GUA[A/G] and UCUU as the most representative sequences. Finally, the heterodimer Nrd1–Nab3 can form a ribonucleoprotein complex capable of recruiting the helicase Sen1 that removes the nascent RNA from the RNAP II active site via a mechanism similar to the Rho-dependent termination in bacteria **(Figure 5) (Arndt and Reines 2015; Schulz et al., 2013; Porrua et al., 2012; Porrua and Libri 2015)**.
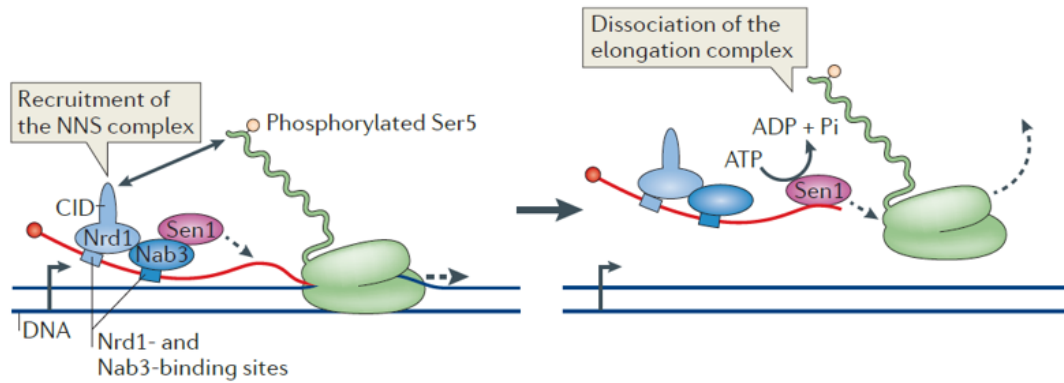
Figure 5: **Transcription termination by the NNS complex in yeast**. Nrd1 and Nab3 are recruited on the emerging RNA through the identification of specific motifs. Later Nrd1 interacts with the Ser5-phosphorylated form of the RNAP II-CTD and the complex Nrd1-Nab3 recruits the RNA and DNA helicase Sen1 that, using the hydrolysis energy of ATP, is able to remove the new RNA transcript from the catalytic site of RNAP II. Modified from (**Porrua and Libri 2015**).

In addition to Nrd1, Nab3 and Sen1, this process requires a subcomplex of CPF called the <u>a</u>ssociated with <u>Pt</u>a1 (APT) complex that is formed by two phosphatases, Glc7 and Ssu72, plus the factors Pta1, Pti1, Syc1, Swd2 and Ref2 **(Lidschreiber et al. 2018)**. The component of the cleavage factor IA, CTD-interacting protein Pcf11, also participates in transcription termination via the NNS complex **(Grzechnik et al. 2015)**. While the role of APT complexes in snoRNAs transcription termination remains to be elucidated, the function of Pcf11 in this process has been well studied. Pcf11 is recruited downstream of the functional NNS-binding sites clusters where it can carry out different activities **(Kufel and Grzechnik 2018)**. However, it is most likely that Pcf11 interacts directly with the NNS complex, alone or in cooperation with some CPF-CFI proteins. Nrd1 recruits Pcf11 co-transcriptionally, which in turn replaces Nrd1 on the RNAP II CTD, further compromising the transcription. This event should support the Sen1-dependent termination of the transcript that requires Pcf11. This hypothesis is reinforced by the observation of defects in the snoRNA transcription termination in a mutant strain of Pcf11. Furthermore, an accumulation of RNA:DNA hybrids downstream of the NNS terminations was also observed in this mutant strain **(Grzechnik et al. 2015)**.

It is interesting to note that the snoRNAs, in addition to the transcription termination site through the NNS complex (site I), have an additional termination site where the sequence resembles the mRNA cleavage/polyadenylation signal (site II) **(Fatica et al.,**

2000; Morlando et al., 2001; Steinmetz and Brow, 2003; Steinmetz et al., 2006). If the first transcription termination site is skipped, the snoRNAs can terminate the transcription at a second site where only the CPF-CFI complex acts in the termination and exclusively Pap1 is used for snoRNA adenylation **(Figure 6) (Grzechnik et al. 2008)**. Although a "fail safe" mRNA-like signal function for the second termination site has been proposed, the precise role of this additional site has yet to be determined. Moreover, there is no detailed information about the maturation pathway of snoRNAs that ends through the second termination site.
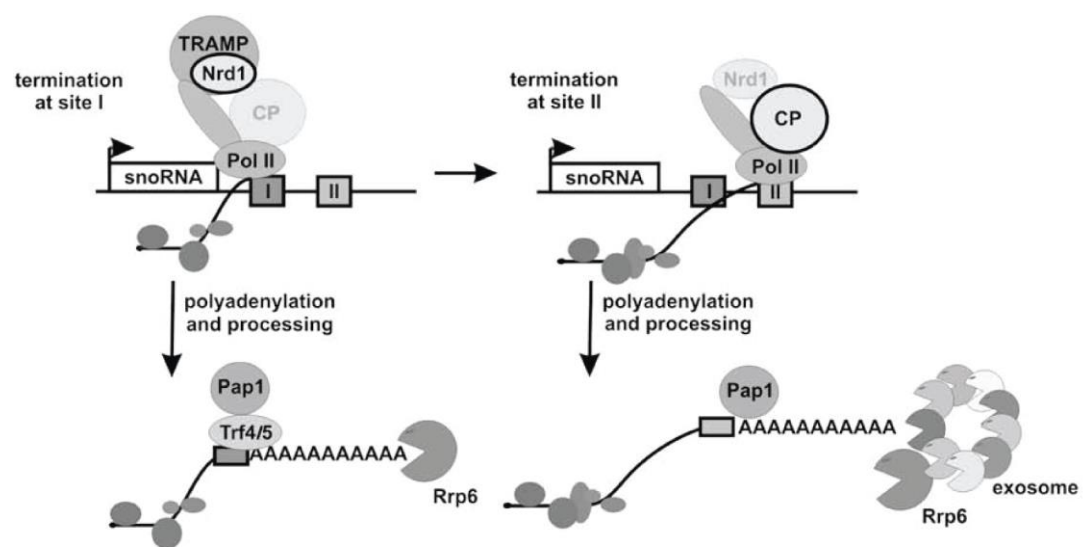
Figure 6: snoRNA 3'-end processing in the first and second transcription termination site. In the picture **I**: First transcription termination site with a sequence for the binding of Nrd1 and Nab3 (NNS complex). **II**: Second transcription termination site with a sequence that resembles the mRNA cleavage/polyadenylation signal and that recruit the CPF-CFI (CP in the picture).
When the transcription ends at site I, the NNS complex recruits the TRAMP complex, which through the poly(A) polymerase Trf4 generates a short oligo(A) tail that is subsequently elongated by the poly(A) polymerase Pap1. The TRAMP complex recruits the exonuclease Rrp6 which trim the snoRNA 3'-end. When the transcription ends at site II, the CPF-CFI complex proceeds to the generation of an oligo(A) tail using Pap1. In this case, the trimming of the 3'-end is performed by the core exosome and followed by Rrp6. Modified from **(Grzechnik and Kufel 2008)**.

2.3.2. snoRNA 3'-end processing

A characteristic of the snoRNAs termination process in yeast is the tight coupling of this reaction to the trimming of the 3'-end extremities. The two main elements that direct snoRNAs to these pathways are the nuclear exosome and the Trf4/Trf5, Air1/Air2, and Mtr4 polyadenylation (TRAMP) complex. First, the NNS complex

recruits the TRAMP complex, which can bind Nrd1 via the Nrd1-interacting motif of the poly(A) polymerase Trf4 **(Tudek et al., 2014)**. Later, Trf4 transiently oligoadenylates the pre-snoRNA at the 3'-end, adding a short oligo(A) tail that is further elongated by the poly(A) polymerase Pap1, a step critical for the subsequent recruitment of the exonuclease **(Grzechnik and Kufel 2008)**. Subsequently, the TRAMP complex recruits the exonuclease Rrp6, which trims the 3'-end pre-snoRNA until the mature extremity is formed **(Tudek et al., 2014; Grzechnik and Kufel 2008)**. There are two exceptions: U3 and snR41, where the 3'-end maturation continues after the trimming with the cutting of a stem-loop by the endoribonuclease Rnt1 (RNase III). This stem-loop is located downstream of the mature sequence, and after it is removed, the exosome-Rrp6 trims the 3'-end until the generation of the mature snoRNA **(Chanfreau G, Legrain P et al., 1998)**.

Rnt1 is also involved in the cleavage of clustered snoRNAs, where each cistron is released from the polycistronic transcript as a singular snoRNA via Rnt1. For these snoRNAs, the termination and maturation is carried out only on the last snoRNA without any difference in this process from other snoRNAs **(Chanfreau G, Rotondo G et al., 1998)**.

Finally, intronic snoRNAs lack an individual termination step and rely exclusively on splicing to be released by the intron-debranching factor Dbr1 or via Rnt1 cleavage **(Ooi et al., 1998)**. Among the eight intronic snoRNAs, some rely exclusively on splicing, such as snR38 and snR24, while others need to be processed by Rnt1 after splicing, for instance snR59 and snR18. The group of intronic snoRNAs is also subject to trimming of the 3'-end extremity by Rrp6, but how this exonuclease is recruited is still unclear. However, it is very likely that the NNS proteins Nrd1 and Nab3 are involved in this step as these proteins can also post-transcriptionally bind and sign many RNAs for exosome-dependent degradation **(Figure 7) (Kufel and Grzechnik 2018)**.

As stated previously, snoRNAs have a second transcription termination site whose function is unclear. If Trf4, a factor of the TRAMP complex, cannot work correctly, the transcription of the snoRNAs is diverted to the second transcription termination site where the CPF-CFI complex proteins act. When the second termination site is selected, Pap1 is exclusively responsible for the polyadenylation, while the trimming

of the 3'-end is started by the core exosome and followed by Rrp6 **(Figure 6)** **(Grzechnik and Kufel 2008)**.
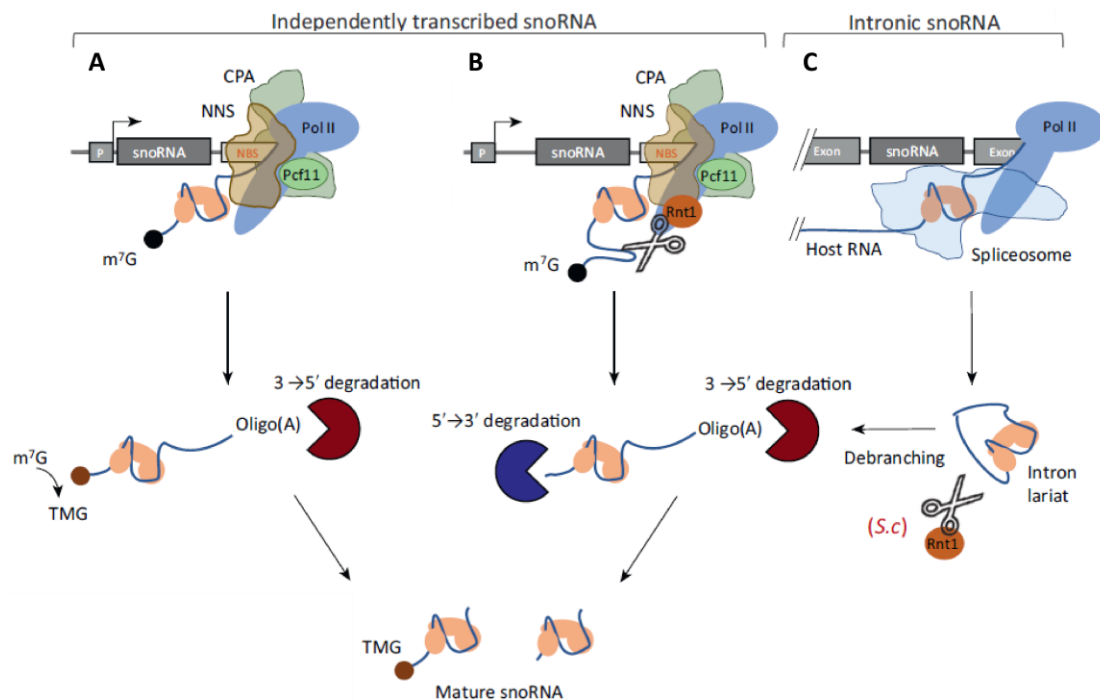
Figure 7: **Maturation pathway of independently transcribed and intronic snoRNA.** For independently transcribed snoRNAs, there are two maturation pathways. **(A)** Most H/ACA maintain the cap that is subject to modification by Tgs1 that converts it to a TMG cap. This is a prerequisite for the 3'-end trimming by Rrp6. **(B)** Most of C/D contain a 5'-end with a stem loop that is cut by Rnt1, generating a snoRNA without the cap. This snoRNA is trimmed at both the 5'-and 3'-ends by Rat1 and Rrp6 respectively. **(C)** Intronic snoRNAs are released after splicing through the debranching enzyme Dbr1 or by Rnt1. Consequently, they will be processed as explained in section (B). Modified from **(Kufel and Grzechnik 2018)**.

2.3.3. snoRNA 5'-end processing

Maturation of the snoRNA 5'-end always includes a co-transcriptional addition of the m^7G cap. However, unlike mRNA, the pre-snoRNA cap is either removed via Rnt1 followed by 5'-end trimming, or it is subject to conversion of the m^7G into a 2,2,7-trimethylguanosine (TMG) cap similar to that of snRNAs **(Figure7) (Becker et al., 2019; Chanfreau et al., 1998; Mouaikel et al., 2002)**.

In *S. cerevisiae*, all snoRNAs that undergo cap removal during maturation, mostly C/D snoRNAs, are transcribed with a long (150–200 nt) 5'-extension that forms a stem loop recognized and cleaved by the endonuclease Rnt1. The unprotected extremity is then processed by the exonucleases Rat1. Failure to remove the cap can result in

the formation of short, oligoadenylated unprocessed 3'-ends that are exported from the nucleus **(Grzechnik et al., 2018)**.

Concerning the H/ACA family, most of them are able to maintain the cap during their whole lifetime. However, differently from the mRNA, the snoRNA cap is modified by the nucleolar trimethylguanosine synthetase Tgs1, which converts the m^7G cap to a TMG cap **(Mouaikel et al. 2002)**. Curiously, the strain *tgs1Δ* shows no change in snoRNA maturation, demonstrating that cap hypermethylation is not a necessary step and does not contribute to the crosstalk between snoRNA ends **(Grzechnik et al., 2018)**.

It remains unknown why snoRNAs are generally devoid of m^7G caps due to either hypermethylation or 5'-end processing. Nevertheless, it is possible to speculate that cap removal is a system developed by the cell to distinguish the 5'-end of snoRNAs from mRNAs and prevent their export, as also suggested for the snRNAs **(Becker et al., 2019)**.

2.4. snoRNP assembly and R2TP complex

Because snoRNPs are involved in the critical process of post-transcriptional modification of non-coding RNAs such as pre-rRNA, their correct biogenesis is required for cell survival **(Watkins and Bohnsack 2012)**. In addition to the snoRNA core proteins previously described, other important proteins, known as assembly factors, are involved in snoRNP biogenesis. One of these assembly factors is called R2TP, a protein complex formed by Rvb1, Rvb2, Tah1, and Pih1 that is active in snoRNP assembly of both classes. Rvb1 and Rvb2 are helicases that belong to the AAA+ family and can form a heterohexamer (Rvbs) **(Huen et al., 2010)**. Pih1 is a 344 amino acid protein that contains no known motifs in its structure and is able to join the R2TP complex with the help of the chaperone Hsp90 that stabilizes its structure. Tah1 act as a co-chaperone of Hsp90, assisting it in the stabilization of Pih1 and forming a link between the R2TP complex and Hsp90 by binding the C-terminal region of Pih1 and the MEEVD motif of the chaperone **(Zhao et al., 2008; Paci et al., 2012)**.

The importance of the R2TP complex in snoRNP maturation was demonstrated in both vertebrates and yeast. In the latter, mutations in RVB2 create a temperature-sensitive phenotype, while the *rvb2Δ* strain causes assembly defects of snoRNPs, probably due to the defective localization of Nop1 and Gar1, which in *rvb2Δ* were found throughout the nucleus and, in a few cells, also in the cytosol, rather than their usual nucleolar localization. Moreover, an increase in U3 precursors and a consequent decrease in the mature form was observed in the *tah1Δ* strain **(Boulon et al., 2008; King et al., 2001; Zhao et al., 2008)**. As a result, the R2TP complex may play a key role in snoRNP maturation, assisting their localization and assembly.

2.4.1. Box C/D snoRNP assembly

The C/D snoRNP is composed of C/D snoRNA and the core proteins, Nop1, Snu13, Nop56, and Nop58 **(Watkins and Bohnsack 2012)**. For the correct C/D snoRNP assembly, the R2TP complex is crucial, and it was proposed that the core proteins interact with the snoRNA structure in a specific order, starting with Snu13, then Nop58, Nop1, and finally Nop56 **(Kakihara and Saeki 2014)**. Nevertheless, when and how the core proteins bind the R2TP complex remains unclear.

One possibility is that Snu13 is the first protein to interact with R2TP supported by the assembly factor Rsa1 **(Boulon et al., 2008)**. Moreover, another assembly factor called Hit1 binds and regulates the steady-state levels of Rsa1, and it was possible to purify the recombinant Snu13–Rsa1–Hit1 heterotrimer combined with C/D snoRNAs and Nop58 **(Rothé et al., 2014)**. However, the unassembled form of Nop58 was also discovered to bind the R2TP complex in the absence of other core proteins **(Kakihara et al., 2014)**.

Another assembly factor, Bcd1, was discovered to promote C/D snoRNP stability **(Peng et al., 2003)** by either directing the loading of Nop58 or Snu13 onto snoRNA **(Khoshnevis et al., 2019; Peng et al., 2003)**.

Even though there is a lot of information about the role of the assembly factors in C/D snoRNP biogenesis in *S. cerevisiae*, there is not a precise model of where and how the core proteins interact with the R2TP complex and when this complex assists in snoRNP formation.

A recent model shows two possibilities. In one of these **(Figure 8 pathway A)**, Rsa1 binds Snu13-Hit1 while the R2TP complex binds Nop58 and Nop1. Snu13 is first loaded onto the snoRNA by Rsa1-Hit1, and then the R2TP complex assembles Nop58 and Nop1 before Nop56 binds to the snoRNP structure. On the other hand **(Figure 8 pathway B)**, the R2TP complex (with Nop58 and Nop1) binds Rsa1-Hit1 (with Snu13) and all together, they load the core proteins onto the snoRNA with Nop56, which is recruited last onto snoRNA **(Rothé et al., 2014)**. The assembly factor Bcd1 was not considered in either case, despite the fact that it has recently been demonstrated to be important in this process, aiding in the binding of Nop58 or Snu13 **(Massenet et al., 2017)**.
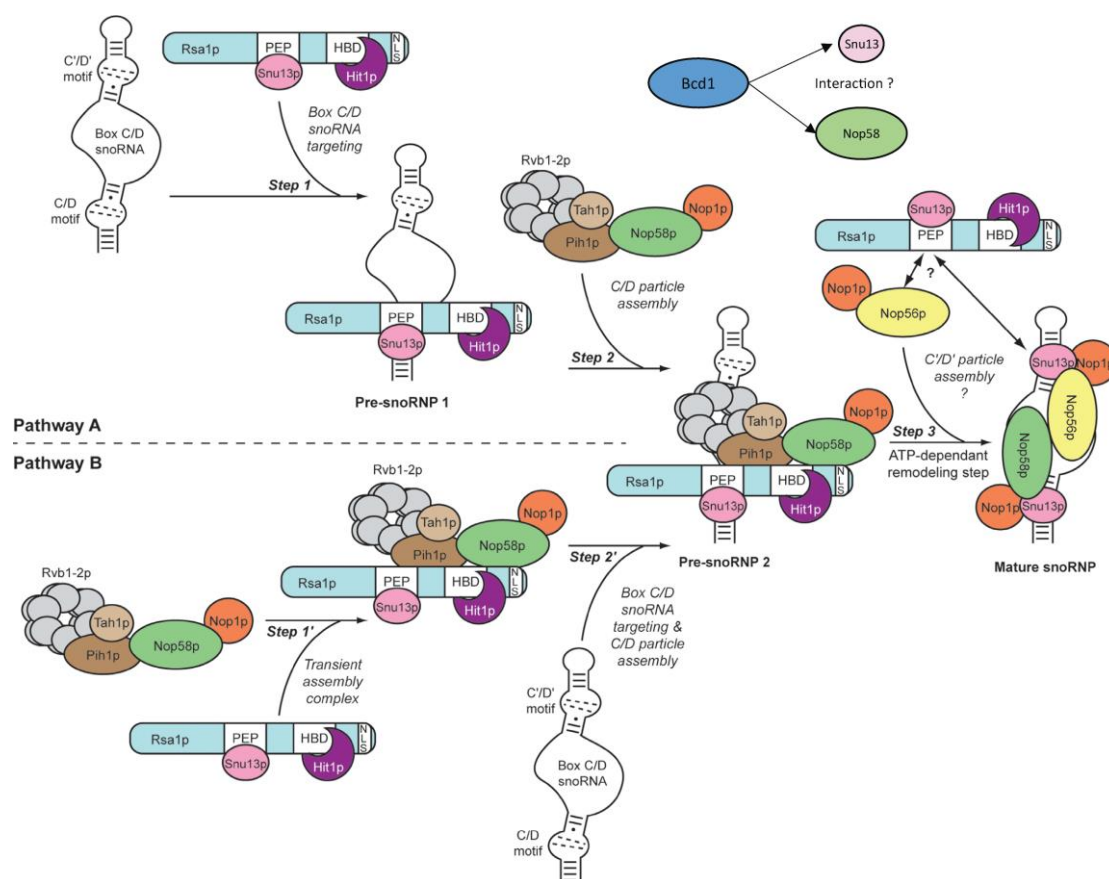
Figure 8: Box C/D snoRNP maturation pathway in *S. cerevisiae*. In pathway A, Rsa1-Snu13-Hit1 binds the snoRNA first, followed by R2TP-Nop58-Nop1. In pathway B, Rsa1-Snu13-Hit1 and R2TP-Nop58-Nop1 bind together and later assemble the core proteins on the snoRNA. In both cases, Nop56 binds the snoRNA separately from the other core proteins. Because the exact location of Bcd1 in the pathway and which core protein it binds are unknown, it was not included in this model. Modified from **(Rothé et al., 2014)**.

Despite extensive research on the biogenesis of C/D snoRNPs in *S. cerevisiae*, a complete understanding of the maturation pathway is lacking. However, it is possible to have a more detailed view of the individual steps through the model designed for vertebrates. It was speculated that the first two core proteins to bind the R2TP complex are SNU13 and NOP58, with the help of the assembly factors NUFIP (Rsa1 in yeast), ZNHIT3 (Hit1 in yeast) and ZNHIT6 (Bcd1). After that, NOP56 and Fibrillarin (Nop1 in yeast) bind this RNA-free complex with the simultaneous exclusion of ZNHIT3. This whole complex is able to bind the C/D snoRNA and, at this point, all the other assembly factors that remained are disassembled, resulting in the formation of the mature snoRNP that only consists of the core proteins SNU13, NOP58, NOP56, and Fibrillarin **(Massenet et al., 2017)**.

2.4.2. Box H/ACA snoRNP assembly

The H/ACA snoRNP consists of the H/ACA snoRNA, and the core proteins, Nhp2, Gar1, Nop10, and Cbf5 (**Kakihara and Saeki 2014**).

In yeast, we know that the assembly factor Shq1 interacts with the free form of Cbf5, forming an RNA-free complex. This complex, together with the assembly factor Naf1, is fundamental for the co-transcriptional assembly of Cbf5 **(Yang et al., 2002; Yang et al, 2005)**. These assembly factors are then removed because they are not integral components of the mature snoRNP. Similar to the C/D family, Rvb proteins are also involved in H/ACA snoRNP biogenesis, although the exact role of Pih1 and Tah1 in this process is unknown **(Zhao et al., 2008; King et al., 2001)**.

Unlike the C/D class, we have less information about the H/ACA snoRNP assembly. As a result, most of what we know about the H/ACA snoRNP maturation pathway comes from studies in vertebrates.

In mammalian systems, the binding of the assembly factor SHQ1 to Dyskerin (Cbf5 in yeast) in its free form is the first steps **(Kakihara and Saeki 2014)** and then there are two possibilities. An RNA-free complex is formed consisting of SHQ1/Dyskerin that is bound by NAF1, NHP2, and NOP10. Alternatively, the binding of NAF1, NHP2, and NOP10 in the second form is preceded by the removal of SHQ1 **(Grozdanov et al., 2009; Li et al., 2011)**. Regardless of how the different proteins are recruited, an RNA-free complex is formed and the R2TP complex will take the place of SHQ1. Later,

with the help of NAF1, the whole complex is recruited to nascent H/ACA RNAs, with the simultaneous exclusion of R2TP. Finally, NAF1 is exchanged with GAR1 after the nascent snoRNP complex is localized in the Cajal bodies. The snoRNP final localization is the nucleolus **(Massenet et al., 2017).**

2.5. snoRNPs released from the ribosome

As explained previously, one of the main functions of snoRNAs is the post-transcriptional modification of pre-rRNAs **(Turowski and Tollervey 2015)**. Typically, the binding between the snoRNA guide region and pre-rRNA occurs co-transcriptionally with the formation of a duplex of 10–21 bp **(Cavaillé et al., 1998)**. Nevertheless, snoRNPs need to be released from the pre-rRNA after successfully completing their task because they were not found as part of the mature ribosome and their presence would probably impede proper ribosome assembly.

The most intuitive model proposes that helicases are used to release snoRNPs from ribosomes, and several studies have shown that inactivation of various helicases can result in snoRNP persistence on pre-ribosomes. In yeast, for example, defects in the helicases Has1, Rok1, and Dbp4 can prevent some snoRNPs from being released from their target **(Liang and Fournier, 2006; Bohnsack et al., 2008; Kos and Tollervey, 2005)**. Moreover, recent studies showed that the helicase Dbp3 can affect the binding of multiple snoRNPs on ribosomes **(Aquino et al., 2021)** and that helicase Dbp2 can also influence the maturation of snoRNAs itself **(Lai et al., 2019)**.

However, it remains possible that the helicases are not the only way to release snoRNP from the pre-ribosome. Even if some helicases can remove multiple snoRNAs from the pre-rRNA, it is likely that they are not able to release all 77 snoRNAs in *S. cerevisiae*. Moreover, direct unwinding of a snoRNA-pre-rRNA duplex was never demonstrated. In conclusion, although there is evidence that helicases are involved in an active mechanism of snoRNP release from the pre-ribosome, passive mechanisms can also play a role in this process **(Bleichert and Baserga, 2007)**.

Even if the release of snoRNP from the pre-ribosome is the most accepted model, recent studies show that in different organisms, including *S. cerevisiae*, a small pool of snoRNA-derived small RNAs (sdRNAs) (small RNAs of ~30 nt formed by the further

processing of the snoRNA) can maintain the binding with the ribosome until their cytosolic localization. It is speculated that these yeast sdRNAs may exert inhibitory activity on translation and their cytosol presence can change depending on stress conditions **(Mleczko et al., 2019)**.

2.6. snoRNAs proteins with unknown function

In addition to the well-known core proteins and assembly factors, the roles of a set of proteins in the snoRNA maturation pathway are still unknown.

2.6.1. The Lsm complex and its role in snoRNAs

Lsm (like Sm) proteins receive their name from their structural resemblance to the Sm family of proteins, which consists of seven small polypeptides linked to several small nuclear RNAs (snRNA). It was proposed that the Lsm proteins can form a heptameric ring complex, obtaining the same configuration as the Sm proteins, which consists of a seven-protein ring with a small central aperture **(Beggs, 2005)**. Two heteroheptameric complexes of Lsm proteins were identified. Lsm2, Lsm3, Lsm4, Lsm5, Lsm6 and Lsm7 are present in both complexes, while the seventh protein can be either Lsm1 or Lsm8 **(Bouveret et al., 2000)**.

Lsm1-7 is found in the cytosol and specifically bind mRNAs with short poly(A) tails of 10 residues or less. Based on Lsm1 depletion, it was possible to propose two functions for this complex: protection of 3'-end mRNAs from premature exonuclease activity and mRNA decapping. Even though its function is not fully understood, it appears that Lsm1-7 plays a role in mRNA decay **(Wilusz and Wilusz, 2013)**.

The Lsm2-8 is localized in the nucleus and the most studied target for this complex is U6, the only snRNA that binds to the Lsm complex rather than the Sm proteins. The Lsm ring binds and stabilizes the 3'-end of U6 on the sequence CGUUUU, which may be the optimal binding sequence. Moreover, Lsm2-8 promotes the assembly of the U4/U6 di-snRNP and chaperon U6 throughout the splicing process **(Achsel et al., 1999; Wilusz and Wilusz, 2013; Zhou et al., 2014)**. In addition to being involved in supporting splicing, the Lsm2-8 complex has other functions in targeting different RNA such as pre-tRNA, pre-mRNA, pre-P RNA, pre-rRNA and pre-snoRNAs.

Lsm2-8 can act as a chaperone between pre-tRNA processing factors and their substrates. On pre-mRNAs, it may play a role in nuclear mRNA turnover by decapping the target. For the rRNA, the depletion of Lsm8 caused a delay in pre-rRNA processing as well as the accumulation of many aberrant processing intermediates, making it therefore important to preserve the regular processing order **(Kufel et al, 2002; Kufel et al, 2004; Kufel et al., 2003a)**.

Finally, some snoRNAs interacted with the Lsm2-8 complex. Depletion of Lsm2, Lsm5, or Lsm8 resulted in the loss of 3'-extended precursors as well as the formation of truncated fragments of both mature and pre-U3 RNAs, indicating that Lsm2-8 stabilizes pre-U3 snoRNAs at their 3'-end. Moreover, it was possible to co-precipitate pre-U3 species with Lsm3, suggesting that Lsm proteins could have transitory interactions with the precursors. Furthermore, the stabilization of pre-U3 snoRNA takes place together with Lhp1, and they may function interdependently because the depletion of one leads to a reduction in the association of the other with the target **(Kufel et al., 2003b)**. To conclude, there may be another Lsm complex containing only six proteins (Lsm2-7) but not Lsm1 or Lsm8. It was shown that Lsm2-7 is able to interact with the H/ACA snoRNA5 and with pre-P RNA **(Fernandez et al., 2004)**.

2.6.2. snoRNA binding with non-canonical proteins

In addition to core proteins and assembly factors, there are proteins whose interaction with snoRNAs is new and not fully understood. Among these proteins are Npl3, Nab2, and Hrp1. Their binding to snoRNAs appears to occur at the 3'-end, a feature shared by Nab2, Hrp1, but also by Npl3, a particular characteristic for Npl3 since in most cases it binds other RNAs at the 5'-end. Even though Npl3 and Hrp1 were proposed to play a role in transcription regulation, this has yet to be confirmed, and there is no information about Nab2's role in snoRNAs **(Chen et al., 20017; Holmes et al., 2015; Kim et al., 2006; Reuter et al., 2015)**. Moreover, even if at a low level, TREX complex components such as Yra1, Sub2, and Hpr1 were discovered to be linked with snoRNAs **(Meinel et al., 2013)**. The TREX complex recruitment on snoRNAs of *S. cerevisiae* can be supported by a study that showed a link between the THO complex and snoRNAs in *Schizosaccharomyces pombe*,

implying that the THO complex may play a role in the regulation of snoRNA expression **(Larochelle et al., 2012)**. Finally, a transcriptome-wide analysis revealed that not only the previously mentioned proteins, but also the serine/arginine (SR)-rich protein Gbp2 and the export factor Mex67, could bind snoRNAs **(Tuck and Tollervey 2012)**.

2.7. General nucleo-cytoplasmic transport

In eukaryotic cells, the separation between the nucleus and the cytosol is a key fact that allows cells to divide various processes throughout their whole lifespan. However, this separation obligates the cell to use a dedicated transport system in order to generate an exchange of macromolecules between the nucleus and cytoplasm. The cargoes that need to be transported across the nuclear membrane pass through nuclear pores known as the nuclear pore complex (NPC), a protein complex made up of proteins called nucleoporins and inserted into the nuclear envelope. Although smaller molecules simply diffuse through the NPC, larger molecules require nuclear transport factors, a group of proteins that recognize the cargoes and bring them through the NPC **(Aitchison and Rout, 2012)**.

One of the most studied transport systems is the Ran-dependent way that uses proteins called karyopherins (Kaps), which can bind different cargos that need to be transported through the nuclear pore complex. In *S. cerevisiae*, there are 14 Kaps functioning as exportins or importins and able to differentially bind multiple targets **(Fried and Kutay, 2003)**. The Ran-dependent transport system use a small protein known as Ran (or Gsp1 in yeast) that exists in two states in the cell: GTP- and GDP-bound. In the nucleus, a GTP exchange factor (Srm1 or Prp20 in yeast) keeps Ran in its GTP form, whereas in the cytosol it is more abundant in the GDP form thanks to the Ran GTPase-activating protein known as RanGAP (Rna1 in yeast) **(Aitchison and Rout, 2012; Sloan et al., 2016)**.

This system enables the cell to maintain the Ran-gradient and, therefore, direct target transport inside and outside the nucleus. In the nucleus, the cargoes with the nuclear export signal (NES) form a trimeric complex with the karyopherin (an exportin in this case) and RanGTP, the most abundant Ran form in this

compartment. Afterwards, the structure of the karyopherin allows the transport of the whole complex through the NPC. Once the complex is in the cytosol, RanGAP stimulates the intrinsic RanGTPase activity, resulting in the hydrolysis of RanGTP in RanGDP and the release of the cargo. Now the exportin and the RanGDP are recycled and transported back to the nucleus independently **(Figure 9a) (Aitchison and Rout 2012)**.

In contrast to export, import only involves the binding between the karyopherin and the cargo with a nuclear localization signal (NLS). This complex can cross the NPC and reach the nucleus where the cargo is released and replaced by the RanGTP via the GTP exchange factor. The formation of the complex karyopherin-RanGTP allows the importer to be recycled back to the cytosol (Figure 9b) **(Sloan et al., 2016)**.

The majority of karyopherins are transported empty back to their original compartment. However, in some cases, a karyopherin can bind another cargo before returning to the original compartment, conducting both an export and import function **(Aitchison and Rout, 2012)**.
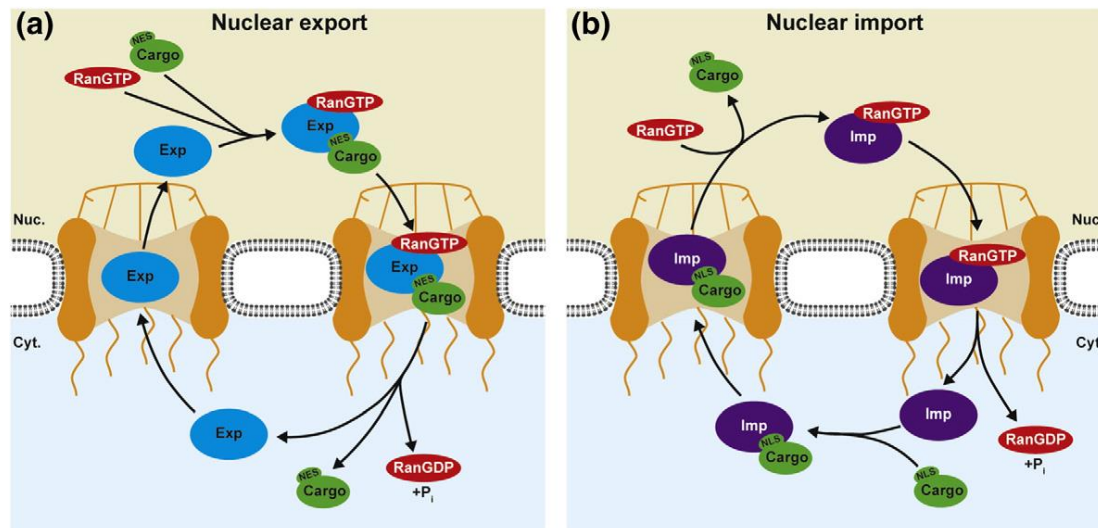
Figure 9: Schematic overview of the Ran-dependent export and import. (a) In the nucleus, the karyopherin involved in the export (Exp) binds the cargo containing the NES together with the RanGTP. Following translocation through the NPC, the cargo is released in the cytosol after RanGTP hydrolysis into RanGDP due to Rna1 activity. After that, the exportin comes back to the nucleus. **(b)** In the cytosol, the cargo containing the NLS binds the karyopherin involved in the import (Imp) and, together, they are transported to the nucleus. Once in the nucleus, via Prp20, the RanGTP takes the place of the cargo that is released. Then the importin-RanGTP complex is recycled back into the cytosol **(Sloan et al., 2016)**.

Another strategy for exporting different targets through the nucleus is the use of the export receptor heterodimer Mex67-Mtr2 (Tap-p15 in humans), which binds mostly mRNAs. Under normal growth conditions, the mRNA needs to overcome several steps before being exported to the cytosol. These steps include the addition of the cap, the excision of introns, and the addition of a 70-90 nucleotide long poly(A) tail. During mRNA maturation, it is possible to identify a group of proteins that have the ability to recruit Mex67-Mtr2 only on correct mRNAs, allowing their export to the cytosol. These proteins in *S. cerevisiae* are the serine/arginine (SR)-rich proteins Npl3, Gbp2, and Hrb1, as well as the poly(A)-binding protein Nab2 **(Figure 10)** **(Zander and Krebber, 2017)**. At the nuclear basket, Mex67-Mtr2 is able to interact with the phenylalanine-glycine (FG) repeat of the NPC and transport the mRNA to the cytosol. It is important to note that Mex67-Mtr2 cannot generate directionality in the process on its own, but requires the DEAD box RNA helicase Dbp5 in order to release its target **(Stewart M., 2010, Tieg and Krebber, 2013)**.
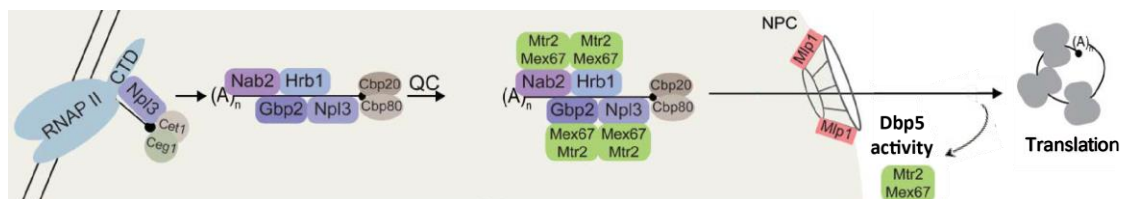
Figure 10: **mRNA export via the Mex67-Mtr2 transport system**. The poly(A)-binding protein Nab2, along with the (SR)-rich proteins Npl3, Gbp2, and Hrb1, carry out a quality control (QC) step in which the export factor Mex67-Mtr2 is recruited only on the correct mRNAs that can then be exported in the cytosol. Modify from **(Zander and Krebber, 2017)**.

2.8. Nucleo-cytoplasmic transport of non-coding RNA

Non-coding RNA (ncRNA) is an RNA class that is not translated and includes different kinds of RNA, some well known, such as rRNA and tRNA, and others whose interest grew in recent years, like long non-coding RNAs. However, even though the function of some of them is clear, recently, studies that have modified their maturation pathways and their localization during these steps have been carried out. Small nuclear RNA (snRNA) and *TLC1* (telomerase *component* 1) are two examples of how new models for the maturation pathway of non-coding RNAs have been developed over the years.

2.8.1. snRNA

In eukaryotic cells, an important mRNA maturation step is splicing, which consists of the removal of introns prior to the export of nuclear mRNA. The RNA-protein complex involved in splicing is known as spliceosome, and it is formed of five spliceosomal subunits called small nuclear ribonucleoprotein (snRNP). Each snRNP is formed of snRNA and several spliceosomal proteins. The snRNAs can be divided into two classes: U1, U2, U4, and U5 belong to the Sm-class, while U6 is part of the Lsm-class.

Unlike in humans, yeast Sm-class snRNAs undergo 3'-end processing and 5'-trimethylation in the nucleus, leading many models to suggest that snRNAs do not shuttle in yeast. The same model was proposed for the Lsm-class, in which no cytosolic step was supported for all eukaryotes **(Matera and Wang, 2014; Matera et al., 2007)**. However, over the years, different research has started to propose the possibility that snRNAs could have a cytosolic phase. According to heterokaryon assay results, both snRNA classes can shuttle into the cytoplasm **(Olson and Siliciano, 2003)**. Furthermore, it was discovered that the Lsm-ring is required for U6 nuclear retention **(Spiller et al., 2007)**. Finally, it was recently shown in *S. cerevisiae* that Mex67 and Xpo1 export both snRNA classes. In the cytosol, the Sm-or Lsm-ring binds the snRNA, which is an important step because the import factors Cse1 and Mtr10 mediate snRNA import through their binding with the Sm-ring. Furthermore, preventing pre-snRNA export or processing causes spliceosome assembly to be incorrect. This suggest that snRNA shuttling functions as a quality control mechanism **(Becker et al., 2019)**.

2.8.2. *TLC1*

Telomerases are RNP complexes that prevent the shortening of chromosome ends, known as telomeres, during replication. In yeast, one of the telomerase components is *TLC1*, a long non-coding RNA of 1158 nucleotides that functions both as a scaffold for the accessory proteins (Est proteins, Pop proteins and Sm-ring) and as a template sequence for telomeres **(Vasianovich and Wellinger, 2017)**.

The maturation pathway of *TLC1* has undergone changes over time. First, the presence of a cytosolic step was proposed, in which *TLC1* is exported exclusively via

Xpo1 and, once in the cytosol, comes into contact with the Est proteins. The only protein involved in the re-import of *TLC1* was the import factor Mtr10 **(Gallardo et al., 2008)**. Subsequently, another export factor, Mex67, was identified, and it was shown that export is a fundamental step for the correct functionality of *TLC1* **(Wu et al., 2014)**. Later, similarly to snRNAs, it was discovered that the binding between *TLC1* and the Sm-ring occurs in the cytosol **(Vasianovich et al., 2020)**. Finally, in the most recent model, the Pop proteins also bind to *TLC1* in the cytosol, and Cse1 was identified as a second import factor that works together with Mtr10. Moreover, the formation of the TMG cap occurs as the final step, following the export phase into the cytosol **(Hirsch et al., 2021)**.

2.9. snoRNA in human

Similarly to *S. cerevisiae*, snoRNAs in humans can be classified into two families based on the same conserved motifs found in specific regions: the C/D box and the H/ACA box. The core proteins that bind to human snoRNAs are also similar to those in *S. cerevisiae* and carry out the same functions **(Laurent et al., 2016; Kufel and Grzechnik 2018)**. However, this class of small non-coding RNAs in humans and other higher eukaryotes differs from *S. cerevisiae* in several ways.

For example, in human both families can show further particularity in the sequence, a long GU repeat for box C/D and an additional conserved sequence (UGAG motif) for box H/ACA that identifies these snoRNAs as small Cajal body-associated RNAs (scaRNA). scaRNAs bind the same core proteins as snoRNAs but are localised in Cajal bodies and mostly guide the modification of snRNAs **(Marnef et al., 2014)**. The genomic organization and the number of snoRNAs also varies significantly. Humans have a different genomic organization, with over 90% of snoRNAs intron-encoded, whereas *S. cerevisiae* has only 10% **(Lui and Lowe 2013)**.

The number dramatically changed as well. Indeed, in humans today, there is no defined number of snoRNAs, but it can be estimated that snoRNA-rRNA targets are around 700. However, when non-canonical target are included, the number increases significantly, reaching over 1000 **(Bouchard-Bourelle et al., 2020)**. Moreover, in humans as well as in other multicellular eukaryotes, there are orphan

snoRNAs that have no known target. However, many orphan snoRNAs were predicted to have complementarities with areas of rRNA that were not known to be modified, suggesting that these modifications are tissue or condition-specific.

It is also possible to identify new snoRNA members that have been discovered in recent years. Some examples of new members are mini-snoRNAs, sdRNAs (snoRNA-derived small RNAs), sno-lncRNAs (snoRNA-long non-coding RNA) and SPA lncRNA (5' snoRNA capped and polyadenylated lncRNA). Mini-snoRNAs are shorter C/D snoRNAs that lack the boxes C' and D'. sdRNAs are formed by the activity of endonucleases or exonucleases and can be further divided into miRNA-like and piRNA-like, with a length of 17-30 nucleotides, and processed snoRNAs (psnoRNAs), a longer form of sdRNA. sno-lncRNAs are formed from loci having two snoRNAs inside the same intron and are usually two box C/D snoRNAs separated from the intronic sequence. SPA lncRNAs, which contain 5' terminal box C/D snoRNPs and are polyadenylated at the 3'-ends, are the longest known variants of snoRNAs to date, with a length of up to 34 kb.

Along with the new members of snoRNA, new targets and function for snoRNAs were discovered. It was shown that snoRNAs can guide modifications to each other. Moreover, other non-canonical targets are vault RNAs, the snRNA 7SK, the signal recognition particle RNA (7SL), and numerous mRNAs. Among the new functions proposed, we can identify their activity as miRNA, regulators of splicing, regulators of lipid traffic and mediators of stress **(Bouchard-Bourelle et al., 2020; Dupuis-Sandoval et al. 2015; Kufel and Grzechnik 2018)**.

2.9.1. snoRNA in human disease

Modifications in snoRNA expression and function could have serious consequences for human health. Many snoRNAs are connected to cancer and other illnesses. Deletion or transcription deficiency of C/D box SNORD116 is correlated with Prader-Willi syndrome **(Duker et al., 2010)**. While elevated expression of box C/D SNORD3A is connected with Creutzfeldt–Jakob disease. Snord3A expression is increased after interaction with misfolded protease-resistant protein aggregates, and this increase may result in the activation of endoplasmic reticulum (ER) stress and designated unfolded protein response arms. Furthermore, it is possible that Snord3A interferes

with the unfolded protein response pathway after ATF6 activation (an ER stress-regulated transmembrane transcription factor that activates ER molecule transcription) and thus inhibits immunoglobulin heavy chain-binding protein (BIP, also known as GRP78) activation and its function as a protective chaperon **(Cohen et al. 2013)**.

Recently, many studies have been able to relate snoRNAs to carcinogenesis. A snoRNA class called small nucleolar RNA non-coding host genes (SNHG) is a snoRNA gene that contains both introns and exons in their sequences and that keeps the full-length transcript, including exons. It was shown that 9 SNHG are involved in carcinogenesis and can be used as a viable biomarker for cancer development and aggressiveness **(Zimta et al., 2020)**. In 10–40% of common tumors, including prostate, lung, liver, and skin cancer, the SNORD50A-SNORD50B locus is lost **(Siprashvili et al. 2016)** and many snoRNAs seem to be directly or indirectly correlated with metastasis and cancer progression **(van der Werf et al. 2021)**. Despite the fact that many studies have found a connection between snoRNAs and carcinogenesis, the molecular basis of this correlation remains unknown.

2.10. Aim of the study

The ribosome is one of the most important ribonucleoprotein complexes in the cell as it is involved in the translation of mRNA. In order to produce a functional ribosome, the pre-rRNA undergoes cutting, trimming, and chemical modification steps **(Turowski and Tollervey 2015; Kos and Tollervey, 2010)**. Chemical modifications are carried out by ribonucleoproteins identified as snoRNPs, whose RNA component is known as snoRNA. The snoRNA maturation pathway consists of several steps, including binding to assembly factors, trimming one or both ends, and finally binding to core proteins, which include the enzyme that modifies the target **(Massenet et al., 2017; Kufel and Grzechnik 2018)**.

The current model predicts no cytosolic steps for snoRNAs, which would complete all maturation steps in the nucleus. However, snoRNA binding to unusual proteins such as the nuclear export factor Mex67, as well as Npl3 and Nab2, which can recruit Mex67, raises doubts on the snoRNAs' exclusive nucleus localization **(Holmes et al., 2015; Reuter et al., 2015; Tuck and Tollervey 2012; Zander and Krebber, 2017)**. Moreover, new cytosolic steps were recently identified for other non-coding RNAs. For *TLC1*, it was shown that the binding to the Sm-ring and Pop proteins occurs in the cytosol **(Hirsch et al., 2021; Vasianovich et al., 2020)**. In the case of snRNA, the unprocessed form is exported to the cytoplasm to bind the Sm-ring and is then re-imported depending on Cse1 and Mtr10 **(Becker et al., 2019)**. Moreover, in a recent study, our group discovered a cytosolic pool of snoRNAs that decreased in the export factor mutant strain *mex67-5 xpo1-1* **(Coban et al. submitted)**.

The aim of the research is to find out whether, like snRNAs and *TLC1*, snoRNAs in *S. cerevisiae* also undergo nucleo-cytoplasmic shuttling and which proteins are involved in this process.

3. Material and Methods

All solutions and media that were prepared in the laboratory were sterilized either by autoclaving at 121 °C for 20 min or by sterile filtration. Glassware was autoclaved, or sterilised at 180 °C for 6 h.

3.1. Material

3.1.1. Chemicals and Consumables

Table 1: List of consumable materials

Materials	Manufacturer/Source
2-Mercapoethanol	Carl Roth (Karlsruhe/Germany)
5-Fluoroortic acid (FOA)	Apollo Scientific (Derbyshire/UK)
Agarose NEEO Ultra	Carl Roth (Karlsruhe/Germany)
Amersham Hybond N+ Nylon Membrane	GE Healthcare (Freiburg/Germany)
Amersham Protran 0.45 µm nitrocellulose membrane	GE Healthcare (Freiburg/Germany)
Blocking Reagent	Roche (Mannheim/Germany)
cOmplete™, EDTA-free Protease Inhibitor	Roche (Mannheim/Germany)
CSPD	Roche (Mannheim/Germany)
Deionized Formamide	Applichem (Munchen/Germany)
Difco Skim Milk	Applichem (Munchen/Germany)
Dithiothreitol (DTT)	Nippon Genetics (Duren/Germany)
dNTPs	Thermo Fisher Scientific (Schwerte/Germany)
Ficoll type 400	Sigma-Aldrich (München/Germany)
Formaldehyde 37 %	AppliChem (Munchen/Germany)
GFP-Selector-beads	NanoTag Biotechnologies (Gottingen/Germany)
GFP-Trap® Beads	ChromoTek GmbH (Planegg-Martinsried/Germany)
Gibson Assembly® Master Mix	New England Biolabs (Frankfurt/Germany)
Glass Beads Type S 0.4-0,6 mm	Carl Roth (Karlsruhe/Germany)
GlycoBlue™ Coprecipitant	Thermo Fisher Scientific (Schwerte/Germany)
HDGreen™ Plus DNA Stain	Intas Science Imaging (Gottingen/Germany)
MF-Millipore™ Membrane Filter, 0.025 µm pore size	Merck Millipore (Darmstadt/Germany)
Microscope slides, 12 well, 5.2 mm, PTFE-coating	Thermo Fisher Scientific (Schwerte/Germany)
Oligonucleotides	Sigma-Aldrich (Munchen/Germany)
Phenol/chloroform/isoamyl alcohol (25:24:1)	Carl Roth (Karlsruhe/Germany)
Poly-L-lysine solution	Sigma-Aldrich (Munchen/Germany)
qPCRBIO SyGreen Mix Lo-ROX	Nippon Genetics (Duren/Germany)
RiboLock RNase Inhibitor	Thermo Fisher Scientific (Schwerte/Germany)

Table 1: List of consumable materials (continued)

Rotiphorese Gel 30 (37.5:1) Acrylamide	Carl Roth (Karlsruhe/Germany)
Salmon sperm DNA	Applichem (Munchen/Germany)
TRIzol™ Reagent	Thermo Fisher Scientific (Schwerte/Germany)
tRNAs	Sigma-Aldrich (Munchen/Germany)
WesternBright™ Quantum™ Western Blotting HRP Substrate	Advansta (San Jose,CA/USA)
Whatman® Blotting Paper	Hahnemuhle (Dassel/Germany)

Kit

DIG RNA labeling mix, 10x	Roche (Mannheim/Germany)
FastGene® Scriptase II cDNA Kit	Nippon Genetics (Duren/Germany)
Maxima First Strand cDNA Synthesis Kit	Thermo Fisher Scientific (Schwerte/Germany)
NucleoSpin® Gel and PCR Clean-up	Macherey-Nagel (Duren/Germany)
NucleoSpin® Plasmid	Macherey-Nagel (Duren/Germany)
NucleoSpin® RNA	Macherey-Nagel (Duren/Germany)
TURBO DNA-free™ DNase Kit	Thermo Fisher Scientific (Schwerte/Germany)

Protein and DNA markers

GeneRuler 100 bp DNA Ladder	Thermo Fisher Scientific (Schwerte/Germany)
GeneRuler 1 kb DNA Ladder	Thermo Fisher Scientific (Schwerte/Germany)
Lambda DNA/EcoRI plus HindIII Marker	Thermo Fisher Scientific (Schwerte/Germany)
PageRuler™ Prestained Protein Ladder	Thermo Fisher Scientific (Schwerte/Germany)

Enzyme

Conventional Restriction Enzymes	Thermo Fisher Scientific (Schwerte/Germany)
DreamTaq DNA-Polymerase	Thermo Fisher Scientific (Schwerte/Germany)
PhusionR High-Fidelity DNA polymerase	New England Biolabs (Frankfurt/Germany)
Q5R High-Fidelity DNA polymerase	New England Biolabs (Frankfurt/Germany)
RNase A	Qiagen (Hilden/Germany)
RNase-Free DNase	Qiagen (Hilden/Germany)
Taq Ligase	New England Biolabs (Frankfurt/Germany)
T5 Exonuclease	New England Biolabs (Frankfurt/Germany)
Zymolyase 20T	Zymo Research (Freiburg/Germany)
DpnI	Nippon Genetics (Duren/Germany)
EcoRI	Thermo Fisher Scientific (Schwerte/Germany)
KpnI	Thermo Fisher Scientific (Schwerte/Germany)

Table 2: Antibody used

Antibody	Dilution	Supplier/Source
Anti-Aco1 (rabbit)	1/2000	Prof. Dr. U. Muhlenhoff (Marburg/Germany)
Anti-GFP (mouse) (monoclonal, GF28R)	1/5000	Thermo Fisher Scientific (Schwerte/Germany)
Anti-Hem15 (rabbit)	1/5000	Prof. Dr. U. Muhlenhoff (Marburg/Germany)
Anti-Nop1 (mouse)	1/4000	Santa Cruz (Heidelberg/Germany)
Anti-Zwf1 (rabbit)	1/4000	Prof. Dr. U. Muhlenhoff (Marburg/Germany)
Anti-rabbit IgG-HRP (goat)	1/10000	Dianova (Hamburg/Germany)

Table 2: Antibody used (continued)

Anti-mouse IgG-HRP (goat)	1/10000	Dianova (Hamburg/Germany)
Anti-Digoxigenin-FITC Fab fragments (sheep)	1/100 (FISH)	Roche (Mannheim/Germany)
Anti-Digoxigenin-Cy3 Fab fragments (sheep)	1/100 (FISH)	Roche (Mannheim/Germany)

3.1.2. Equipment, Hardware and Software

Table 3: Equipment and hardware used

Machine	Supplier / Source
AF6000 microscope with Leica DFC360 FX camera	Leica (Wetzlar/Germany)
Bio-Link 254 UV-crosslinking chamber	Vilber Lourmat (Eberhardzell/Germany)
CFX Connect 96FX2 qPCR cycler	Bio-Rad (München/Germany)
Eclipse E400 tetrad microscope	Nikon (Düsseldorf/Germany)
Electro Blotter PerfectBlue Semi-Dry, Sedec M	Peqlab (Erlangen/Germany)
FastPrep-24® Cell homogenizer	MP Biomedicals (Illkirch/France)
Fusion-SL-3500.WL	Vilber Lourmat (Eberhardzell/Germany)
Fusion FX	Vilber Lourmat (Eberhardzell/Germany)
Gene Pulser Xcell™ Electroporation System	Bio-Rad (München/Germany)
Heraeus™ Pico™ 21	Thermo Fisher Scientific (Schwerte/Germany)
Heraeus™ Multifuge™ X3 with TX-750 or F15-8x50cy rotor	Thermo Fisher Scientific (Schwerte/Germany)
Improved Neubauer counting chamber	Carl Roth (Karlsruhe/Germany)
Innova42R Incubator Shaker	Eppendorf (Hamburg/Germany)
INTAS UV gel detection system	INTAS (Göttingen/Germany)
Milli-Q® Water purification system	Millipore (Eschborn/Germany)
Nano Drop 2000 spectrophotometer	Peqlab (Erlangen/Germany)
Primo Star light microscope	Zeiss (Jena/Germany)
T100™ Thermal Cycler	BioRad (Feldkirchen/Germany)

Table 4: Software used

Software	Supplier/Source
Ape Plasmid Editor	M. Wayne Davis (University of Utah/USA)
CFX manager 3.1	BioRad (Feldkirchen/Germany)
Fusion Capt Software	Vilber Lourmat (Eberhardzell/Germany)
Illustrator CS6	Adobe Systems (San Jose/USA)
Leica AF 2.7.3.9723	Leica (Wetzlar/Germany)
Office® 2011/2019	Microsoft Corporation (Redmond/USA)
Photoshop CS6	Adobe Systems (San Jose/USA)
Snapgene	GSL Biotech LLC (Chicago/USA)

3.1.3. Media

Table 5: *Saccharomyces cerevisiae* media used

YPD

Yeast extract	1 % (w/v)
Peptone	2 % (w/v)
Glucose	2 % (w/v)
Agar-Agar	1.8 % (w/v)

Selective Media

Nitrogen base	1.7 g/l
Ammonium sulphate	40 mM
Glucose*	2 % (w/v)
Agar-Agar*	1.8 % (w/v)
L-Alanine	80 mg/l
L-Arginine	80 mg/l
L-Asparagine	80 mg/l
L-Aspartic acid	80 mg/l
L-Cysteine	80 mg/l
L-Glutamine	80 mg/l
L-Glutamic acid	80 mg/l
L-Glycine	80 mg/l
Inositol	80 mg/l
L-Isoleucine	80 mg/l
L-Methionine	80 mg/l
Para-aminobenzoic acid	8 mg/l
L-Phenylalanine	80 mg/l
L-Proline	80 mg/l
L-Serine	80 mg/l
L-Threonine	80 mg/l
L-Tyrosine	80 mg/l
L-Valine	80 mg/l
optional metabolites according to selectivity	
L-Adenine	20 mg/l
L-Histidine	80 mg/l
L-Leucine	400 mg/l
L-Lysine	80 mg/l
L-Tryptophan	80 mg/l
Uracil	80 mg/l

Sporulation medium

Yeast extract	0.25 % (w/v)
Potassium acetate	150 mM
Glucose**	0.05 % (w/v)
Uracil**	40 mg/l
Adenine**	40 mg/l
Tyrosine**	40 mg/l
Histidine**	20 mg/l
Leucine**	20 mg/l
Lysine**	20 mg/l
Tryptophan**	20 mg/l
Methionine**	20 mg/l
Arginine**	20 mg/l
Phenylalanine**	100 mg/l
Threonine**	350 mg/l

FOA plates

Drop out mix (-URA)	0.2 %
Glucose	2.0 %
Nitrogen Base	0.17 %
Ammonium sulphate	0.51 %
5-fluoroorotic acid	0.1 %
Agar-Agar	1.8 %

B-plates

Nitrogen Base	0.17 % (w/v)
Ammonium sulphate	3 mM
Agar-Agar*	3 % (w/v)
Glucose*	2%

(Sherman, 2002; Sprague, 1991; modified)

*components were autoclaved separately

**components were sterile filtered (0.2 μm)

Table 6: *Escherichia coli* media used

LB medium	
Tryptone	1 % (w/v)
Yeast extract	0.5 % (w/v)
NaCl	85 mM
Ampicillin* (if added)	100 µg/ml
Agar-Agar (for plates only)	1.5 % (w/v)

*Ampicillin was added after autoclaving and cooling the medium to ~ 60 °C **(Sambrook et al., 1989)**.

3.1.4. Strains

Table 7: *Saccharomyces cerevisiae* strains used

Number	Genotype	Source	Parental strains
HKY36	*MATα ura3-52 leu2Δ1 his3Δ200*	(Winston et al.,1995)	
HKY82	*MATα ura3 leu2 trp1 his3 ade2 Mtr10Δ pURA-Mtr10 (pRS316)*	(Senger et al.,1998)	
HKY208	*MATα ura3-52 ade2-101 his3-11,15, trp1-Δ901 cse1-1*	(Xiao et al., 1993)	
HKY644	*MATα ade2, his3, leu2, trp1, ura3 mex67::HIS3 pUN100-mex67-5 (LEU2, CEN)*	(Segref et al.,1997)	
HKY1112	*MATa trf4::kanMX4 ura3Δ0 leuΔ0 his3Δ1 met15Δ0*	Euroscarf	
HKY1854	*MATa lsm8-1 uraΔ hisΔ trpΔ lysΔ leuΔ*	(Spiller et al. 2007)	
HKY2087	*MATα his ura cse1-1 mtr10:kanMX4*	Prof. Dr. H. Krebber	
HKY2109	*MATa Lsm8::GFP:HISMX6 his3Δ1 leu2Δ0 met15Δ0 ura3Δ0*	Laboratory of Prof. Dr. G. Braus	
HKY2122	*MATα mex67::HIS3 trf4::kanMX4 ade2 ura3*	This study	HKY1112 x HKY644
HKY2305	*MATα snoRNA13::URA3 ura3Δ0 leu2Δ0 his3Δ1 met15Δ0*	This study	
HKY2316	*MATα snoRNA65::URA3 ura3Δ0 leu2Δ0 his3Δ1 met15Δ0*	This study	
HKY2328	*MATα snoRNA13Δ ura3Δ0 leu2Δ0 his3Δ1 met15Δ0*	This study	
HKY2329	*MATα snoRNA65Δ ura3Δ0 leu2Δ0 his3Δ1 met15Δ0*	This study	

Table 8: *Escherichia coli* strain used

Strain	Genotype	Application
DH5α™	F⁻ φ80*lacZ*ΔM15 Δ(*lacZYA-arg*F)U169 *rec*A1 *end*A1 *hsd*R17 (rₖ⁻, mₖ⁺) *pho*A *sup*E44 λ⁻*thi*-1 *gyr*A96 *rel*A1	Plasmid amplification

3.1.5. Plasmid

Table 9: Plasmid used

Number	Genotype	Source/reference	Origin and construction
pHK1894	*pSNR13-snR13 URA3 CEN*	This study	Restriction free cloning on pHK1819 using HK4653 + HK4654
pHK1895	*pSNR13-snR13 URA3 CEN NNS sites mutated*	This study	Restriction free cloning on pHK1859 using HK4653 + HK4654
pHK88	*CEN URA3 (pRS316), AMPR*	(Sikorski and Hieter, 1989)	
pHK385	*pGAL1 GBP2-GFP, CEN URA3*	Prof. Dr. H. Krebber	
pHK640	*HIS3 GAL1-cre*	Euroscarf	
pHK1705	*pADH1:Lsm8:GFP CEN URA3*	Prof. Dr. H. Krebber	pHK1335
pHK1711	*pLsm8:Lsm8:GFP CEN URA3*	This study	Restriction free cloning on pHK1705 using HK3880 + HK3881
pHK1725	*pUC19 Cloning Vector*	Prof. Dr. H. Krebber	
pHK1819	*pGAL1-snoRNA13 URA3 CEN*	This study	Gibson assembly on pHK385 using HK4414 + HK4415
pHK1820	*pGAL1-snoRNA65 URA3 CEN*	This study	Gibson assembly on pHK385 using HK4418 + HK4419
pHK1839	*pGAL1-snoRNA13 URA3 CEN NNS sites mutation GTAG -> GCCG (139/140*) TCTT -> TACT (147/148*)*	This study	Mutagenic PCR on pHK1819 using HK4601-4602
pHK1840	*pGAL1-snoRNA65 URA3 CEN NNS sites mutation GTAA -> GCCA (109/110*) TCTT -> TACT (114/115*) GTAA --> GCCA (119/120*)*	This study	Mutagenic PCR on pHK1820 using HK4603 + HK4604
pHK1859	*pGAL1-snoRNA13 URA3 CEN NNS sites mutation GTAA -> GCCA (152/153*) TCTT -> TACT (160/161*)*	This study	Mutagenic PCR on pHK1839 using HK4669 + HK4670
pHK1868	*pSNR65-snR65 URA3 CEN*	This study	Restriction free cloning on pHK1820 using HK4655 + HK4656
pHK1871	*pSNR65-snR65 URA3 CEN NNS sites mutated*	This study	Restriction free cloning on pHK1840 using HK4655 + HK4656

* Indicates the number of the mutated nucleotide starting from the 5'-end.

3.1.6. Oligonucleotides

Oligonucleotides were provided by Sigma-Aldrich. They were delivered dry and then suspended in DEPC water to a concentration of 100 µM stock solution before being stored at - 20 °C. After suspension in DEPC water, fluorescently labeled

oligonucleotides were aliquoted and stored at -20 °C. When used, the fluorescently labeled oligonucleotide aliquotes were stored at 4°C. Fluorescently labeled oligonucleotides were always stored in the dark.

Table 10: Primers used for cloning

Cloned plasmids	Number	Sequence (5' → 3')	Orientation	Use of the oligo
pHK1711	**HK3880**	GTCGCGCCATTCGCCATTCAGGCTGCG CAACTGTTGGGAATTCCGTCTCATGCT GCTT	Forward	For restriction free cloning in pHK1705
	HK3881	CAACTCTTTTATTTAAGTAGTCTTTCAA GGTGGCTGACATGGTGCACGATAGTG TGTTCT	Reverse	
pHK1819	**HK4414**	TCTATACTTTAACGTCAAGGAGAAAAA ACTATAGAATTCAAGGAAGTTTTTTCCT TTTTATATG	Forward	For gibson assembly in pHK385
	HK4415	ACAAAAGCTGGGTACCTTCACATGTTC CGCAGATTTTGATACTCCAGTATTATG GATGG	Reverse	
pHK1820	**HK4418**	TCTATACTTTAACGTCAAGGAGAAAAA ACTATAGAATTCaTAAAATGATGATTTT TTTAAACACA	Forward	For gibson assembly in pHK385
	HK4419	ACAAAAGCTGGGTACCTTCACATGTTC CGCAGATTTTGATCAGATCTGGTTTGA GAATTG	Reverse	
pHK1839	**HK4601**	CTACCTTTTTTTACTTTTATCTGACCTTT TAACTTCCCCGCCGAAAATACTAGTAA TCCTTCT	Forward	For mutagenic restriction free cloning in pHK1819
	HK4602	CGCATTATATATGCAGCGCTACGATAC AATGTAAGAAGGATTACTAGTATTTTC GGC	Reverse	
pHK1840	**HK4603**	ATTACAGTGTTTTCGACAGTTTTAAATC TCTGAACCGATTTTGCCACTACTGGCC ATTGT	Forward	For mutagenic restriction free cloning in pHK1820
	HK4604	TGCGATTTGATTAACGTCATTACGGAA ATGTAAGGACACAATGGCCAGTAGTG GC	Reverse	
pHK1859	**HK4669**	TGACCTTTTAACTTCCCCGCCGAAAATA CTAGCCATCCTTACTACATTGTAT	Forward	For mutagenic restriction free cloning in pHK1839
	HK4670	GAAAATTTTACGCATTATATATGCAGC GCTACGATACAATGTAGTAAGGATGG CTAGTAT	Reverse	
pHK1868	**HK4655**	GTGGCGGCCGCTCTAGATTTCCTGCGG AGTCAAAACA	Forward	For mutagenic restriction free cloning in pHK1820
	HK4656	GCATAAATTGTGTTTAAAAAAATCATC ATTTTATGAATTCGAATTTTGTTGACAA GAACATCTGG	Reverse	
pHK1871	**HK4655**	GTGGCGGCCGCTCTAGATTTCCTGCGG AGTCAAAACA	Forward	For mutagenic restriction free cloning in pHK1840
	HK4656	GCATAAATTGTGTTTAAAAAAATCATC ATTTTATGAATTCGAATTTTGTTGACAA GAACATCTGG	Reverse	

Table 10: Primers used for cloning (continued)

pHK1894	**HK4653**	GTGGCGGCCGCTCTAGATGATTGTATT GTCATTGTAGGAGGT	Forward	For restriction free cloning in pHK1819
	HK4654	ACTCATATTCATCATATAAAAAGGAAA AAACTTCCTTGAATTCGACCCTTTAAAA AATCCAATTAACA	Reverse	
pHK1895	**HK4653**	GTGGCGGCCGCTCTAGATGATTGTATT GTCATTGTAGGAGGT	Forward	For restriction free cloning in pHK1859
	HK4654	ACTCATATTCATCATATAAAAAGGAAA AAACTTCCTTGAATTCGACCCTTTAAAA AATCCAATTAACA	Reverse	

Table 11: Primers for qPCR

Target	Number	Sequence (5' → 3')	Use of the oligo
snR13	**HK3530**	GAAGTTTTTTCCTTTTTATATGATGAA	Forward
	HK3531	GGTCAGATAAAAGTAAAAAAAGGTAGC	Reverse
	HK3533	TTACTAAGATTTTCTACGGGGAAG	Reverse for 3'-extended unprocessed form
	HK3784	GAACAAGCCAAACCCAAC	Reverse over NNS termination site
	HK4690	GGCATCTCAAATCGTCTCTATATC	Forward promoter
snR17a (U3a)	**HK3542**	GTTGATGAGTCCCATAACCTTT	Forward
	HK3543	GAGCCCTATCCCTTCAAAA	Reverse
	HK3545	CAATTTAGAAAAGGAAAAAAGTGG	Reverse for 3'-extended unprocessed form
	HK3785	CGCTCTTGACGAATTTTAGG	Reverse over NNS termination site
snR24	**HK2797**	TCAAATGATGTAATAACATATTTGCTACTTC	Forward
	HK2798	CATCAGAGATCTTGGTGATAATTGG	Reverse
	HK3405	GAGAAGAGCAGAGTAATGCTAAACC	Reverse for 3'-extended unprocessed form
snR59	**HK3447**	CTTAATGATGAAAACTATTCCTTATTCTCGA	Forward
	HK3448	AGTCAGCCGAAAGATGGTG	Reverse
snR65	**HK3789**	TAAAATGATGATTTTTTTAAACACAA	Forward
	HK3790	GTTCAGAGATTTAAAACTGTCGAA	Reverse
	HK3791	CCCATAATCAAATCAGCTCATA	Reverse over NNS termination site
snR68	**HK3402**	ATCATGATGAGCATTTATTTTACTGCG	Forward
	HK3403	CAGCAAATCTGTTAAGAGTCAATTTCC	Reverse
	HK3411	AGTTTTCCAATTTTTTTGTAAGATGAACC	Reverse for 3'-extended unprocessed form
	HK3787	GACCATATTATCAAGAGCTTCCTGCT	Reverse over NNS termination site
snR42	**HK2799**	TTGTGATGCTTTAGGGAGCC	Forward
	HK2800	ATCCTTTCTCTATCTCACCCTG	Reverse
snR42	**HK3413**	CATACTATAAATACGTATATATAACAAAGTAACCAT CAAG	Reverse for 3'-extended unprocessed form
	HK3786	AATATTGATCTCAATGTCATCAGCTG	Reverse over NNS termination site

Table 11: Primers for qPCR (continued)

	HK3554	GTTACCGGGAGTTTTTCTTG	Forward
	HK3555	GTGGGAATACTCAGTCATTGTTAG	Reverse
snR82	HK3557	GCAATCACTATACGTACGTAAATATACTC	Reverse for 3'-extended unprocessed form
	HK3788	GACCGACATCTGTAACAGGTAT	Reverse over NNS termination site

Table 12: Oligonucleotides used for synthesis of digoxigenin labeled RNA probes

Target	Number	Sequence (5' → 3')	Orientation	Use of the oligo
snR13	HK3303	TAATAGGACTCACTATAGGGGAAGTTTTTTCCTTTTTATATGATG	Forward	For antisense probe synthesis
	HK3304	GGTCAGATAAAAGTAAAAAAGGTAGC	Reverse	
	HK3324	GGAAGTTTTTTCCTTTTTATATGATG	Forward	For sense probe synthesis
	HK3325	TAATAGGACTCACTATAGGGGTCAGATAAAAGTAAAAAAGGTAGC	Reverse	
	HK4362	CTGACCTTTTAACTTCCCC	Forward	For 3'-extended probe synthesis
	HK4363	TAATAGGACTCACTATAGGGTCACTTTCGTTTTTTTACAAG	Reverse	
snR42	HK3307	TAATAGGACTCACTATAGGGATGCTTTAGGGAGCCTATTG	Forward	For antisense probe synthesis
	HK3308	GGATTACCTCAGCACCAAC	Reverse	
	HK2605	GATGCTTTAGGGAGCCTATTG	Forward	For sense probe synthesis
	HK2606	TAATAGGACTCACTATAGGGGATTACCTCAGCACCAAC	Reverse	
	HK4364	GATGACCTGAGGTATGGAA	Forward	For 3'-extended probe synthesis
	HK4365	TAATAGGACTCACTATAGGGATGTCTTTGTGATAGCAATC	Reverse	
snR68	HK3309	TAATAGGACTCACTATAGGATGATGAGCATTTATTTTACTGCGT	Forward	For antisense probe synthesis
	HK3310	TTTCAGCAAATCTGTTAAGAGTC	Reverse	
	HK3326	ATGATGAGCATTTATTTTACTGCGT	Forward	For sense probe synthesis
	HK3327	TAATAGGACTCACTATAGGTTTCAGCAAATCTGTTAAGAGTC	Reverse	
snR17 (U3)	HK3572	GGTTGATGAGTCCCATAACC	Forward	For sense probe synthesis
	HK3573	TAATAGGACTCACTATAGGGTCAGACTGCCATTTGTACC	Reverse	
	HK4295	GGTACAAATGGCAGTCTGAC	Forward	For 3'-extended probe synthesis
	HK4296	TAATAGGACTCACTATAGGGTCGCTCTTGACGAATTTTAG	Reverse	
snR24	HK3305	TAATAGGACTCACTATAGGTCAAATGATGTAATAACATATTTGC	Forward	For antisense probe synthesis
	HK3306	TTCATCAGAGATCTTGGTG	Reverse	
	HK2607	TCAAATGATGTAATAACATATTTGC	Forward	For sense probe synthesis
	HK2608	TAATAGGACTCACTATAGGTTCATCAGAGATCTTGGTG	Reverse	

Table 13: Oligonucleotide probes labeled with Cy3 dye

Target	Number	Sequence (Cy3-5' → 3'-Cy3)
snR13	**HK3413**	GAGTTTTTCCACACCGTTACTGATTTGGCAAAAGCCAAACAGCAACTCGA
snR17a (U3a)	**HK3563**	GTTTCTCACTCTGGGGTACAAAGGTTATGGGACTCATCAACCAAGTTGGA
snR24	**HK2802**	GTGATAATTGGTATGTCTCATTCGGAACTCAAAGTTCCATCTGAAGTAGC
snR42	**HK2801**	CGATGGTTTTAAAGATGGATTACCTCAGCACCAACAGTTACACTATTCGG
snR65	**HK4727**	GAATGCTTTCAGATACTATCTAGCATAAAT
snR68	**HK3562**	GCCCCCGTCAATACGATAACGCAGTAAAAT

Table 14: Primers for Knock Out generation

Deleted gene	Number	Sequence (5' → 3')	Orientation
SNR13	**HK4229**	GCCATATTGGTCGTAACACAAAATGCCCAATGGAG CCTGGGGATCTATCGATCTCGACAACCCG	Forward
	HK4188	AAAATTTTACGCATTATATATGCAGCGCTACGATAC AATGCCCAGTCACGACGTTGTAAAACG	Reverse
SNR65	**HK4413**	AGTTGTTTTCACTCTTCAAAACTAAATTCAGTATTAG CGAGGATCTATCGATCTCGACAACCCG	Forward
	HK4190	TTTAGTTAAGAAGATTCAAGATTGCGATTTGATTAA CGTCCCCAGTCACGACGTTGTAAAACG	Reverse

3.2. Cell biology methods

3.2.1. Cell cultivation

Prior to application, all media were autoclaved and heat-sensitive components, including antibiotics and galactose, were sterile-filtered and added after autoclaving. Plates were prepared by adding to the suitable liquid medium 1.5 % agar for *E. coli* or 1.8 % agar for *S. cerevisiae*. When synthetic selective media were used for *S. cerevisiae*, the solutions were autoclaved separately before being combined.

3.2.1.1. Cultivation of *E. coli*

Cultures of *E. coli* were carried out in LB medium **(Table 6)** according to **(Sambrook et al., 1989)**. Single colonies were selected and utilized as inoculum for liquid cultures grown overnight at 37 °C. The appropriate antibiotics were applied to the medium to select resistance genes.

3.2.1.2. Cultivation of *S. cerevisiae*

YPD media was used to grow yeast cells without plasmid DNA **(for yeast media see Table 5)**. Strains with a plasmid-encoded selection marker that complements the

strain's auxotrophy were cultivated in the proper selective medium **(Sherman, 2002)**. The loss of URA3 gene containing plasmids was selected using 5-fluorotic acid (FOA) plates prepared with a mix that contained every amino acid and nucleobase except uracil. FOA plates can select the deletion of a URA3 gene-containing plasmid because 5-Fluorotic acid is decarboxylated by the URA3 encoded Orotidine 5'-phosphate decarboxylase, resulting in the toxic metabolite 5-fluorouracil. Unless otherwise noted, yeast cells were grown at 25°C on YPD or synthetic selective medium plates and were stored at 4°C. For long-term storage at -80 °C, cells were suspended in 50% glycerol. Based on the experiment to be carried out, single colonies from plates were inoculated into 5 ml or 50 ml pre-cultures and incubated overnight at 25 °C with agitation. The pre-culture concentration was measured using a hemocytometer and diluted to $0.5 - 0.8 \times 10^6$ cells/ml in the main-culture (see section 3.2.2). The main culture was grown at 25 °C with agitation until log-phase ($1 - 3 \times 10^7$ cells/ml) and if temperature-sensitive mutants were used, the culture was also shifted to the restrictive temperature (37 °C or 16 °C). The liquid culture was harvested by centrifugation at 4,000 rpm for 3 minutes, and the cell pellet was resuspended in 5 ml of sterile water before being transferred to a 15 ml tube and centrifuged again at 4,000 rpm for 3 minutes. The supernatant was then removed, and the cells were either used immediately or frozen in liquid nitrogen and stored at -20 °C.

3.2.2. Measurement of yeast cell density in liquid culture

The cell density of yeast cell cultures was calculated using a hemocytometer. A sample of the cell culture was diluted 1/20 (for pre-cultures) or 1/5 (for log phase cultures) and 10 µl were pipetted into the counting chamber.

Before pipetting into the hemocytometer, the diluted sample was mixed to avoid errors due to cell sedimentation. The cell density was calculated using the formula:

$$1x10^4 \; x \; dilution \; factor \; x \; counted \; cells = cells/ml$$

3.2.3. Transformation of *E. coli* via electroporation

Electrocompetent cells were produced according to **(Dower et al., 1988)**. Prior to the transformation, the DNA sample was dialyzed to ensure that no free ions cause a

bypass during the electroporation. The plasmid DNA was pipetted on a nitrocellulose membrane (0.025 μm pore size) placed on deionised water in a Petri dish. The DNA sample was dialysed for 30 min - 60 min. The dialysate plasmid DNA was gently added and mixed to an aliquot of 50 μl of electro competent *E. coli* cells stored at -80 °C and that were thawed on ice. The cell suspension was pipetted into an electroporation cuvette (1 mm gap), which was precooled on ice. With an electroporator, a pulse of 1.8 kV, 50 μF, 150 W was generated. After electroporation, 1 ml of LB medium was immediately added into the cuvette and, after being gently mixed, it was transferred into a new 1.5 ml tube. The cells were incubated for 60 min at 37 °C and then centrifuged at 2500 rpm for 5 min and resuspended in 1 ml of sterile water. The sample was centrifuged again, resuspended in 100 μl sterile water and plated on ampicillin containing LB-plates. The plate was incubated over night at 37 °C.

3.2.4. Transformation of *S. cerevisiae*

The transformation of yeast cells was carried out by the lithium acetate heat shock transformation **(Gietz et al., 1992)**. A pre-culture was grown over night and used to inoculate a 5 ml liquid culture with a concentration of 0.5 - 0.8 x 10^7 cells/ml. When the main culture reached a concentration of 1 - 3 x 10^7 cells/ml, it was harvested by centrifugation at 4000 rpm for 5 min. The pellet was washed once with 1 ml of TE lithium acetate buffer (10 mM Tris/Cl, 1 mM EDTA, 100 mM lithium acetate, pH 7.5), centrifuged again at 4000 rpm for 5 min, and resuspended in 50 μl of TE lithium acetate buffer ($\sim$ 0.5 x 10^8 cells). The cell suspension was mixed with 1 μg of plasmid DNA, 50 μg of salmon sperm carrier DNA, which was boiled for 5 min at 95 °C and then cooled on ice for 5 min, and 300 μl of PEG TE lithium acetate buffer (10 mM Tris pH 7.5, 1 mM EDTA, 100 mM lithium acetate, 40 % (v/v) poly ethylene glycol 4000). The sample was incubated for 30 min at 25 °C on a rotator, followed by 15 min heat shock at 42 °C. Afterwards, the cells were centrifuged at 13000 rpm for 1 min and the pellet was washed with 1 ml of sterile water. The cell suspension was centrifuged again, resuspended in 100 μl of sterile water and plated on the required selective media plate. The plate was incubated at 25 °C until colonies were visible.

3.2.5. Crossing of *S. cerevisiae* strains

Under nutrient depletion conditions, a diploid strain is able to sporulate, a process in which it undergoes miosis, resulting in the formation of 4 haploid cells in an ascus. **(Sherman, 2002; Sherman and Hicks, 1991)**. The crossing is carried out by mating two haploid strains with opposite mating types (MATa or MATα, determined by the gene cassette in the MAT locus).

Two different strains were streaked out and mixed on a YPD plate and incubated for 1 - 2 days. To select the diploid cells, the strain mix was stamped from YPD onto the suitable selective media plate, according to the selection markers of the parental strains, and grown for 2 - 3 days. The sporulation was induced by inoculating 2 ml of sporulation medium **(see Table 5)** with the diploid strain. After 5 - 8 days at 25 °C in a rotator, if the presence of tetrads (asci with 4 spores) was confirmed, 100 µl of the culture was harvested by centrifugation at 13000 rpm for 1 min, washed once with 1 ml sterile water, and resuspended in 50 µl P-solution (0.1 M phosphate buffer - pH 6.5, 1.2 M sorbitol). The digestion of the ascus wall was carried out by adding 1 µg/µl Zymolyase (Zymo Research) for 5 - 10 min at room temperature. The cells were then centrifuged at 4000 rpm for 1 min, washed once with 100 µl P-solution, and resuspended in 200 µl P-solution. From this cell suspension, 2.5 – 5 µl were mixed with 100 µl of sterile water and pipetted on one third of a YPD plate. The tetrads were picked and separated into single spores using a tetrade microscope. After 2 – 3 days of incubation, the single spores were restreaked on YPD plates and grown for 2 – 3 days. The spores were transferred to a 96-well plate with 200 µl of 50 % glycerol per well. For long term storage, the 96-well plate was kept at - 80 °C. Cell material was stamped onto different YPD and selective plates to analyse the genotypes. The temperature sensitivity was tested by incubating YPD plates at 16 °C and 37 °C. For the identification of the mating types, the spores were stamped on MATa and MATα plates and grown for one day at 25 °C. Afterwards, the cells were stamped on selective B-plates and further incubated. The MATa and MATα strains were isoleucine and valine auxotrophs, and the tested strain with the opposite mating type was the only one that could complement them **(Sprague, 1991)**.

3.3. Methods using DNA

3.3.1. Plasmid isolation from *E. coli*

Plasmids were purified using the NucleoSpin Plasmid purification kit (Macherey-Nagel) following the manufacturer's instructions. *E. coli* culture were grown in 10 ml LB as described in section 3.2.1.1 and DNA was purified according to the manufacturer's instructions. The yield was determined by photometric analysis (see 3.3.3).

3.3.2. Extraction of genomic DNA from *S. cerevisiae*

Yeast chromosomal DNA was extracted by phenol/chloroform extraction based on **(Rose et al., 1990)**. Yeast culture was grown in 10 ml of YPD medium until saturation. The culture was harvested by centrifugation at 4000 rpm for 3 min, the supernatant was removed and the pellet was transferred into a 2 ml screw top tube after resuspension in 1 ml of sterile water. For the lysis, the cell sample was centrifuged and the supernatant removed, followed by the addition of 500 µl of detergent lysis buffer (2 % Triton X-100, 1 % SDS, 100 mM NaCl, 10 mM Tris pH 8, 1 mM EDTA), 500 µl of phenol, and 300 µl glass beads (0.4 - 0.6 mm). The cells were homogenized using the FastPrep machine twice at 6 m/s for 20 sec. The samples were centrifuged at 16000 x g for 5 min to separate the aquatic and the organic phase. The aquatic upper phase, which contained the hydrophilic DNA, was transferred into a new 1.5 ml tube, vigorously shaken with an equal amount of phenol, and the phases were separated again by centrifugation at top speed for 5 min. The procedure was repeated with phenol-chloroform-isoamyl alcohol (25:24:1) and then with chloroform-isoamyl alcohol (24:1). The aquatic phase was then transferred to a new tube and mixed with 1/10 volume of 3 M sodium acetate (pH 5.2) and 2.5 volumes of 100% ethanol. After mixing, the sample was incubated over night at -20 °C for precipitation of the DNA. The DNA precipitated was then pelleted by centrifugation at top speed for 30 min at 4 °C, the supernatant was removed, and the DNA pellet was washed twice with 70 % ethanol. The DNA pellet was dried for 5 min at 65 °C, suspended in 100 µl of sterile water and incubated at 65 °C for 10 minutes with shaking.

3.3.3. Measurement of DNA and RNA concentration

The concentrations of nucleic acids were determined using a NanoDrop spectrophotometer that measured the absorbance of light at 260 nm wavelength, and the concentration was calculated using a modification of the Lambert-Beer law. The calculation includes the absorbance at 260 nm, a baseline correction at 340 nm and extinction coefficients of 50 ng × cm/µl for double stranded DNA, 33 ng-cm/µl for single-stranded DNA and 40 ng × cm/µl for RNA.

3.3.4. Amplification of DNA by Polymerase chain reaction

Depending on the purpose, different DNA polymerases were used. The DreamTaq polymerase was used for analytical purposes, while when it was needed to prepare amplifications of DNA to be used for cloning, site-directed mutagenesis, or digoxigenin labeled RNA probes, proof-reading polymerases Q5 or Phusion were used. The DNA template used was either 100 ng of plasmid DNA or 1 µg of yeast genomic DNA. The reaction mixes and cycling conditions are based on the supplied protocol of the respective polymerase **(Table 15 and Table 16)**. The PCR products were analyzed using agarose gel electrophoresis (see section 3.3.5).

Table 15: PCR reaction mix composition

Polymerase	DreamTaq	Phusion	Q5
dNTPs	200 µM each	200 µM each	200 µM each
Primers	0.2 µM each	0.5 µM each	0.5 µM each
Polymerase	0.025 U/µl	0.02 U/µl	0.02 U/µl

Table 16: PCR protocols

Polymerase	DreamTaq	Phusion	Q5
Initial denaturation	95 °C - 3 min	98 °C - 30 sec	98 °C - 30 sec
Denaturation	95 °C - 30 sec	98 °C - 10 sec	98 °C - 10 sec
Annealing	55 - 65 °C - 30 sec	55 - 65 °C - 30 sec	55 - 65 °C - 30 sec
Elongation	72 °C - 1 min/kb	72 °C - 30 sec/kb	72 °C - 30 sec/kb
35 cycles			
Final elongation	72 °C - 10 min	72 °C - 10 min	72 °C - 10 min

3.3.5. Agarose gel electrophoresis

DNA samples were separated based on their size using agarose gel electrophoresis. For gel preparation, 1 % (w/v) agarose was dissolved in TAE buffer (40 mM Tris base, 0.1 (v/v) Acetic acid, 1 mM EDTA, pH 8.5) and warmed in the microwave until the agarose was fully dissolved. The mixture was cooled down to approximately 60 °C under constant stirring before adding 5 µl/100 ml HDGreen Plus DNA Stain (Intas Science Imaging). The solution was cast into a gel mould (10 cm x 15 cm x 2 cm) with a comb already inserted in order to form sample wells. Once the gel was solidified, it was immediately used or stored at 4 °C. When used, the gel was placed in an agarose gel running chamber and completely covered with TAE buffer. Before pipetting the DNA samples into the gel pockets, they were mixed with 6x loading buffer (10 mM Tris pH 7.6, 60 mM EDTA, 60% (v/v) glycerol, 0.03 (w/v) bromophenol blue). The separation of the DNA fragments took place by applying a voltage of 120 V to the electrodes of the gel chamber for 30 - 90 min. Finally, DNA bands were visualized on UV-transilluminator at 320 nm and, if required, excised for DNA extraction.

3.3.6. DNA extraction from agarose gels

To extract the DNA from the agarose gel, a NucleoSpin Gel and PCR Clean-up kit (Macherey-Nagel) based on silica membranes was used. The DNA purification was carried out following the manufacturer's instructions, and the DNA was eluted in sterile or DEPC treated water.

3.3.7. Cleavage of DNA by restriction digestion

Restriction endonucleases (Thermo Fisher Scientific) were used to cleave DNA samples. For the digestion, 0.5 µg of the plasmid or 3 µg of a purified PCR product was mixed with 5 units of the required enzyme in one of the provided buffers. For PCR products, a total volume of 30 µl was used, while plasmids were digested in a final volume of 20 µl. The samples were incubated at 37 °C for 4 – 15 h and then the enzyme was inactivated by heat at 80 °C for 20 min, according to the manufacturer's description. Digested DNA was separated by agarose gel electrophoresis (see 3.3.5) and then purified (3.3.6). The restriction enzymes used in this work are *EcoRI* and *KpnI* **(Table 1)**, both with Tango buffer.

3.3.8. Gibson Assembly

The Gibson assembly was carried out in a total volume of 10 µl by combining a 2 - 3 fold molar amount of insert fragment (5-fold molar excess for insert fragments shorter than 200 bp) with 100 - 150 ng of vector. Subsequently, 10 µl of the Gibson Assembly Master Mix (New England Biolabs) were added. The sample was incubated at 50 °C for 1 h and then used for *E. coli* transformation **(Gibson et al., 2009)**. All primers used for Gibson assembly were drawn with a 30 – 40 bp overhangs that overlap with the vector in order to generate the insert fragments **(Table 10)**.

3.3.9. Restriction free cloning

Restriction-free (RF) cloning is a method that allows the inserting of a DNA fragment in any position of a plasmid without the use of restriction enzymes **(Zeng et al., 2017)**. All primers used for RF cloning have 30 - 40 bp overhangs that are complementary to the region of the plasmid where we want to insert the DNA fragment **(Table 10)**. These primers were used to generate by PCR a product known as 'mega-primer', which consists of the DNA insert with the complementary regions to the plasmid. The RF cloning was carried out running a PCR with a mix containing the components shown in **(Table 17)**. Subsequently, the sample was digested with the enzyme DpnI, for 10 h at 37 °C. DpnI recognizes methylated adenosine sites and cut the sequence 5'-GATC-3'. Because only the plasmid isolated from *E. coli* contains methylated adenosine, only this plasmid will be digested. DpnI was then deactivated incubating the sample at 80°C for 20 min. Finally, the sample was either stored at 4 °C or directly transformed in *E. coli* (see 3.2.3).

The plasmids pHK1868 and pHK1871 were created in collaboration with the Ph.D. Student Fei Yu.

Table 17: Component used in Restriction-free cloning

RF cloning Mix

Polymerase Buffer	1x
10mM dNTPs	0.5 µM
Phusion/Q5 DNA Polymerase	0.025 U/µl
Plasmid DNA	80 – 150 ng
DNA fragment (mega-primer)	20-fold of plasmid DNA
Nuclease-free water	to 20 µl

3.3.10. Site directed mutagenesis by restriction free cloning

The Restriction Free cloning was used to carry out site-directed mutagenesis of plasmid DNA. Using Restriction Free cloning, it was possible to generate more mutations at the same time in close regions of the target. The primers used to generate the "mega-primer" contained the desired mutation(s) and specific overhangs to overlap the plasmid region where the mutations should be inserted. For Restriction Free cloning protocol, see section 3.3.9.

The plasmids pHK1839, pHK1840, pHK1859, pHK1894 and pHK1895 were created in collaboration with the Ph.D. Student Fei Yu.

3.3.11. Knockout strain generation using Cre/Lox system

During this study, knockout strains were generated with the Cre/Lox system. The primers used have to amplified a marker gene, URA3 in this work, flanked by LoxP regions. Moreover these primers contain 30 – 40 bp overhangs that are complementary to the region the we want to excise **(see Table 14)**. A PCR with these primers synthesized a cassette (*loxP* – marker gene – *loxP*) and *S. cerevisiae* was transformed with it in order to replace the target gene by homologue recombination **(Gueldener et al. 2002)**. The protocol used is a modify version of the protocol in section 3.2.4. After that the cell culture was resuspended in 50 µl of TE lithium acetate buffer, were added the same amount of salmon sperm carrier DNA, PEG TE lithium acetate buffer, but an higher quantity of DNA, at least 3 µg of the cassette. The sample was incubated for 30 min at 25 °C on a rotator, followed by adding of 1/9 volume of DMSO and 15 min heat shock at 42 °C. Afterwards, the cells were centrifuged at 13000 rpm for 1 min, the pellet was resuspended in 5 ml of YPD and incubated at 25 °C for 3 - 4 h with agitation. The cell suspension was then centrifuged at 4000 rpm for 3 min and washed with 1ml of sterile water. Finally, the cell sample was centrifuged, resuspended in 100 µl of sterile water, and plated on the selective media plate for the marker gene of the cassette. The plate was incubated at 25 °C until colonies were visible. The grown colonies were tested for the excision of the target gene by PCR.

The marker gene was then removed using the Cre recombinase. The strain was transformed with a plasmid containing the Cre recombinase under control of the

GAL1 promoter. The transformed strain was plated on the selective media for the plasmid containing Cre recombinase, and the colonies obtained from the transformation were grown in the same liquid selective media containing galactose in order to express the Cre recombinase. The loss of the marker gene was tested by PCR.

3.3.12. Sequencing

To verify all DNA constructs, the region of interest was sequenced by LGC Genomics, using Sanger sequencing.

3.4. Molecular biological methods

3.4.1. RNA isolation from yeast

In this study, were used two different methods for RNA extraction:

RNA from cell lysates was extracted with the NucleoSpin RNA kit (Macherey-Nagel), following the manufacturer's instructions except for two steps. The cells were lysed twice at 5.5 m/s for 30 s using the FastPrep machine. The DNA digestion with DNase was extended to 30 min.

RNA purification for RNA Co-Immunoprecipitation experiments was carried out via TRIzol Reagent (Invitrogen). 1 ml of TRIzol was added to the samples before incubation for 10 min at 65 °C on the shaker at 1300 rpm. Afterwards 200 µl of Chloroform were added and mixed vigorously. Next, the samples were centrifuged at 16000 x g for 15 min with the consequent separation of the phases, and the upper, aquatic phase was transferred into a new 1.5 ml tube and mixed with the same volume of 2-propanol. Finally, were added 20 µg glycogen for lysate samples and 15 µg GlycoBlue (Thermo Fisher Scientific) for eluate samples. The samples were mixed and incubated over night at - 20 °C. Samples were then centrifuged for 30 min at top speed at 4 °C, the supernatant was removed and the RNA pellet was washed twice with 70 % ethanol-DEPC treated water (pre-cooled to -20 °C). During the washing steps, to completely remove the supernatant, the samples were briefly centrifuged again and the remaining supernatant was removed. The RNA pellet was then dried at 37 °C and resolved in 20 µl DEPC treated water. To further remove DNA, the samples

were treated with the Turbo DNAfree kit following the manufacturer's instructions, and then the RNA was precipitated again by adding 0.1 volumes 3 M sodium acetate pH 5.2, 2.5 volumes 100 % ethanol, and 20 µg glycogen or 15 µg GlycoBlue (for lysate and eluate samples, respectively), followed by incubation over night at - 20 °C. RNA concentrations were measured using a NanoDrop spectrophotometer (see 3.3.3).

3.4.2. Complementary DNA (cDNA) synthesis from RNA

To reverse transcribed RNA in cDNA, the FastGene Scriptase II Kit (NIPPON Genetics) was used, following the manufacturer's instructions. In all experiments, were used random hexamer primers and the reverse transcription was carried out at 42 °C. As a negative control for DNA contamination, all samples were processed twice in the same manner, but the reverse transcriptase was added to only one of them. After reverse transcription, the cDNA was diluted 1:2.5 – 1:5 with DEPC treated water. For each qPCR 2 µl of cDNA were used per well.

3.4.3. Quantitative Real time PCR (qPCR)

During qPCR, the cDNA serves as a template that amplifies the target via specific primers **(Table 11)**. The fluorescence dye used is SYBR Green and the primer sequence was selected to achieve amplification efficiencies of 0.8 – 1. Excluding the negative controls, all qPCR samples were prepared at least in triplicates. The qPCR was carried out in a total volume of 10 µl per well containing 5 µl qPCR master mix (qPCRBIO SyGreen Mix Lo-ROX, Nippon Genetics), 10 µM forward and reverse primers (0.2 µl each), 2.6 µl DEPC treated water, and 2 µl cDNA.

3.4.4. Nucleo-cytoplasmic fractionation experiments

The nucleo-cytoplasmic fractionation was carried out with modifications according to **(Sklenar and Parthun 2004)**. It was used to isolate the cytoplasmic fraction of a cell lysate. A pre-culture of 50 ml of the required strain was prepared and diluted at $5 - 8 \times 10^6$ cells/ml in 200 ml of the main culture. The main culture was harvested by centrifugation at 4000 rpm for 3 min when it reached mid-log phase ($1 - 2 \times 10^7$ cells/ml), and the pellet was resuspended in 5 ml of sterile water and transferred to a 15 ml tube. The cell sample was then centrifuged, the pellet resuspended in 1 ml of

YPD, 1 M sorbitol, 2 mM DTT, and transferred into a 2 ml tube. The cell suspension was centrifuged again, the supernatant was discarded, and the pellet was resuspended in 1 ml YPD, 1 M sorbitol, 1 mM DTT. In order to degrade the cell wall, the cell sample was mixed with 1 mg Zymolyase and incubated until 70 % were spheroblasted. Digestion was carried out at 25 °C. Next, the cell suspension was transferred in 50 ml YPD/1 M sorbitol and incubated for 30 min at 25 °C under shaking. If required, the culture was shifted to the restrictive temperature of 16 °C or 37 °C, depending on the used strain. Afterwards, the cell culture was split in two; 10 ml were transferred to a 15 ml tube, while 40 ml were transferred to a 50 ml tube. The 10 ml served as total RNA and total protein controls while the 40 ml were used to obtain the cytoplasmic fractionation. Next, the two cell samples were centrifuged for 10 min at 2000 rpm and the pellet was treated differently.

The pellet from the 10 ml sample was resuspended in 1ml DEPC treated water and then split in two, one of 700 µl for total RNA isolation and the other of 300 µl for total protein control. Both samples were collected in 2 ml screw top tubes for cell lysis with the FastPrep machine. The total RNA was treated as described in section 3.4.1. The protein control sample was lysate (see 3.6.1) and mixed with an equal amount of 2x SDS sample buffer (125 mM Tris pH 6.8, 4 % SDS, 20 % (v/v) glycerol, 0.05 % (w/v) Bromophenol blue, 5 % (v/v) 2-mercaptoethanol) before being boiled for 5 min at 95 °C, and loaded on a SDS gel (see 3.6.3).

The pellet from the 40 ml sample was resuspended in 500 µl Lysis buffer (18 % Ficoll 400, 10 mM HEPES pH 6.0) plus 1 µl Ribolock and transferred into a new 1.5 ml tube. Next, 1 ml Buffer A (50 mM NaCl, 1 mM MgCl2, 10 mM HEPES pH 6.0) was added and the tube was vortexed thoroughly. The sample was then centrifuged at 4000 rpm at 4 °C for 15 min to separate the cytoplasmic fraction. The supernatant containing the cytoplasmic fraction was transferred into a new 1.5 ml tube and centrifuged again at 4000 rpm at 4 °C for 15 min. The supernatant obtained was collected into a new 1.5 ml tube and either used directly or frozen in liquid nitrogen and kept at -20 °C. For the RNA extraction, 300 µl of the cytoplasmic fraction were mixed with 250 µl of 70 % ethanol-DEPC treated water and 150 µl of the buffer RA1 of the NucleoSpin RNA kit (Macherey-Nagel) and then pipetted into the blue column of the NucleoSpin RNA kit. From this point, RNA extraction was carried out as

described in 3.4.1. For the protein control, 30 µl of the cytoplasmic fraction were mixed with an equal amount of 2x SDS sample buffer, boiled for 5 min at 95 °C and loaded on a SDS gel (see 3.6.3). For both total and cytoplasmic samples, a control Western blot was carried out using specific antibodies to detect the cytoplasmic protein Zwf1 and the nucleolar protein Nop1, as described in section 3.6.4.

3.4.5. Synthesis of digoxigenin labeled RNA probes

Synthesis of digoxigenin (DIG)-labeled probes was carried out in vitro using the T7-polymerase (Thermo Scientific) and the DIG RNA labeling Mix (Roche). The size of the DIG-probes varied depending on the target selected. The first step was the amplification via PCR followed by purification (see 3.3.4 and 3.3.6) of the target region using genomic DNA and a pair of primers, one of which contained a T7-promotor sequence **(Table 12)**. Afterwards, the purified target DNA was used as a template for the in vitro transcription with the T7 RNA polymerase, DIG-labeled UTP, and all four natural RNA-NTPs. The transcription was performed as described by the manufacturer's protocol. After the incubation of the sample at 37 °C for 2 h, the reaction was stopped by adding 1 µl 0.5 M EDTA (pH 8.0 made with DEPC treated water). The DIG-RNA was precipitated by adding LiCl (final 200 mM), glycogen (final 80 ng/µl) and 70 % (v/v) ethanol-DEPC treated water to the sample, which was then incubated overnight at -20 °C. Next, the DIG-RNA was pelleted by centrifugation at top speed for 30 min, washed twice with 70 % (v/v) ethanol-DEPC water, and air dried. The DIG-probe was then resuspended in 20 µl 0.5 x TE pH 7.5 (10 mM Tris/HCl, 1 mM EDTA, DEPC water), 20 µl deionized formamide, and 60 µl HybMix. The probe was stored at -20 °C.

50x Denharts solution
1 % (w/v) Ficoll
1 % (w/v) Polyvinylpyrrolidone
1 % (w/v) Bovine serum albumin

HybMix
50 % (v/v) deionized formamide
5x SSC
500 µM EDTA
0.1 % (v/v) TWEEN-20
1x Denharts solution
0.1 mg/ml Heparin

3.5. Microscopic

The microscopic analysis was carried out using the Leica DMI6000B fluorescence microscope with the Leica DFC360 FX camera.

3.5.1. Fluorescence *in situ* hybridization experiments (FISH)

Fluorescence *in situ* hybridization (FISH) experiment was used for visualization of individual RNA species and it was carried out as described in **(Hackmann et al. 2014)**. The detection of snoRNAs was conducted with DIG-labeled probes and Cy3-labled DNA probes with Cy3 at the 5'- and 3'-end (Sigma Aldrich) **(Table 13)**.

The main culture with the desired strain was grown to mid-log phase (1 x 10^7 cells/ml) at 25 °C and, if required, was carried out a temperature shift to the restrictive temperature (37 °C or 16 °C). Next, the cells were fixed using formaldehyde to a final concentration of 4 % and the fixation was carried out for 60 min at room temperature or for 15 min at the restrictive temperature followed by 45 min at room temperature under agitation. The sample was then centrifuged for 2 min at 4000 rpm at 4 °C, washed twice with 1 ml P-solution, centrifuged again and resuspended in 200 µl P-solution. The cell sample was stored at 4 °C or used directly. When used, the sample was mixed with 2 µl 1 M DTT and 20 µl of Zymolyase (10 mg/ml) followed by incubation at 25 °C until 70 % of the cells were spheroblasted. The cells were collected by centrifugation at 4000 rpm for 2 min at 4 °C and resuspended in 200 - 400 µl P-solution depending on the concentration of the sample. 20 µl of the cell sample were pipetted onto a well of a Poly-L-lysine coated slide and incubated for 30 min at 4 °C. Then, the cells were permeabilized for 10 min using P-solution mixed with 0.5 % Triton X-100. The solution in excess was aspirated and the well washed once with P-solution. If a Cy3 probe was used, the well was directly treated with pre-hybridization mix. When the DIG-probe was used, the P-solution was aspired and the well equilibrated with 0.1 M TEA pH 8.0 for 2 min. Next, the polar groups were blocked with 0.25 % acetic anhydride in 0.1 M TEA for 10 min and finally the well was washed with P-solution.

During the pre-hybridization step, first it was prepared a pre-hybridization mix containing 1 µl salmon sperm DNA (boiled for 5 min at 95 °C and chilled for 5 min on

ice), 1 µl tRNA (10 mg/ml), and 18 µl HybMix for a total volume of 20 µl that was needed for each well used. 20 µl of the pre-hybridization mix was pipetted onto the well and the slide incubated for 1 h at 37 °C in a humidified chamber. During the incubation, the hybridization mix was prepared, containing the same component as the pre-hybridization mix with the addition of the probe at a concentration depending on the target and the kind of probe used. Finally, the pre-hybridization mix was aspirated from the well, 20 µl of the hybridization mix was pipetted onto the well, and the slide was incubated over night at 37 °C in a humidified chamber. The next day, the well was washed at room temperature with 2x SSC and afterwards with 1x SSC, both for 1 h. The well was then washed once with 0.5x SSC at 37 °C for 30 min and once with 0.5x SSC at room temperature for 30 min.

If a Cy3 probe was used, the slide was treated directly with DAPI for nuclear staining. When DIG-probe was used, the SSC buffer was aspired and the well was rinsed with the antibody blocking buffer (0.1 M Tris pH 9.0, 0.2 M NaCl, 5 % heat-inactivated FCS, 0.3 % tween) (ABB) for 1 h. The ABB was then aspired and 20 µl of ABB mixed with the anti-Digoxigenin-Fab fragments was applied onto the well. The slide was incubated over night at 4 °C in a humidified chamber. Subsequently, the well was washed twice with ABB for 15 min, once with ABB for 30 min and finally with 1x PBS, 0.1 % tween-20. Next, as for the Cy3 probes, the slide was treated for the nuclear staining. The following steps are the same for both probes used. For nuclear staining, DAPI (1:8000 diluted in 1x PBS) was pipetted onto the well and incubated for 2 min in the dark. The well was then washed once with 1x PBS, 0.1 % Tween-20 for 5 min and twice with 1x PBS for each 5 min. All of the washing steps were carried out at room temperature. The slide was dried in the dark and finally mounted with the mounting medium. The slide was stored at - 20 °C.

1x PBS pH 7.4
137 mM NaCl
2,7 mM KCl
10 mM Na2HPO4
1.8 mM KH2PO4

Mounting medium
2 % (w/v) n-propyl gallate
80 % (v/v) glycerol
20 % (v/v) PBS pH 8.0

P-solution
0.1 M phosphate buffer pH 6.5
1.2 M sorbitol

20x SSC pH 7.0
3 M NaCl
300 mM Sodium citrate

3.6. Biochemical methods with protein and RNA

3.6.1. Preparation of yeast cell lysate

The main culture with the selected strain was grown to mid-log phase ($1 - 2 \times 10^7$ cells/ml), if required, shifted to the restrictive temperature (37 °C or 16 °C) and harvested by centrifugation at 4000 rpm for 3 min at 4 °C. Afterwards, the pellet was washed with 5 ml of sterile water and transferred to a 15 ml tube. The cells were then centrifuged again at 4000 rpm for 3 min at 4 °C, the supernatant was removed, and the pellet was either frozen in liquid nitrogen and stored at -20 °C or stored on ice for direct use. The pellet was lysed by adding 1x pellet-volume of glass beads (0.4 – 0.6 mm) and, depending on the experiment, 1x pellet-volume of the appropriate buffer. See 3.6.2 for Immunoprecipitation and see 3.6.5 for RNA Co-Immunoprecipitation. The pellet was lysed using the FastPrep machine three times at 5.5 m/s for 30 sec with a 5 min incubation on ice in-between. To remove all cell debris, the lysate was centrifuged at 13000 rpm for 5 min at 4 °C. The centrifugation step was repeated until the lysate was clear.

3.6.2. Immunoprecipitation (IP) of GFP-tagged proteins

GFP tagged proteins were purified using GFP-selector beads (Nanotag Biotechnologies) or GFP-Trap beads (Chromotek), following the manufacturer's instructions with modifications. For each immunoprecipitation (IP) sample, a 400 ml culture was harvested and lysate as described in 3.6.1. The buffer used was PBSKM-T (1x PBS pH 7.4 (137 mM NaCl, 2.7 mM KCl, 10 mM KH_2PO_4, 2 mM Na_2HPO_4), 2.5 mM $MgCl_2$, 3 mM KCl and added fresh every time, 0.5 % Triton X-100 and protease inhibitor (5 µl per 100 µl cell pellet; cOmplete™, EDTA-free Protease Inhibitor Cocktail, Roche)). All preparation steps were carried out on ice. For each sample, a 10 µl slurry of GFP-beads was used and prepared by washing 3 times with 1 ml PBSKM-T buffer (after each washing step, the beads were centrifuged at 2000 rpm for 2 min and the supernatant was removed). As a lysate control for Western blot analysis, 20 µl of the clarified lysate was taken, mixed with 2x SDS sample buffer and kept on ice. To each sample of washed GFP-beads was added the same volume of the remaining clarified lysate and was incubated for 2 hours on a rotator at 4 °C. The

sample including the beads is termed "eluate". Subsequently, the beads were washed 5 times with 1 ml PBSKM-T buffer by inverting the tubes. After the last washing step, the beads were centrifuged at 2000 rpm for 2 min and the supernatant was discarded, leaving approximately 30 µl of liquid in the tube. The eluate was mixed with 30 µl 2 x SDS sample buffer. Both eluate and lysate samples were heated to 95 °C for 5 min and then loaded on an SDS gel (see 3.6.3).

3.6.3. SDS-Polyacrylamide gel-electrophoresis (SDS-PAGE)

In this study, the proteins were separated according to their size using the standard, vertical, discontinuous SDS polyacrylamide gel electrophoresis **(Garfin, 2009)**. All the components for the preparation of the stacking and the separation gel are listed in **(Table 18)**. For both gels, APS and TEMED were added last before pouring. The preparation gel mix was cast between two 25 x 20 glass plates with 2 mm thick spacers and it was covered with a layer of 2-propanol to generate an even surface. After polymerisation, the 2-propanol was removed. The stacking gel mix was cast on top of the separation gel and a comb was immediately inserted to form sample wells. After polymerisation of the stacking gel, the comb was removed and the gel was put in a running chamber containing two reservoirs with electrodes. Both reservoirs of the chamber were filled with SDS running buffer (25 mM Tris Base, 0.1 % (w/v) SDS, 190 mM glycine). Using a syringe, air bubbles underneath the gel and remaining non-polymerised acrylamide from the wells were removed. The prepared samples, and the pre-stained protein marker (PageRuler Prestained Protein Ladder, Thermo Fisher Scientific) were loaded into the wells. The power source was connected with the two electrodes of the chamber and the gel was run for approximately 15 h at 14 mA.

Table 18: Composition of SDS polyacrylamide gels

Components	Stacking gel	Separation gel
Bis-/Acrylamide mixture 37,5:1	5 % (v/v)	10 % (v/v)
Tris/HCl pH 8.8	-	375 mM
Tris/HCl pH 6.8	125 mM	-
SDS	0.1 % (w/v)	0.1 % (w/v)
APS	0.1 % (w/v)	0.1 % (w/v)
TEMED	0.1 % (v/v)	0.04 % (v/v)

3.6.4. Western blot analysis

After SDS-PAGE, proteins were transferred to an Amersham Protran 0.45 µm nitrocellulose membrane (GE Healthcare Life Sciences) using a semi-dry blotting chamber **(Alegria-Schaffer, 2014)**. The anode plate was covered with blotting buffer (25 mM Tris Base, 192 mM glycine, 20 %(v/v) Methanol) and a pre-soaked whatman paper was put onto the anode, followed by the nitrocellulose membrane, the SDS-Gel, and another pre-soaked whatman paper. Air bubbles were removed, and additional blotting buffer was poured on the stack. Finally, the cathode plate was placed on top and fixed with screws. Depending on the size of the membrane, the mA used to transfer the proteins on the nitrocellulose membrane was calculated (1.2 mA/cm²) and the timing for transfer was 2 h. All subsequent washing or incubation steps were carried out on a shaker. After transfer, the membrane was first blocked in 5 % (w/v) milk powder in TBS-T (50 mM Tris pH 7.4, 150 mM NaCl, 0.1 % (v/v) Tween 20) for 1 h and then incubated with the primary antibody solution (antibody diluted in 2 % milk powder in TBS-T) either overnight at 4 °C or at room temperature for 2 h.

Afterwards, the primary antibody solution was removed and the membrane was washed three times for 10 min with TBS-T. Next, the membrane was incubated with the secondary antibody solution (antibody diluted in 2 % milk powder in TBS-T) for 2 h at room temperature. The secondary antibody selected was anti-mouse or anti-rabbit, depending on the primary antibody used. All secondary antibodies used were connected to the horseradish peroxidase (HRP). After the incubation, the membrane was washed three times for 5 min with TBS-T. The membrane was then rinsed two times with TBS and covered with ECL substrate solution (Amersham ECL, GE healthcare or WesternBright Quantum, Advansta). Afterwards, the membrane was put into a plastic sheet, the excess liquid was removed, and the signals were detected on a chemiluminescence imaging system (Fusion SL and Fusion FX (Vilber)).

3.6.5. RNA Co-Immunoprecipitation (RIP) of GFP-tagged proteins

To analyse the RNA-Protein interactions, was carried out a GFP-tagged protein Immunoprecipitation followed by RNA isolation. For each RIP sample, a 400 ml culture was harvested and lysate as described in 3.6.1. The buffer used was the RIP

buffer (25 mM Tris/HCl pH 7.5, 150 mM NaCl, 2 mM MgCl2), to which was added freshly every time 0.2 mM PMSF, 0.5 mM DTT, 0.2 % (v/v) Triton X-100, protease inhibitor (5 µl per 100 µl cell pellet; cOmplete™, EDTA-free Protease Inhibitor Cocktail, Roche) and RNase inhibitor (0.6 µl / 500 µl pellet-volume Ribolock, Thermo Scientific). All preparation steps were carried out on ice. For each sample, a 10 µl slurry of GFP-beads was used and prepared by washing 3 times with 1 ml RIP buffer (after each washing step, the beads were centrifuged at 2000 rpm for 2 min and the supernatant was removed). After the last wash, in each sample, 10 µl of DNAse (Qiagen) was added.

For the lysate samples, in addition to the 20 µl for the protein lysate control added with 2x SDS sample buffer, 50 µl of the clarified lysate were also taken to use as a whole-cell lysate sample for RNA purification (RNA lysate sample). 10 µl of DNAse (Qiagen) was added to the RNA lysate samples and they were incubated for 1 h at 25 °C on a rotator. After that, both protein and RNA lysate samples were kept on ice.

To each sample of washed GFP-beads was added the same volume of the remaining clarified lysate and was incubated for 2 hours on a rotator at 4 °C followed by incubation for 30 min at 25 °C on a rotator. The sample including the beads is termed "eluate". Subsequently, the eluate was washed 5 times with 1 ml RIP buffer by inverting the tubes. Prior to the last washing step, from the 1 ml RIP sample 300 µl of the bead suspension were transferred into a new 1.5 ml tube, that served as protein eluate control for Western blot analysis. The remaining 700 µl were used for RNA isolation. From both protein and RNA eluate samples, the supernatant was removed after the last washing step.

The eluate protein samples were mixed with 2x SDS loading buffer and, together with the protein lysate control, were boiled at 95 °C for 5 min and loaded on an SDS gel (see 3.6.3) followed by Western blot analysis (see 3.6.4).

The eluate RNA together with the lysate RNA, were mixed with 1 ml TRIzol and RNA Isolation was carried out as described in section 3.4.1. After the Turbo DNAse and washing steps, the RNA obtained was used for cDNA synthesis and analyzed using qPCR as described in sections 3.4.2 and 3.4.3, respectively.

3.7. Quantification and statistical analysis

All experiments were carried out in at least three independent biological replicates, and qPCR additionally in three technical replicates. The error bars show the standard deviation of biological replicates. Statistical significance was calculated by unpaired, two tailed, unequal variance student´s t-test. The p-values are indicated by * ($p < 0.05$), ** ($p < 0.01$) and *** ($p < 0.001$).

4. RESULTS

4.1. Mex67 interact with snoRNAs *in vivo*

As previously reported, Mex67 is required for the export of mRNAs as well as the ncRNAs *TLC1* and snRNAs to the cytoplasm **(Becker et al., 2019; Wu et al., 2014; Zander and Krebber, 2017)**. Moreover, recent data from RNA sequencing (RNA seq) showed a small cytosolic pool of snoRNAs that decreases in the double mutant *mex67-5 xpo1-1* after a 1 h shift to 37 °C **(Figure 11) (Coban et al. submitted)**.
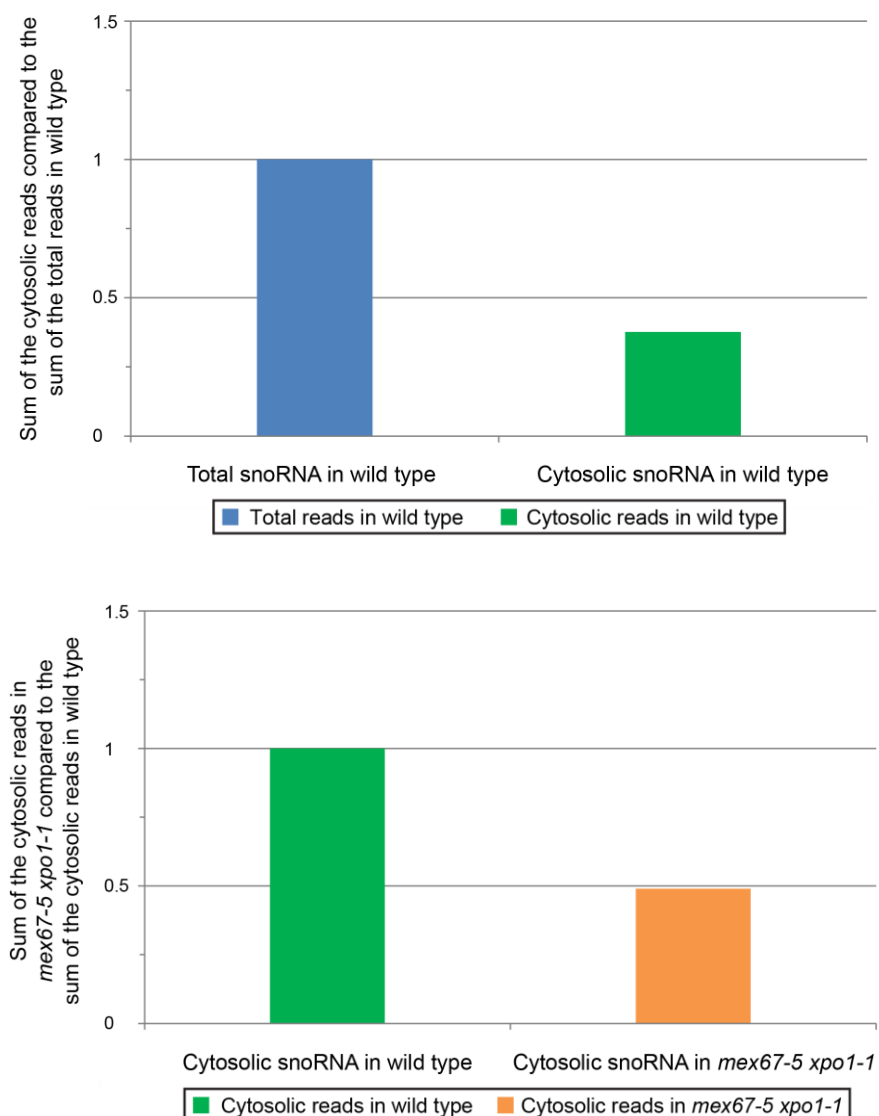
Figure 11: Cytosolic snoRNAs concentration decrease in the double mutant *mex67-5 xpo1-1*. The wild type and the *mex67-5 xpo1-1* strains were shifted for 1 h at 37 °C prior to isolating the cytoplasmic fraction. The RNA was isolated and the sequencing of RNA sample was carried out. **(Coban et al. submitted)**.

Taking into account the results shown in a study that via a transcriptome-wide analysis revealed an interaction between snoRNAs and Mex67 **(Tuck and Tollervey 2012)**, we carried out RNA Co-Immunoprecipitation experiments *in vivo* to confirm if snoRNAs are able to bind the export factor Mex67. In this experiment, the GFP-tagged Mex67 strain was used, and five different snoRNAs were tested: capped C/D snR13, capped C/D U3 (snR17), intronic C/D snR24, uncapped C/D snR68, and capped H/ACA snR42. Following cell lysis, Mex67-GFP was precipitated with GFP beads, and the RNA was isolated, reverse-transcribed, and analyzed via qPCR. To verify that Mex67-GFP was successfully precipitated, a Western blot analysis was carried out. Detection of both the pull down and a control protein was observed **(Figure 12A)**. Specific primers were used to detect the 3'-extended immature form of snoRNAs, which was enriched from 2 to 6 times over the no tag. This indicates that snoRNAs and Mex67 physically interact **(Figure 12B)**. Interestingly, the intronic snR24 has lower binding than the other snoRNAs, despite the fact that its interaction with Mex67 has previously been reported **(Tuck and Tollervey 2012)**.
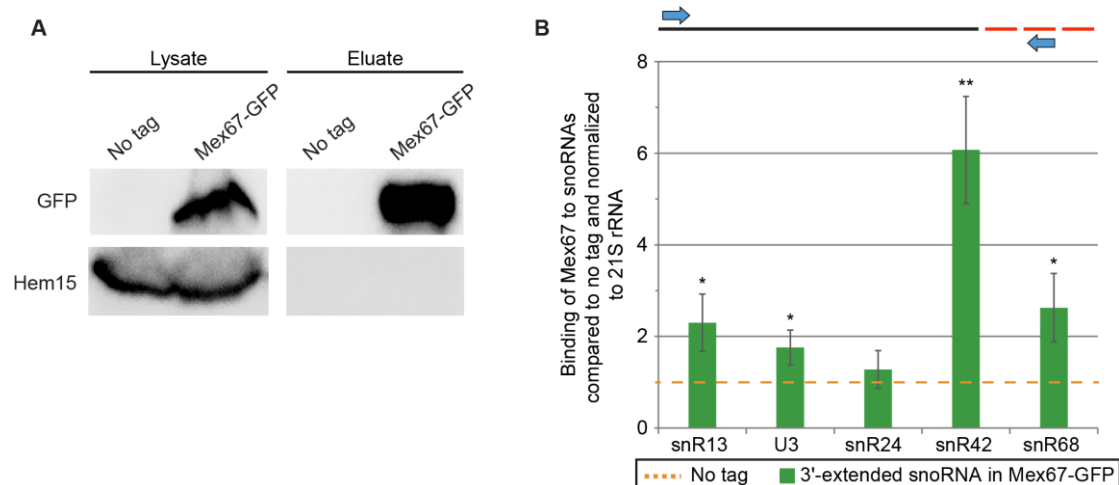
Figure 12: Mex67 physically interact with the snoRNAs *in vivo*. The used strains were grown to mid-log phase prior to cell lysis. Mex67-GFP was precipitated with GFP-beads. Co-immunoprecipitated RNA was isolated, reverse transcribed and analyzed via qPCR. **(A)** Western blot analysis of the immunoprecipitated Mex67-GFP. Hem15 (Ferrochelatase) served as a control for unspecific protein binding to the GFP-beads. Mex67-GFP was detected with a GFP-specific antibody. **(B)** qPCR data shows the binding of 3'-extended snoRNAs to Mex67-GFP compared to no tag. In the upper part, the black line indicates mature snoRNA, the red dashed line indicates the 3'-extensions, and the arrows indicate the positions of the primers used. The error bars represent the standard deviation. p-values were calculated by unpaired two-tailed unequal variance student's t-test (* = $p < 0.05$, ** = $p < 0.01$, *** = $p < 0.001$). n=5

4.2. snoRNAs are exported to the cytoplasm by Mex67

After confirming Mex67 binding to snoRNAs, we wanted to know if snoRNAs could shuttle into the cytosol using this export factor. To answer the question, a fluorescent *in situ* hybridization (FISH) was carried out using the temperature-sensitive strain *mex67-5*. Four different snoRNAs were tested: capped C/D snR13, intronic C/D snR24, uncapped C/D snR68, and capped H/ACA snR42. To carry out this experiment, we used long DIG-labeled RNA probes ranging in size from 100 to 300 nucleotides, depending on the snoRNAs tested, and detected them with a FITC conjugated α-DIG-antibody. Due to the length of the DIG-labeled RNAs, the probes are less likely to penetrate the nuclear envelope, allowing for better visualization of cytoplasmic snoRNAs and possible nuclear snoRNA accumulation **(Becker et al., 2019)**. The used strains were shifted to the restrictive temperature for 1 h before fixation with formaldehyde **(Figure 13)**.
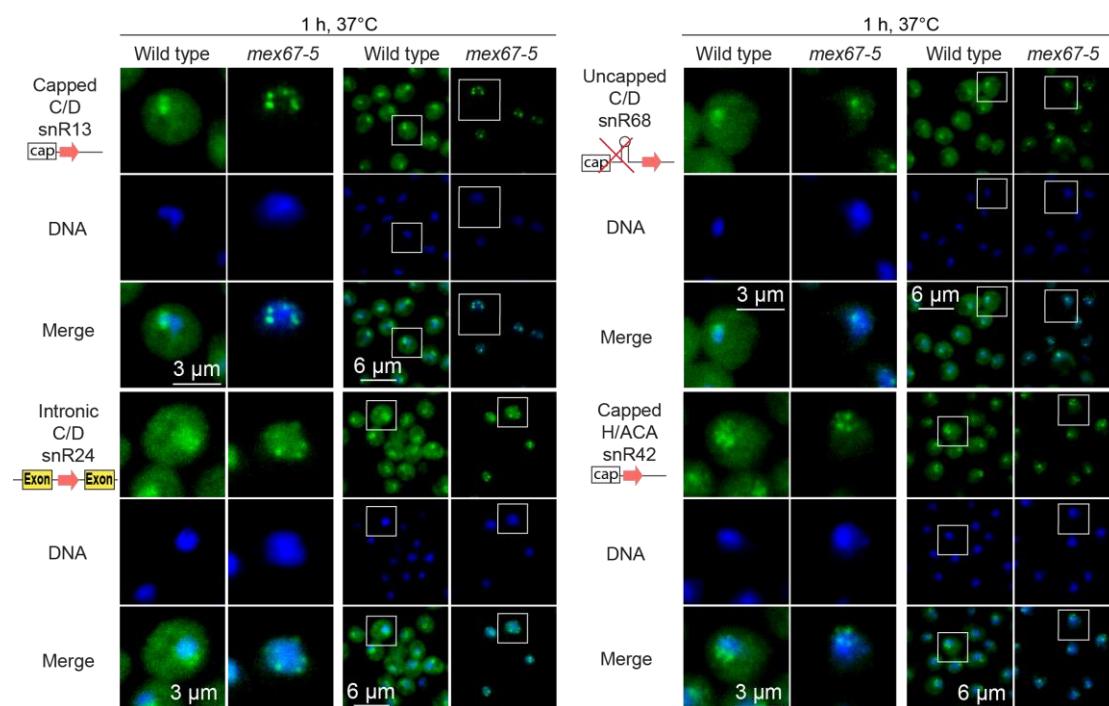
Figure 13: FISH analysis shows snoRNA nuclear export defects in the *mex67-5* mutant strain.
The indicated strains were incubated for 1 h at 37 °C prior to fixation. Cells were fixed with 4 % formaldehyde and snoRNAs were hybridized with 100-300 nucleotide long, DIG-labeled RNA probes and detected via FITC conjugated α-DIG-antibody (green). The DNA was stained with DAPI (blue). The two columns on the right represent the main picture. A cell was chosen from the main picture and placed inside a white square for a close-up shown in the two columns on the left. As a negative control, DIG-labeled RNA probes for antisense snoRNAs were used, see figure 33 appendix.

In wild type strain, the signal for snoRNAs appeared to be distributed throughout the cell, with the highest concentration in the nucleolus. In contrast, *mex67-5* showed significant nuclear retention of snoRNAs. These findings suggest that snoRNAs may leave the nucleus via the export receptor Mex67.

To better understand the effects of the *mex67-5* temperature sensitive phenotype on snoRNAs, we investigated how the relative amounts of different snoRNAs changed in *mex67-5*. Using specific primers, the total snoRNA and the immature 3'-extended form were analyzed. Because the primers used for the total can amplify both the mature and immature forms, the total snoRNA pool includes the immature form. Before cell lysis, the strains were shifted to 37 °C for 1 h. The RNA was then isolated, reverse transcribed, and analyzed via qPCR. In this experiment, the capped C/D U3 snoRNA was also tested. The analysis revealed that the amounts of total and immature snoRNA change differently in *mex67-5* depending on the snoRNA examined **(Figure 14)**.
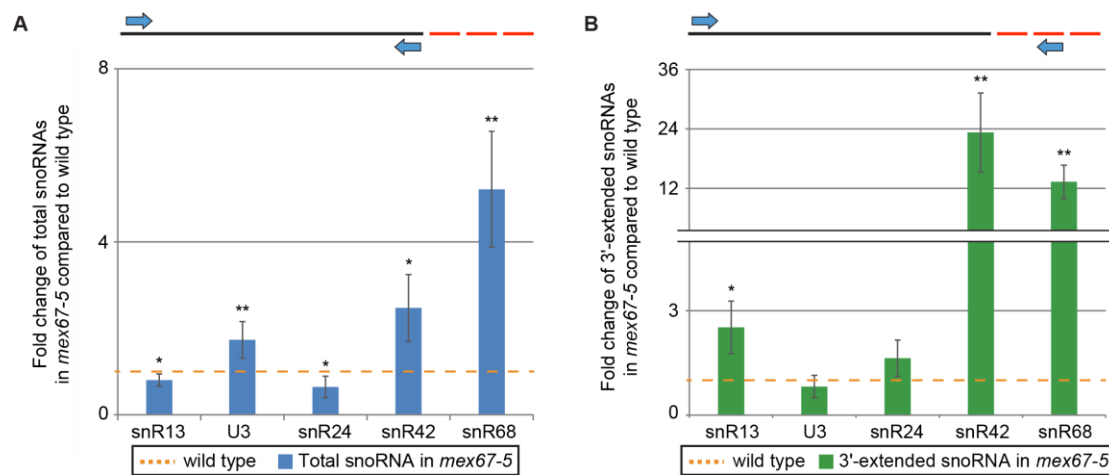
Figure 14: qPCR analysis of snoRNAs in *mex67-5* mutant strain. The indicated strains were incubated for 1 h at 37 °C prior to cell lysis. The total RNA was isolated, reverse transcribed into cDNA and analyzed via qPCR. Data of **(A)** the total or **(B)** the 3'-extended snoRNA was obtained using specific primers. In the upper part, the black line indicates mature snoRNA, the red dashed line indicates the 3'-extensions, and the arrows indicate the positions of the primers used. The error bars represent the standard deviation. p-values were calculated by unpaired two-tailed unequal variance student´s t-test (* = p< 0.05, ** = p< 0.01, *** = p< 0.001); n=4.

For snR42 and snR68, an increase in both total and 3'-extended amounts was observed, indicating that the immature form was stable in this condition and could not be processed or degraded. **(Figure 14)**. Although the total concentration of

snR13 and snR24 decreased slightly, the 3'-extended form increased, possibly due to the inability of new snoRNAs to be processed into the mature form **(Figure 14)**. Because U3 is the only snoRNA whose immature form did not change while increasing the total pool, Mex67 may not play a role in the maturation of this unique snoRNA **(Figure 14)**.

## 4.3. Immature 3'-extended snoRNAs are located in the cytoplasm

Once it was established that some snoRNAs move in the cytoplasm via Mex67 and that inactivation of this export factor causes a change in the concentration of the snoRNAs immature form, we wondered about the effective localization of the 3'-extended snoRNAs. To answer the question, a FISH was carried out using the wild type strain. Three different snoRNAs were tested: capped C/D snR13, capped C/D U3 and capped H/ACA snR42. These snoRNAs were chosen because of their higher expression, which allowed us to detect the immature form.

The probe size for 3'-extended snoRNAs was 200 nucleotides. To carry out this FISH experiment, we used DIG-labeled RNA probes for both mature and 3'-extended snoRNA and detected them with a Cy3 conjugated α-DIG-antibody **(Figure 15B)**. When using the probe for the mature form of snR13 and snR42, we reduced the exposure time until only the nucleolar signal was visible, to remove the cytosolic signal, and the same setting was used for the samples with the probe for the 3'-extended form.

For snR13 and snR42, in contrast to the mature form, which is mostly localized in the nucleolus, the 3'-extended immature form appeared to be distributed all over the cell **(Figure 15A)**.

When U3 was analyzed, it was never to possible identify a cytosolic pool using the probe for the mature form. This could be due to the very high expression of U3 **(Hughes et al., 1987)** that may have impeded the precise identification of the immature snoRNA present in a lower amount. However, when the probe for the 3'-extended form was used, the high expression of this snoRNA in the cell allowed an easy identification of its immature form, which was interestingly present throughout the cell, with a higher localization in the nucleus **(Figure 15A)**.

This data suggests that when in the immature form, the snoRNAs are localized in the cytoplasm and that the cytosolic pool observed in the previous experiment was probably composed mainly of immature snoRNAs.
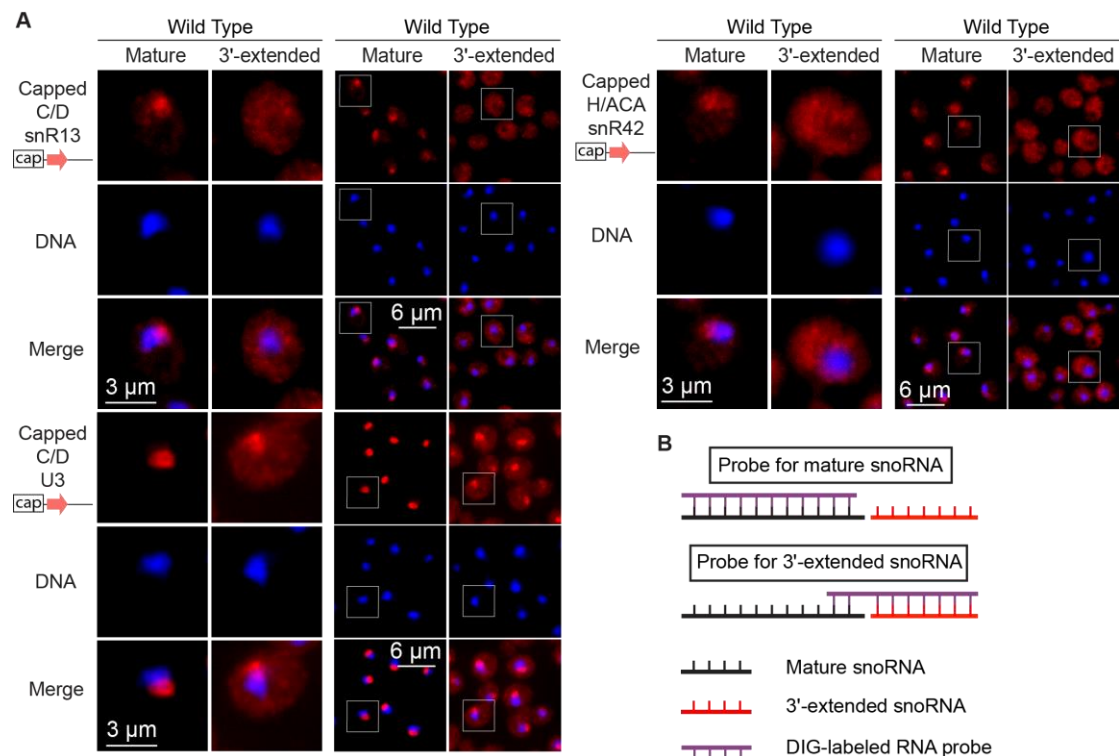
Figure 15: FISH analysis shows that 3'-extended snoRNAs are distributed all over the cell.
Fluorescent *in situ* hybridization analysis was carried out. **(A)** Cells were fixed with 4 % formaldehyde and 3'-extended snoRNAs were hybridized with 200 nucleotide long, DIG-labeled RNA probes and detected via Cy3 conjugated α-DIG-antibody (red). The DNA was stained with DAPI (blue). **(B)** Schematic representation of the snoRNA probes used for the mature and 3'-extended form.

4.4. snoRNAs are re-imported into the nucleus via Cse1 and Mtr10

Because snoRNAs are exported to the cytoplasm, we wanted to investigate how they return to the nucleus. Recently, it was shown for *TLC1* and snRNAs that Cse1 and Mtr10 are involved in the re-import of these non-coding RNAs into the nucleus **(Becker et al., 2019; Hirsch et al., 2021)**. Therefore, we wondered if Cse1 and Mtr10 could also influence snoRNA localization. To investigate this, FISH experiments were carried out in the *cse1-1*, *mtr10Δ* and *cse1-1 mtr10Δ* mutants. The *mtr10Δ* strain was shifted to 37 °C for 1 h, while the *cse1-1* and the double mutant *cse1-1 mtr10Δ* strains were shifted to 16 °C for 1 h and 15 min because their growth defect was strongest at this temperature **(Xiao et al., 1993)**.

Five different snoRNAs were tested: capped C/D U3, intronic C/D snR24 **(Figure 16)**, capped C/D snR13, uncapped C/D snR68 and capped H/ACA snR42 **(Figure 17)**. For labeling of the snoRNAs, we used a short, 30 nucleotide long, DNA-probe that was conjugated with Cy3 at its 5'- and 3'-ends. Short probes were used because they could penetrate the nucleus and stain the nucleolar snoRNAs more effectively, allowing us to easily identify any cytosolic snoRNA accumulation.
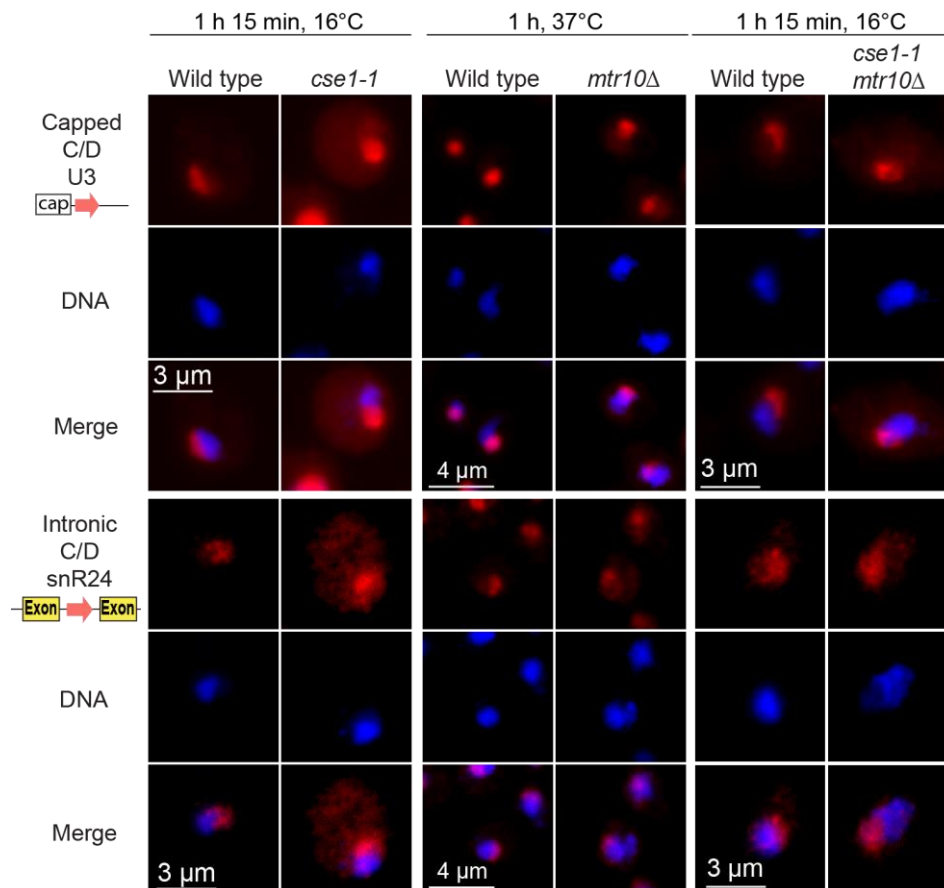
Figure 16: FISH analysis shows that Cse1 and Mtr10 do not block the re-import of U3 and snR24. FISH analysis was carried out after shifting to 37 °C or 16 °C for the indicated times. Cells were fixed with 4 % formaldehyde and snoRNAs were hybridized with 30 nucleotide long, Cy3-labelled probes (red). DNA was stained with DAPI (blue).

In wild type cells, all snoRNAs are mostly found in the nucleolus, whereas mutant strains show different results depending on the snoRNAs examined. We observed that U3 and snR24 showed no localization defects in the mutant strains **(Figure 16)**. For this reason, we decided to not continue to work with the intronic snR24. However, unlike the intronic snR24, the very high expression and long half-life of U3 may have impeded the potential cytoplasmic localization of this snoRNA. Moreover, U3 is one of the most important snoRNAs and it is highly conserved and studied in

many different organisms, including humans. For this reason, we decided to continue investigating U3.
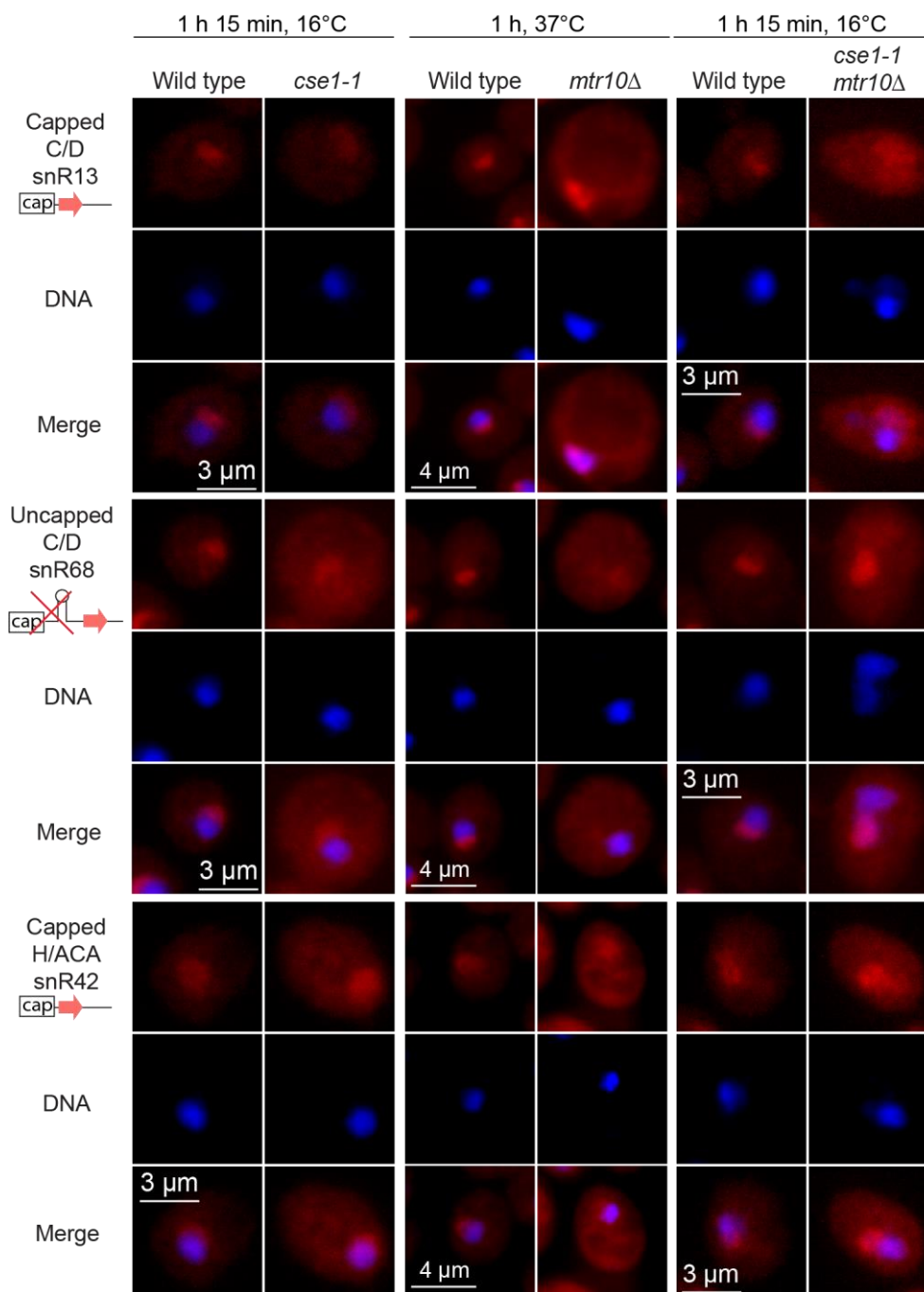
Figure 17: snR13, snR68 and snR42 mislocalize to the cytoplasm in the *cse1-1*, *mtr10Δ* and *cse1-1 mtr10Δ* mutants. FISH analysis was carried out after shifting to 37 °C or 16 °C for the indicated times. Cells were fixed with 4 % formaldehyde and snoRNAs were hybridized with 30 nucleotide long, Cy3-labelled probes (red). DNA was stained with DAPI (blue).

For snR13, snR68, and snR42, we identified that when mutated, Cse1 and Mtr10 caused a cytoplasmic accumulation of snoRNAs **(Figure 17)**. For snR13, only *mtr10Δ* mutants mislocalize the snoRNA to the cytoplasm, whereas both single mutants

cause cytoplasmic accumulation for both snR68 and snR42. When the double mutant *cse1-1 mtr10Δ* was used, all three snoRNAs showed a cytosolic mislocalization that appeared to be stronger than that observed in single mutants.

The cytoplasmic increase in the mutant strains for these snoRNAs suggests that these two karyopherins are important for snoRNA nuclear re-import.

Because of the results obtained, we investigated how the amounts of snoRNAs changed in these import factor mutants. Using specific primers, the total snoRNA and the immature 3'-extended form were analyzed. After shifting *cse1-1* to 16 °C for 1 h and 15 min, and *mtr10Δ* to 37 °C for 1 h, the strains were lysed, the RNA was isolated, reverse transcribed, and then analyzed via qPCR **(Figure 18)**.
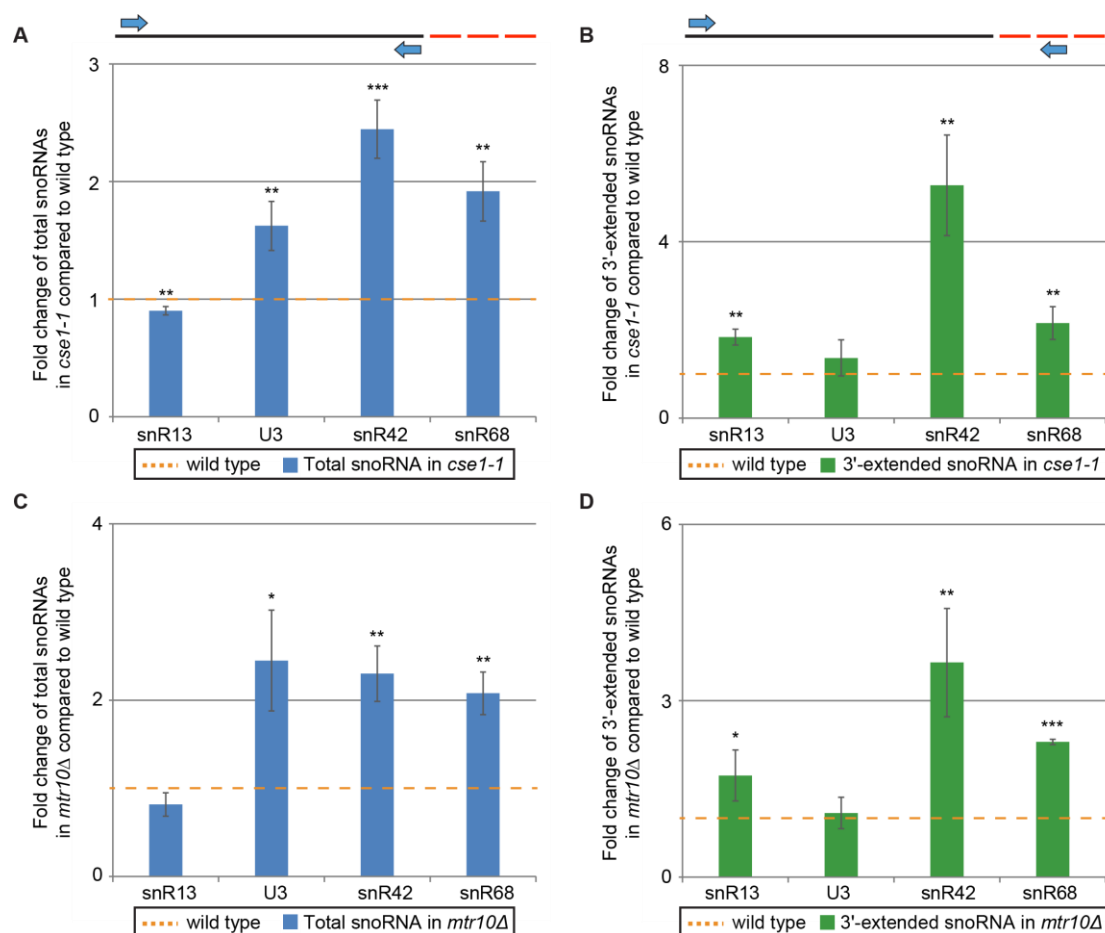
Figure 18: qPCR analysis of snoRNAs in *cse1-1* and *mtr10Δ* mutant strain. The indicated strains were incubated for 1 h at 37 °C for *mtr10Δ* and for 1 h 15 min at 16 °C for *cse1-1*. After cell lysis, the total RNA was isolated, reverse transcribed into cDNA and analyzed via qPCR. Data of **(A and C)** the total or **(B and D)** the 3'-extended snoRNAs was obtained using specific primers. In the upper part, the black line indicates mature snoRNA, the red dashed line indicates the 3'-extensions, and the arrows indicate the positions of the primers used. The error bars represent the standard deviation. p-values were calculated by unpaired two-tailed unequal variance student´s t-test (* = p< 0.05, ** = p< 0.01, *** = p< 0.001); n=3

In both *cse1-1* and *mtr10Δ*, the total amount was significantly enriched for all snoRNAs, excluding snR13, whose concentration remained unchanged **(Figure 18A and C)**. The 3'-extended snoRNAs also accumulated in these mutants, but in this case, the concentration of snoRNA U3 held steady, with only a slight increase in *cse1-1* **(Figure 18B and D)**. Only U3 exhibits a different pattern, with the increase in concentration appearing to be probably composed of the mature form.

To further confirm our results, we carried out cytoplasmic fractionation experiments in the *cse1-1 mtr10Δ* double mutant strain **(Figure 19)**.
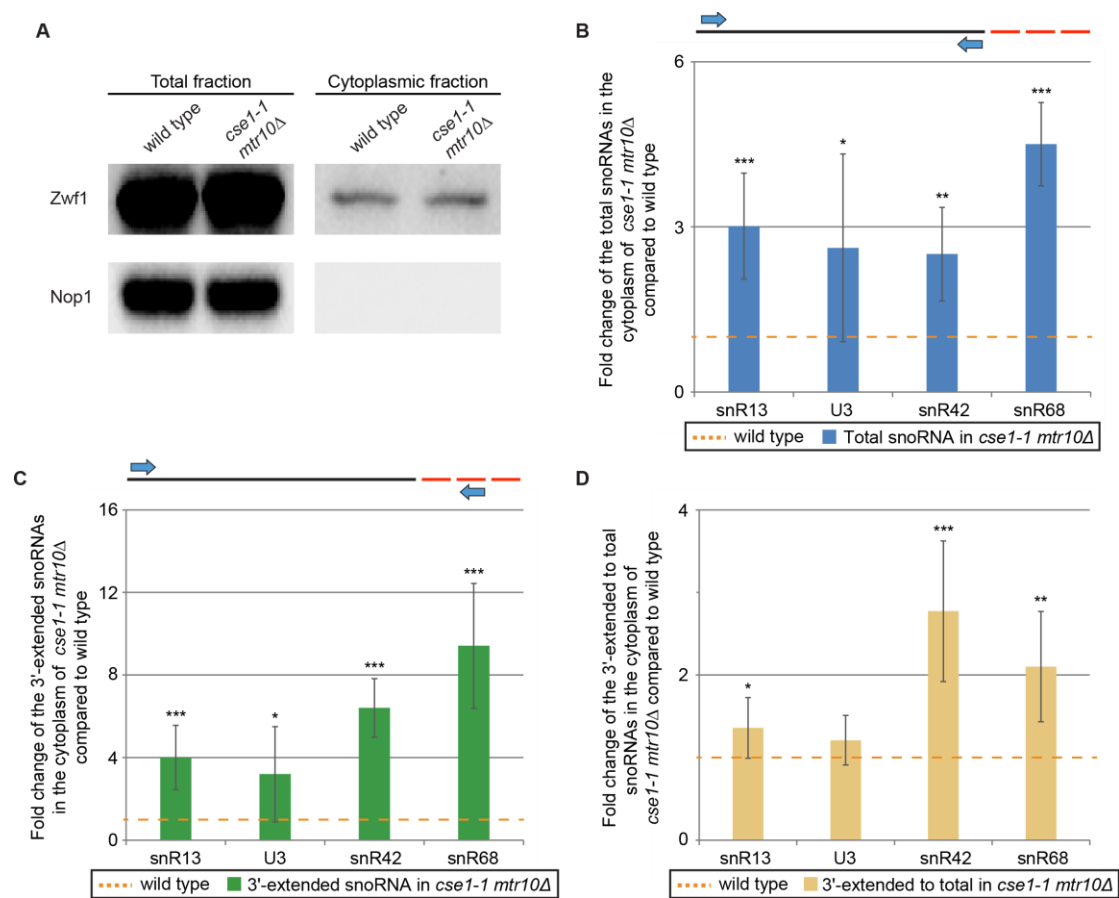
Figure 19: snoRNAs amount increases in the cytoplasmic fractions of *cse1-1 mtr10Δ*. The *cse1-1 mtr10Δ* strain was incubated for 1 h and 15 min at 16 °C prior to isolating the cytoplasmic fraction. **(A)** Western blot analysis of the cytoplasmic fractionation. The total and cytoplasmic fractions were analyzed by detecting the cytoplasmic protein Zwf1 and the nucleolar protein Nop1. **(B - D)** qPCR data that show the cytosolic amount of **(B)** total snoRNAs, **(C)** 3'-extended snoRNAs, and **(D)** the ratio of 3'-extended to total snoRNAs level. In the upper part, the black line indicates mature snoRNA, the red dashed line indicates the 3'-extensions, and the arrows indicate the positions of the primers used. The error bars represent the standard deviation. p-values were calculated by the unpaired two-tailed unequal variance student´s t-test (* = p< 0.05, ** = p< 0.01, *** = p< 0.001); n= 6

Four different snoRNAs were tested: capped C/D snR13 capped C/D U3, uncapped C/D snR68, and capped H/ACA snR42. Isolation of the cytoplasmic fraction was carried out after a temperature shift to 16 °C for 1 h and 15 min. As a control for the successful isolation of the cytoplasmic fraction, a Western blot analysis was conducted **(Figure 19A)** to detect the cytoplasmic protein Zwf1 (Glucose-6-phosphate dehydrogenase) and the nucleolar protein Nop1 (Histone glutamine methyltransferase).

The RNA was isolated from the cytoplasmic fraction, reverse transcribed into cDNA and analysed via qPCR **(Figure 19)**. Both, total and 3'-extended snoRNAs accumulate in the cytoplasm of the *cse1-1 mtr10Δ* double mutant, with a higher enrichment of the 3'-extended form **(Figure 19B and C)**. Therefore, it is possible that snoRNAs are mostly exported in their immature form. However, the ratio of the 3'-extended to total snoRNAs in the cytoplasmic fraction shows a significant increase only for snR42 and snR68, while the two capped C/D snR13 and U3 have almost no increment **(Figure 19D)**.

These results suggest that *cse1-1* and *mtr10Δ* are important for snoRNA nuclear re-import and that snR42 and snR68 accumulate in the cytoplasm of this mutant in the 3'-extended form, unlike snR13 and U3, which do not show a predominance of the immature form. However, even though for snR13 and U3 we could not confirm the exclusive presence of the 3'-extended form, we have to remember that when using the primer for the total snoRNAs, the pool includes both the immature and the mature form. Therefore, we cannot totally exclude the possibility that these capped C/D snoRNAs are also mostly exported in their immature form.

4.5. Lsm8 binds all snoRNAs *in vivo*

An important component for the maturation of non-coding RNAs *TLC1* and snRNAs is the Sm-ring **(Becker et al., 2019; Hirsch et al., 2021)**, with the exception of snRNA U6 that binds the Lsm2-8 complex **(Achsel et al., 1999)**. An interaction with the Lsm-ring was also shown for two snoRNAs. The pre-snoRNA U3 is able to bind the Lsm2-8 complex **(Kufel et al., 2003b)**, while snR5 can bind a peculiar form of the Lsm-ring containing only six proteins, the Lsm2-7 complex **(Fernandez et al., 2004)**. Because

of the importance of the Lsm-ring on the snRNA U6 and the finding that two snoRNAs can bind this complex, we wanted to determine if other snoRNAs are also able to interact with the Lsm2-8 complex. Therefore, we carried out RNA Co-Immunoprecipitation experiments *in vivo* to confirm if other snoRNAs are able to bind Lsm8. In this experiment, the GFP-tagged Lsm8 strain was used, and eight different snoRNAs were tested. Following cell lysis, Lsm8-GFP was precipitated using GFP beads, and the RNA was isolated, reverse transcribed, and analyzed via qPCR. A Western blot analysis was used to control the successful precipitation of the Lsm8-GFP **(Figure 20A)**. Specific primers were used to detect the 3'-extended immature form of snoRNAs, which was enriched from 2 to 100 times compared to no tag. The values dramatically change depending on the snoRNA analysed **(Figure 20B)**.
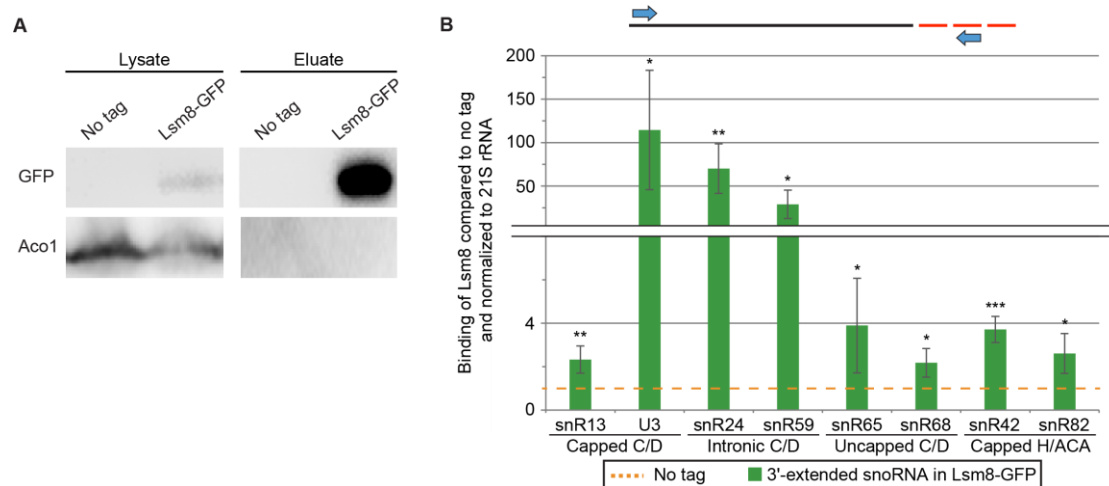
Figure 20: Lsm8 physically interact with the snoRNAs *in vivo*. The used strains were grown to mid-log phase prior to cell lysis. Lsm8-GFP was precipitated with GFP-beads. Co-immunoprecipitated RNA was isolated, reverse transcribed and analyzed via qPCR. **(A)** Western blot analysis of the immunoprecipitated Lsm8-GFP. Aco1 (Aconitase 1) served as control for unspecific protein binding to the GFP-beads. Lsm8-GFP was detected with a GFP-specific antibody. **(B)** qPCR data shows the binding of 3'-extended snoRNAs to Lsm8-GFP compared to no tag. In the upper part, the black line indicates mature snoRNA, the red dashed line indicates the 3'-extensions, and the arrows indicate the positions of the primers used. The error bars represent the standard deviation. p-values were calculated by unpaired two-tailed unequal variance student´s t-test (* = p< 0.05, ** = p< 0.01, *** = p< 0.001). n=3

The majority of snoRNAs have an enrichment of 2 to 4 times, but U3 and intronic snoRNAs show a stronger binding. For U3, this can be explained by its high expression, as it turns out to be one of the most abundant RNA molecules in *S. cerevisiae*, constituting about 0.06% of the total yeast RNA, which corresponds to about 400-1000 copies per cell **(Hughes et al., 1987)**. For intronic snoRNAs, it was shown that Lsm2-8 can bind the pre-mRNA containing the intronic snoRNA **(Kufel et**

al, 2004), which could increase the fold enrichment of the RIP experiment because the primers used cannot distinguish between snoRNA that is part of an intron and snoRNA that has undergone splicing.

4.6. Lsm2-8 is involved in snoRNA nuclear import

Because it has been previously shown that Lsm2-8 can bind different snoRNAs and that Lsm8 is important for nuclear re-import of U6 **(Becker et al., 2019)**, we carried out fluorescent *in situ* hybridization experiments to identify whether Lsm8 is also important for nuclear re-import of the snoRNAs. A FISH experiment was carried out using the temperature sensitive *lsm8-1* mutant strain, which leads to an Lsm-ring assembly defect **(Figure 21) (Pannone et al., 1998)**.
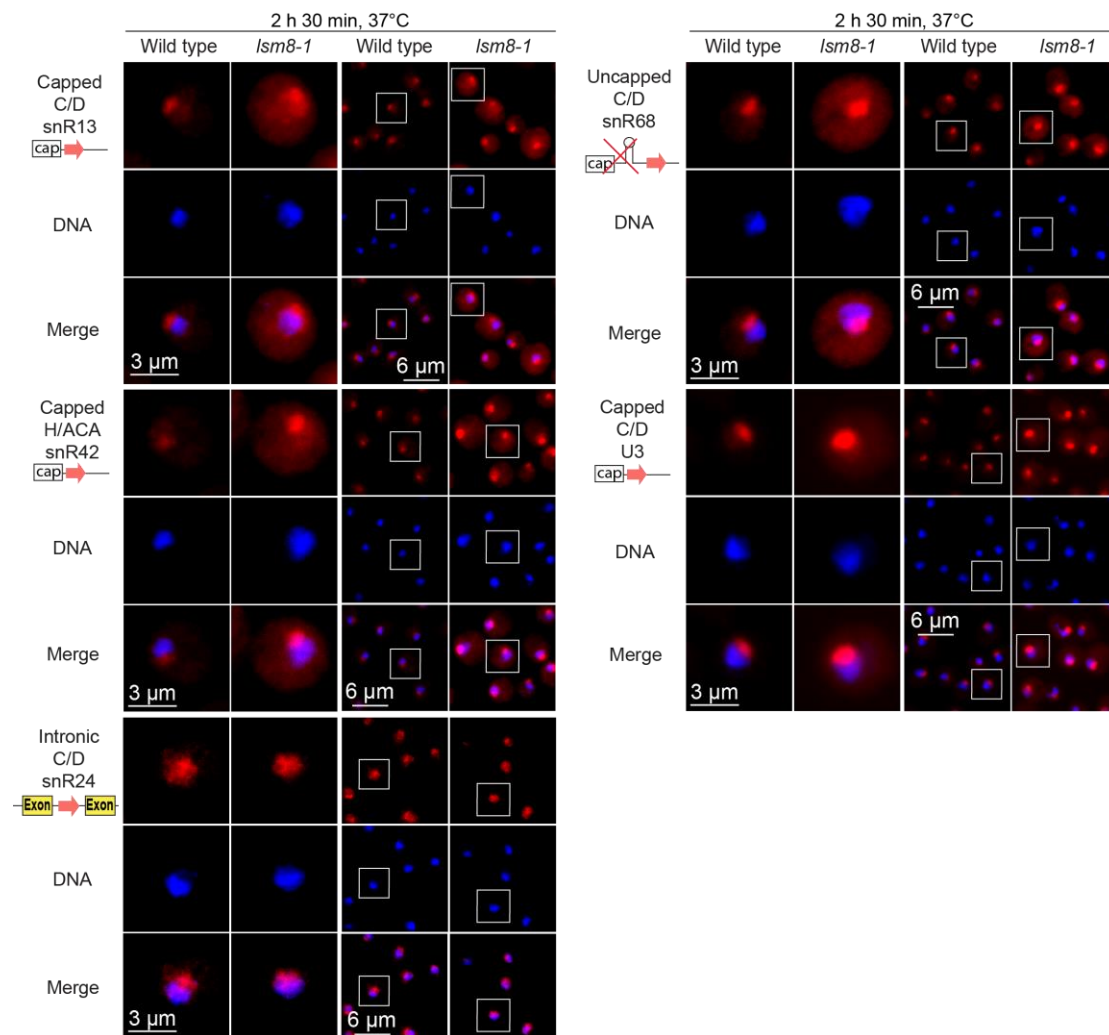
Figure 21: Defects in Lsm2-8 complex assembly lead to a cytoplasmic accumulation of snR13, snR68 and snR42. FISH analysis was carried out after incubation to 37 °C for the indicated times. Cells were fixed with 4 % formaldehyde and snoRNAs were hybridized with 30 nucleotide long, Cy3-labelled probes (red). DNA was stained with DAPI (blue).

The used strains were shifted to 37 °C for 2 h and 30 min before fixation with formaldehyde. Five different snoRNAs were tested: capped C/D snR13, capped C/D U3, intronic C/D snR24, uncapped C/D snR68 and capped H/ACA snR42. For staining of the snoRNAs, we used a short, 30 nucleotide long, DNA-probe that was conjugated with Cy3 at its 5'- and 3'-ends **(Figure 21)**.

For snR13, snR68 and snR42, the *lsm8* mutation resulted in a cytoplasmic enrichment of these snoRNAs. This result suggest that the Lsm2-8 complex could be involved in the re-import of snoRNAs. The mutated strain had no effect on intronic snR24 localization, which, when combined with the findings in **Figure 16**, suggests that intronic snoRNAs may have a different maturation pathway than the other snoRNAs studied. U3 also did not show a mislocation in *lsm8-1*, but its very high expression and long half-life of U3 may have impeded the potential cytoplasmic localization of this snoRNA. Therefore, we decided to keep looking into U3.

To confirm this result, we carried out cytoplasmic fractionation experiments in the *lsm8-1* mutant strain. Four different snoRNAs were tested: capped C/D snR13 capped C/D U3, uncapped C/D snR68, and capped H/ACA snR42.

Isolation of the cytoplasmic fraction was carried out after a temperature shift to 37 °C for 2 h and 30 min. As a control for the correct isolation of the cytoplasmic fraction, the cytoplasmic protein Zwf1 and the nucleolar protein Nop1 were detected by Western blot **(Figure 22A)**.

The cytosolic RNA was isolated, reverse transcribed into cDNA and analysed via qPCR **(Figure 22)**. Both total and 3'-extended snoRNAs accumulate in the cytoplasm of the *lsm8-1* mutant, with a higher increase of the 3'-extended form for snR13 and snR42, while for U3 and snR68, an increase of the same level was visible for both tested forms **(Figure 22B and C)**. When analyzing the ratio of the 3'-extended to total snoRNAs in the cytoplasmic fraction **(Figure 22D)**, there was a visible enrichment only for snR13 and snR42.

From these results, it is possible to deduce that in *lsm8-1* there is an increase in the cytosolic concentration of all tested snoRNAs. This enrichment appears to be higher in the 3'-extended form for capped C/D snR13 and the capped H/ACA snR42, so it is possible that these two snoRNAs are mostly exported in their immature form. However, for capped C/D U3 and uncapped C/D snR68, it is not possible to deduce

which form, whether mature or 3'-extended, is more abundant in the cytoplasmic fraction. Regardless of the detectable form, an increase in the cytosolic concentration of snoRNAs is visible when the Lsm-ring assembly is defective, providing further evidence that this complex may be involved in snoRNA re-import. Furthermore, the Lsm2-8 complex appears to be able to bind Cse1 and Mtr10 **(Wang X. and Krebber H., personal communication)**, similar to the Sm-ring **(Becker et al., 2019)**, thus increasing the possibility that the Lsm ring is involved in the re-import of snoRNAs.
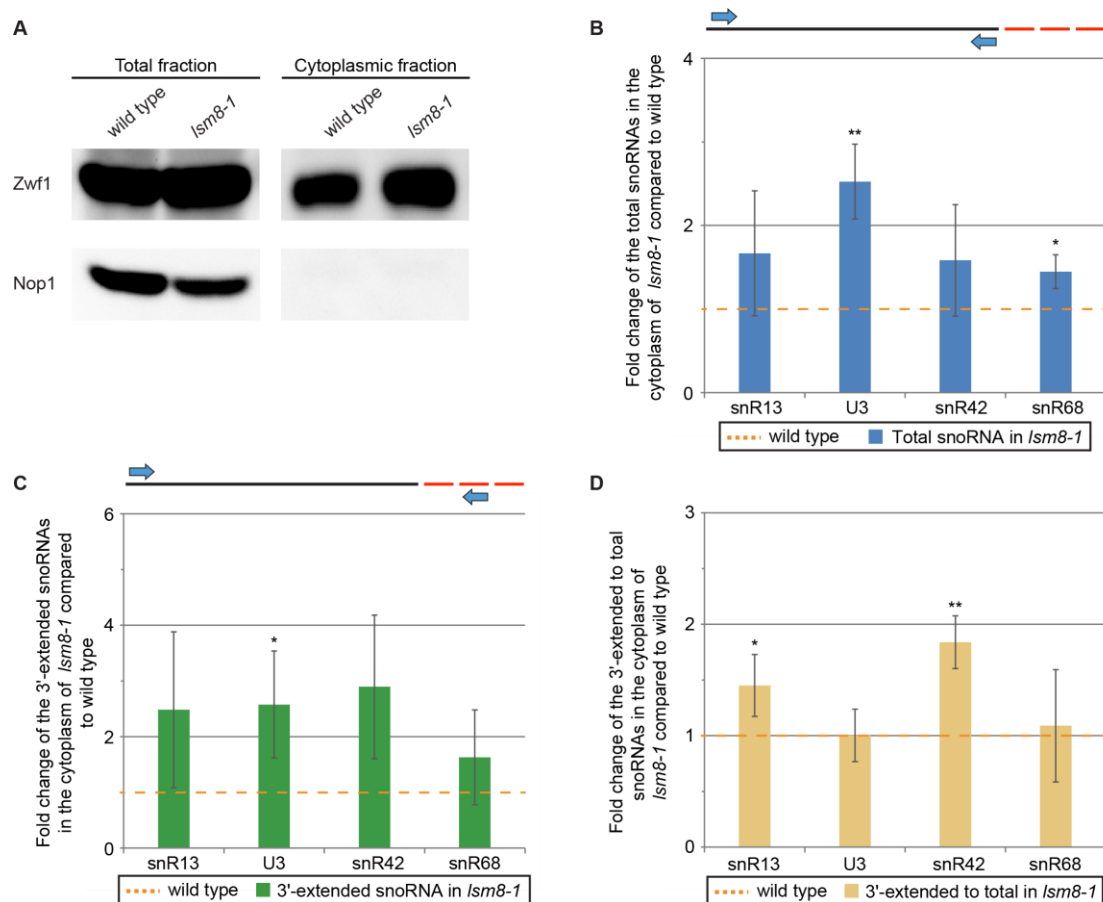
Figure 22: snoRNAs amount increases in the cytoplasmic fractions of *lsm8-1*. The *lsm8-1* strain was incubated for 2 h and 30 min at 37 °C prior to isolating the cytoplasmic fraction. **(A)** Western blot analysis of the cytoplasmic fractionation. The total and cytoplasmic fractions were analysed by detecting the cytoplasmic protein Zwf1 and the nucleolar protein Nop1. **(B - D)** qPCR data that show the cytosolic amount of **(B)** total snoRNAs, **(C)** 3'-extended snoRNAs, and **(D)** the ratio of 3'-extended to total snoRNAs level. In the upper part, the black line indicates mature snoRNA, the red dashed line indicates the 3'-extensions, and the arrows indicate the positions of the primers used. The error bars represent the standard deviation. p-values were calculated by the unpaired two-tailed unequal variance student´s t-test (* = p< 0.05, ** = p< 0.01, *** = p< 0.001); n= 3

4.7. Lsm2-8 assembles on snoRNAs in the nucleus, excluding for U3

Because for non-coding RNAs, *TLC1* and snRNAs, it has been shown that binding of the Sm-ring occurs during the cytosolic step of the maturation pathway **(Becker et al., 2019; Vasianovich et al., 2020)**, we wanted to fins out if binding between the Lsm2-8 complex and snoRNAs occurs during the cytosolic step. Therefore, RIP of Lsm8-GFP was carried out in different mutant strains, including *mex67-5* in order to trap the snoRNAs in the nucleus, as well as *cse1-1* and *mtr10Δ* to accumulate snoRNAs in the cytosol. In all the RNA co-immunoprecipitations carried out, specific primers were used to detect the 3'-extended immature form of snoRNAs.

When the *mex67-5* strain was used, the main culture of both the wild type and mutant strains was shifted for 1 h at 37 °C before harvesting. Following the cell lysis and Lsm8-GFP precipitation via GFP-beads, the protein precipitation was analysed via Western blot **(Figure 23A)**, while the RNA was isolated, reverse transcribed into cDNA and analysed by qPCR **(Figure 23B)**.
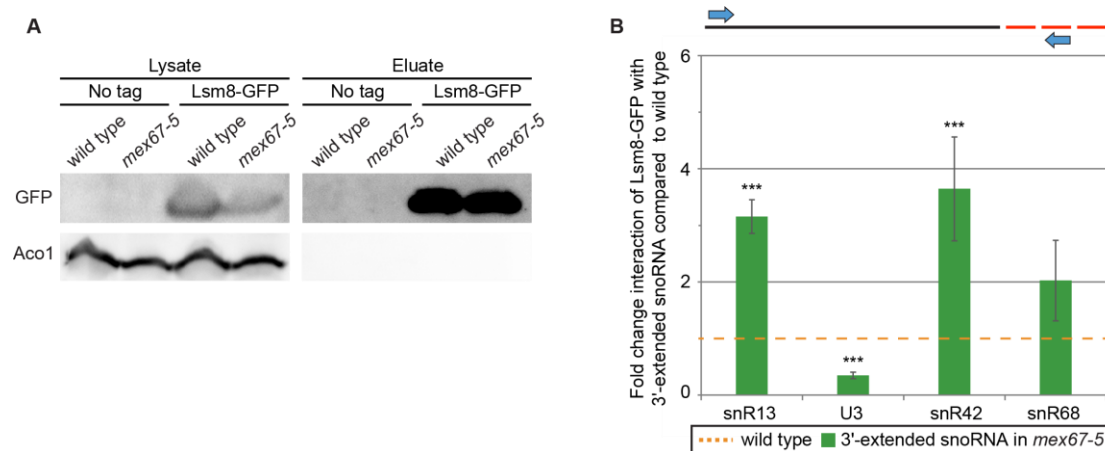
Figure 23: Binding of Lsm8 to snoRNAs change in *mex67-5* mutant. All strains used were grown to mid-log phase and shifted to the restrictive temperature prior cell lysis. Lsm8-GFP was precipitated with GFP-beads. The RNA co-immunoprecipitated was isolated, reverse transcribed and analyzed via qPCR. **(A)** Western blot analysis of the immunoprecipitated Lsm8-GFP. Aco1 served as control for unspecific binding. Lsm8-GFP was detected with a GFP-specific antibody. **(B)** qPCR data shows the binding of 3'-extended snoRNAs to Lsm8-GFP in *mex67-5* compared to the wild type. In the upper part, the black line indicates mature snoRNA, the red dashed line indicates the 3'-extensions, and the arrows indicate the positions of the primers used. The error bars represent the standard deviation. p-values were calculated by unpaired two-tailed unequal variance student´s t-test (* = p< 0.05, ** = p< 0.01, *** = p< 0.001). n=3

It was observed that in the mutant strain *mex67-5*, the amount of binding between Lsm8 and snR13, snR42, and snR68 increased by 2 - 3 times, in contrast to U3, which

showed a decrease in binding of ~ 65 %. This result indicated that U3 is the only snoRNA tested that most likely binds the Lsm2-8 complex in the cytosol as opposed to the other snoRNAs that bind the Lsm-ring in the nucleus.

The next step was to confirm the Lsm8 binding in the mutant strains *cse1-1* and *mtr10Δ* where snoRNAs tend to accumulate in the cytosol.

For the RIP experiment with *mtr10Δ*, the main culture was harvested and a Western blot analysis was used to ensure that the precipitation was successful **(Figure 24A)**, while immunoprecipitated RNA was isolated, reverse transcribed into cDNA, and analyzed using qPCR **(Figure 24B)**.

The qPCR analysis showed that in this case, the amount of binding of all snoRNAs with Lsm8 increased by 2 - 6 times depending on the snoRNAs examined. However, the high error bar for U3 prevents us from having a clear picture of this snoRNA. This result could confirm that for U3, the binding with the Lsm2-8 complex takes place in the cytosol, while for the other snoRNAs analyzed, blocking the re-import probably prevents the Lsm-ring dissociation from the snoRNA, as it is not part of the mature snoRNP.
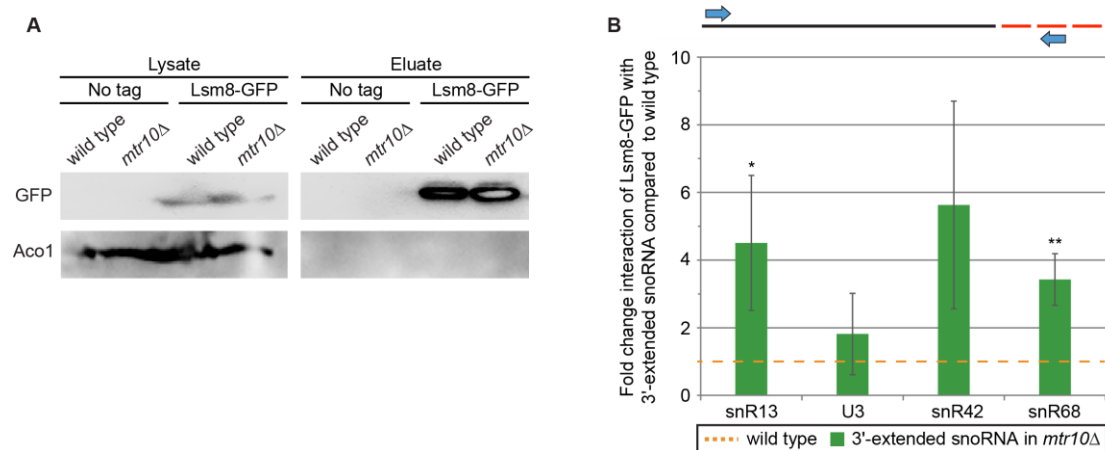
Figure 24: Binding of Lsm8 to snoRNAs increase in *mtr10Δ* mutant. All strains used were grown to mid-log phase and harvested prior cell lysis. Lsm8-GFP was precipitated with GFP-beads. The RNA co-immunoprecipitated was isolated, reverse transcribed and analyzed via qPCR. **(A)** Western blot analysis of the immunoprecipitated Lsm8-GFP. Aco1 served as control for unspecific binding. Lsm8-GFP was detected with a GFP-specific antibody. **(B)** qPCR data shows the binding of 3'-extended snoRNAs to Lsm8-GFP in *mtr10Δ* compared to the wild type. In the upper part, the black line indicates mature snoRNA, the red dashed line indicates the 3'-extensions, and the arrows indicate the positions of the primers used. The error bars represent the standard deviation. p-values were calculated by unpaired two-tailed unequal variance student´s t-test (* = p< 0.05, ** = p< 0.01, *** = p< 0.001). n=3

For the RIP experiment with *cse1-1*, the main culture was shifted at 16 °C for 1h and 15 min before harvest and lysis. The correct protein precipitation was confirmed via Western blot analysis **(Figure 25A)**, while immunoprecipitated RNA was isolated, reverse transcribed into cDNA, and analyzed using qPCR **(Figure 25B)**.

In contrast to the previous result obtained in *mtr10Δ*, binding decreased for all snoRNAs in *cse1-1*, with the exception of snR13, which showed a slight increase **(Figure 25B)**. However, due to the large disparity in the results obtained in the individual tests, the binding increase of snR13 with Lsm8 cannot be established with certainty. The same issue was found for the other snoRNAs, even though the trend of the individual results always showed a decrease in binding.
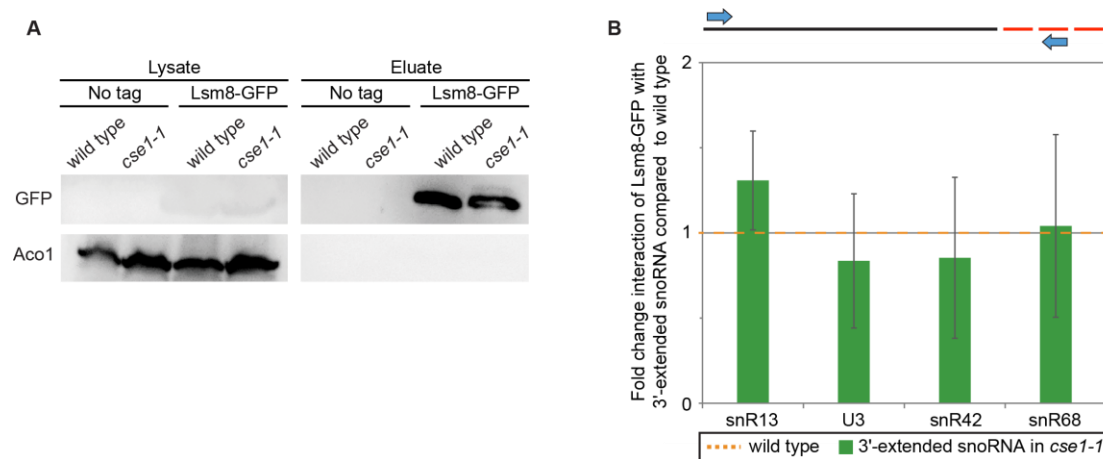
Figure 25: Binding of Lsm8 to snoRNAs decrease in *cse1-1* mutant. All strains used were grown to mid-log phase and shifted to the restrictive temperature prior cell lysis. Lsm8-GFP was precipitated with GFP-beads. The RNA co-immunoprecipitated was isolated, reverse transcribed and analyzed via qPCR. **(A)** Western blot analysis of the immunoprecipitated Lsm8-GFP. Aco1 served as control for unspecific binding. Lsm8-GFP was detected with a GFP-specific antibody. **(B)** qPCR data shows the binding of 3'-extended snoRNAs to Lsm8-GFP in *cse1-1* compared to the wild type. In the upper part, the black line indicates mature snoRNA, the red dashed line indicates the 3'-extensions, and the arrows indicate the positions of the primers used. The error bars represent the standard deviation. p-values were calculated by unpaired two-tailed unequal variance student´s t-test (* = p< 0.05, ** = p< 0.01, *** = p< 0.001). n=3

Although both Mtr10 and Cse1 proteins bind Lsm8 and appear to be involved in snoRNAs re-import, only *mtr10Δ* increased the binding between snoRNAs and Lsm8. This event can be explained by the hypothesis that Cse1 is involved in the stabilization of the Sm-ring **(Hirsch et al., 2021)** and, therefore, could have a similar role for the Lsm-complex.

4.8. *tr4Δ* causes snoRNA transcription termination over the NNS site and increases the cytosolic concentration of the snoRNAs

The transcription termination of independently transcribed snoRNAs in *S. cerevisiae* is mainly mediated by the NNS (Nrd1-Nab3-Sen1) complex. However, snoRNA termination can also occur at a second site where only the mRNA transcription termination factors CPF-CFI complex act. Interestingly, when the Trf4 factor of the TRAMP complex is deleted, snoRNA termination shifts to the second transcription termination site **(Figure 6) (Grzechnik et al., 2008)**. Although a "fail safe" function for the second termination site was proposed, the precise role of this additional termination site is unknown. To gain insight into the role of this second termination site, we used the mutant strain *trf4Δ* to analyze the amount of snoRNAs transcribed via the second termination site **(Figure 26)**.
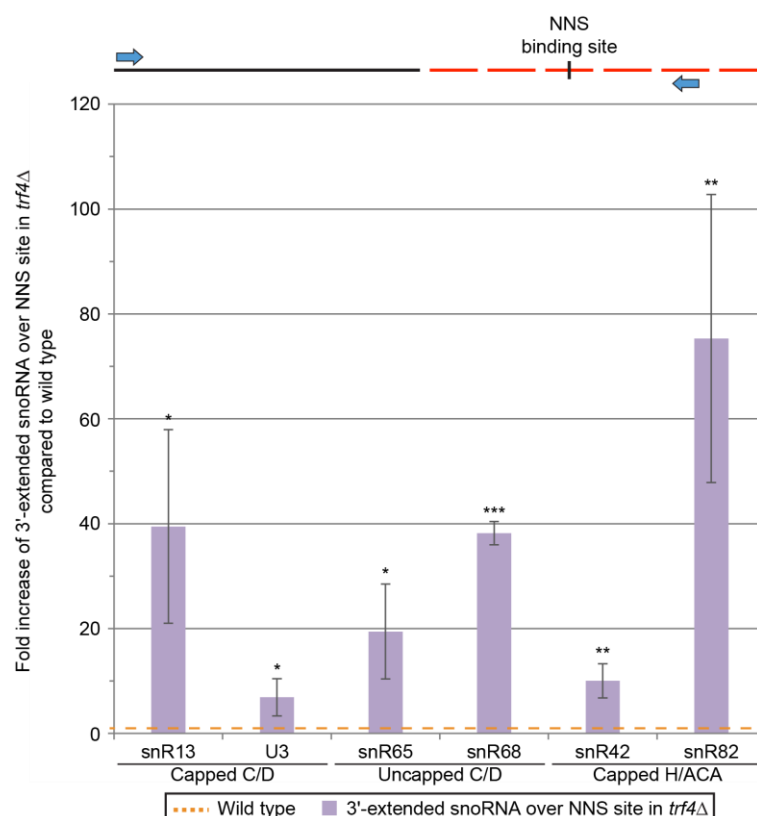
Figure 26: qPCR analysis of snoRNAs in a *trf4Δ* mutant strain shows an enrichment of snoRNAs that overcome the NNS termination site. The indicated strains were grown to mid-log phase prior to cell lysis. Total RNA was isolated, reverse transcribed into cDNA and analyzed via qPCR. qPCR data of the snoRNAs terminated over the NNS site was obtained using specific primers. In the upper part, the black line indicates mature snoRNA, the red dashed line indicates the 3'-extensions, and the arrows indicate the positions of the primers used. The error bars represent the standard deviation. p-values were calculated by unpaired two-tailed unequal variance student´s t-test (* = p< 0.05, ** = p< 0.01, *** = p< 0.001). n= 3

The snoRNA that terminate in the second site, were analyzed using specific primers where the reverse primer bind a snoRNA region that is over the NNS binding site. The used strains were lyzed, and then the RNA was isolated, reverse transcribed, and finally analyzed via qPCR. Analysis revealed that the amount of snoRNAs that skipped the NNS termination site increased for all targets tested, from 6 times for U3 to 75 times for snR82 **(Figure 26)**.

This result shows that snoRNAs in *trf4Δ* cannot terminate transcription at the NNS site and that probably the transcription termination occurs at the second site, where the CPF-CFI complex is used.

After confirming that most snoRNAs in *trf4Δ* terminate the transcription at the second site, we wanted to examine the localization of these snoRNAs to see if there was a change in their cytosolic concentration. To achieve this goal, a cytoplasmic fractionation experiment in the *trf4Δ* mutant strain was carried out. Four different snoRNAs were tested: capped C/D snR13, capped C/D U3, uncapped C/D snR68, and capped H/ACA snR42. The correct isolation of the cytosolic fraction was tested by detecting, via Western blot, the cytoplasmic protein Zwf1 and the nucleolar protein Nop1 **(Figure 27A)**. The cytosolic RNA was isolated, reverse transcribed into cDNA and analysed via qPCR **(Figure 27)**.

Among the snoRNAs analysed, U3 was the only one to remain unaffected when the primers for the total were used, but it showed an increase of 2 times of the immature form. For all the other snoRNAs tested, it was observed in both forms a huge increase in their cytosolic concentration, especially for the 3'-extended form, where it was visible an increase of between 20 – 60 times **(Figure 27B and C)**. Furthermore, the ratio of 3'-extended to total snoRNA present in the cytoplasm was enriched for all snoRNAs tested in *trf4Δ,* meaning that the immature form is probably the most abundant in the cytoplasm of this mutant strain **(Figure 27D)**.

These results supported previous findings that *TRF4* deletion increases snoRNAs transcription termination at the second site **(Grzechnik et al. 2008)**. However, we also observed a significant increase in the cytosolic concentration of snoRNAs in this mutant, especially in the 3'-extended form. Together, these findings suggest that in the *trf4Δ* mutant strain, when the transcription termination is moved to the second site, more snoRNAs tend to be exported.
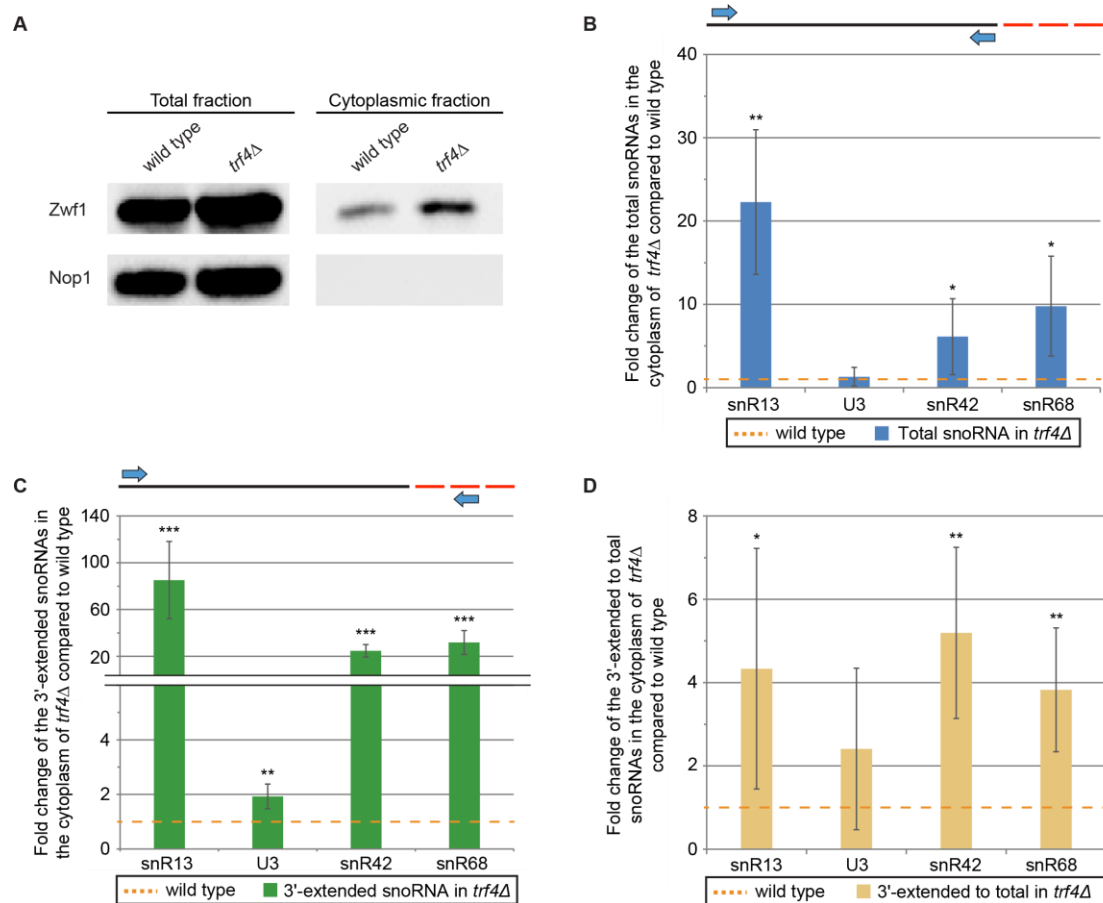
Figure 27: snoRNAs amount increases in the cytoplasmic fractions of *trf4Δ*. (A) Western blot analysis of the cytoplasmic fractionation. The total and cytoplasmic fractions were analysed by detecting the cytoplasmic protein Zwf1 and the nucleolar protein Nop1. **(B - D)** qPCR data that show the cytosolic amount of **(B)** total snoRNAs, **(C)** 3'-extended snoRNAs, and **(D)** the ratio of 3'-extended to total snoRNAs level. In the upper part, the black line indicates mature snoRNA, the red dashed line indicates the 3'-extensions, and the arrows indicate the positions of the primers used. The error bars represent the standard deviation. p-values were calculated by the unpaired two-tailed unequal variance student's t-test (* = $p < 0.05$, ** = $p < 0.01$, *** = $p < 0.001$); n= 5 (The analyses were partly carried out by Carmen Wassong in the laboratory of Prof. Dr. H. Krebber).

4.9. Cytosolic localization of snR65 increases when NNS site is deleted

The results obtained with the *trf4Δ* strain showed a correlation between the increase of snoRNAs that terminate transcription in the second site and their export into the cytosol. Thus, it is possible that the cytosolic export of snoRNAs is limited to or primarily associated with the snoRNAs that terminate transcription via the second termination site. However, because a component of the TRAMP complex was deleted, we cannot exclude that some of the snoRNAs generated in *trf4Δ* are defective and not degraded.

To address this issue, two knockout strains were created: the capped C/D *snR13Δ* and the uncapped C/D *snR65Δ*. At the same time, were generated plasmids containing these snoRNAs under control of the *GAL1* promoter and with the endogenous transcription termination site. Finally, plasmids containing mutations at the NNS transcription termination site were also generated in order to force the snoRNA to terminate the transcription at the second site **(Figure 28)**.
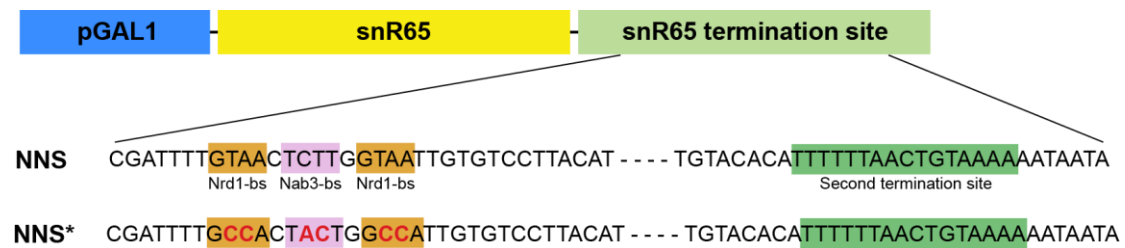
Figure 28: snR65 termination site mutant used. Schematic representation of the snR65 termination site. Nrd1 and Nab3 binding sites are highlighted in orange and purple respectively. The second termination site is highlighted in green. The point mutations are highlighted in red.

The strain *snR65Δ* was transformed with the plasmids containing the correct (NNS) or the mutated termination site (NNS*) and the snoRNA localization was tested via fluorescent *in situ* hybridisation experiments **(Figure 29)**. The snoRNA transcription was induced by replacing glucose with galactose, and two samples were collected and analyzed after 5 and 30 min of induction.

For labeling of the snR65, we used a short, 30 nucleotide long, DNA-probe that was conjugated with Cy3 at its 5'- and 3'-ends.

In wild type cells, the snoRNAs is mostly found in the nucleolus, and a similar result was visible for the NNS strain. However, we observed that in NNS*, even though the highest signal is in the nucleolus, there was an evident increase of the cytosolic localization of the snR65. The highest cytosolic localization of snR65 in NNS* was also more evident after a 30 min induction by galactose **(Figure 29)**.

From this first test we can speculate that when snoRNAs terminate the transcription at the second site, they have a higher chance of being exported to the cytosol. However, this hypothesis needs to be confirmed by additional experiments in which snoRNAs should also be tested under the control of the endogenous promoter.
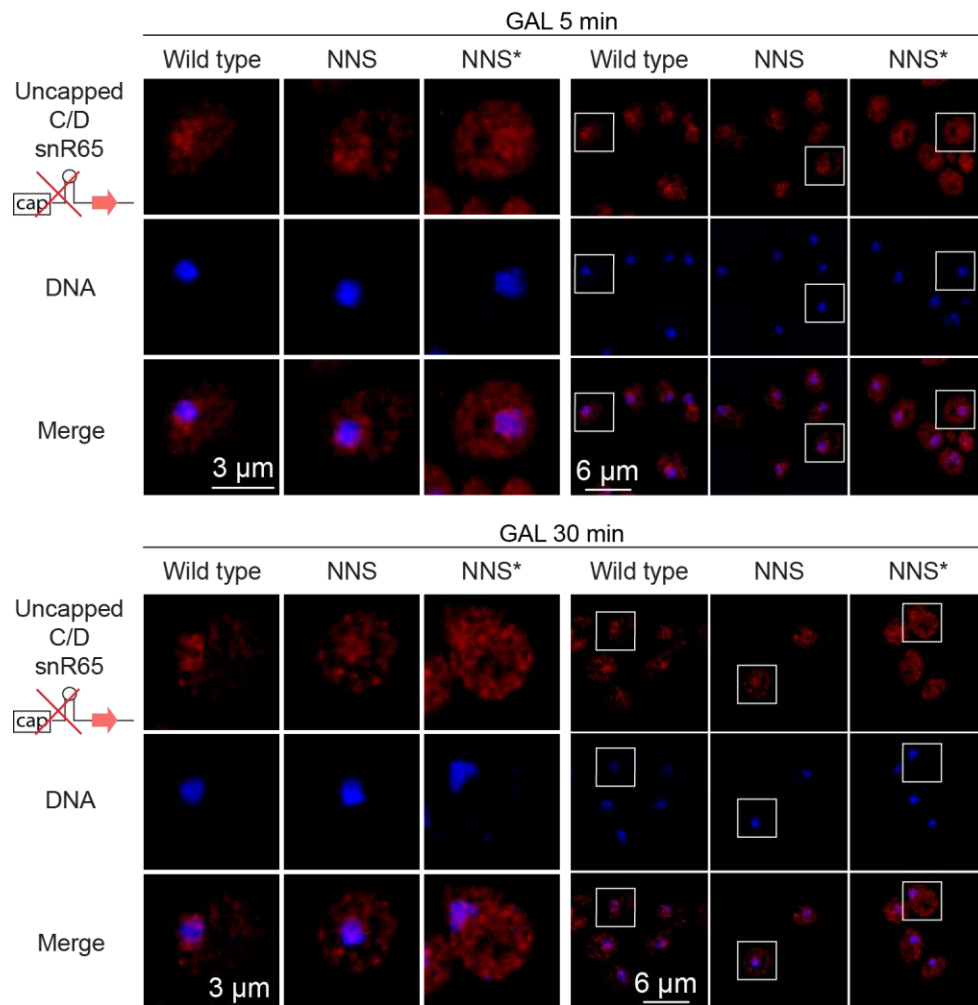
Figure 29: Defects in NNS termination site increase the cytosolic localization of the snoRNA. FISH analysis was carried out after inducing snoRNA transcription for the indicated times. Cells were fixed with 4 % formaldehyde and snoRNAs were hybridized with 30 nucleotide long, Cy3-labelled probes (red). DNA was stained with DAPI (blue). NNS: *snR65Δ* transformed with GAL1:snR65; NNS*: *snR65Δ* transformed with GAL1:snR65 NNS binding site mutated (The experiment was carried out in collaboration with the Ph.D. Student Fei Yu).

5. Discussion

Despite the fact that the precise function of the modifications carried out by snoRNA remains unclear, the rRNA regions subject to these post-transcriptional modifications have been identified as highly conserved throughout evolution, indicating the critical role played by snoRNAs in rRNA development **(Turowski and Tollervey 2015)**. According to the current knowledge about snoRNA biogenesis, these small non-coding RNAs are retained in the nucleus throughout their life cycle without ever being exported to the cytosol **(Kufel and Grzechnik 2018)**. However, recent studies have shown that snoRNAs can bind proteins involved in RNA export, such as Mex67, as well as other non-canonical snoRNA proteins, like Nab2 and Npl3, which can help the cytosolic export by binding the RNA and the Mex67 export factor **(Holmes et al., 2015; Reuter et al., 2015; Tuck and Tollervey 2012; Zander and Krebber, 2017)**. In recent years, there has been more and more confirmation of functional RNAs in yeast, such as *TLC1* and snRNAs, which assemble into RNP after undergoing a nucleocytoplasmic shift **(Becker et al., 2019; Hirsch et al., 2021)**. The export of these non coding RNAs probably allows them to separate the assembly site in RNP from the nuclear final destination where they carry out their activity. In this way, it may be possible to reduce the accumulation of aberrant RNAs in the nucleus that could impede the proper functioning. However, up to date, there is no evidence for such a model for snoRNAs. Therefore, in this study, we investigated whether snoRNAs also undergo a nucleo-cytoplasmic shuttle and which proteins are involved in this process.

5.1. snoRNAs bind Mex67 and undergo nuclear export

The export factor Mex67 is essential for the transport of different RNA targets through the nuclear pore complex in yeast. Mex67 is mostly involved in mRNA export **(Zander and Krebber, 2017)**, but it was shown that it can also export non-coding RNA such as *TLC1* **(Wu et al., 2014)** and snRNAs **(Becker et al., 2019)**. Furthermore, in one study, Mex67 was also found to bind to snoRNAs **(Tuck and Tollervey 2012)**. Because the current snoRNA maturation model does not include a

cytosolic step and Mex67 is primarily involved in RNA export, we first wanted to confirm the existence of a binding between snoRNAs and Mex67.

Through RNA co-immunoprecipitation experiments, we identified a physical interaction between immature snoRNAs and Mex67 **(Figure 12)**. Because we detected the 3-extended snoRNA form in this experiment, we suggest that this interaction occurs prior to the 3'-end processing step of snoRNAs. Interestingly, the intronic snoRNA examined, snR24, was the only one that did not show a clear binding with Mex67, with a small fold enrichment of 1.28 when compared to the other snoRNAs with fold enrichments greater than 2. However, the interaction between snR24 and Mex67 was shown in the work of **(Tuck and Tollervey 2012)**, so it is possible that further experiments are needed to confirm the binding of Mex67 and intronic snoRNAs.

Because Mex67 is an export factor, it is probable that this protein is involved in the export of snoRNAs. This possibility is supported by data from a study conducted in our laboratory using cytosolic fractionation followed by RNA sequencing of the wild type and the double mutant strain *mex67-5 xpo1-1*. It was found that there was not only a cytosolic pool of snoRNAs in the wild type, but also a decrease in the concentration of cytosolic snoRNAs in the export factors mutant strain *mex67-5 xpo1-1* **(Figure 11) (Coban et al., submitted)**.

The next step was to figure out if Mex67 has really a role in snoRNA export. Therefore, we investigated the influence of the mutant *mex67-5* on the localization of snoRNAs via a fluorescent *in situ* hybridization experiment. Because the final and main localization of snoRNAs is nucleolar, we used a method to enhance visualization of cytoplasmic snoRNAs so that it was possible to confirm an eventual nuclear retention in the mutant strain. This was achieved by using relatively large DIG-labeled RNA probes ranging in size from 100 to 300 nucleotides, which are less likely to penetrate the nuclear envelope due to their size **(Becker et al., 2019)**. This fluorescent *in situ* hybridization experiment allowed us to see a snoRNA cytosolic pool in wild type cells **(Figure 13)**, confirming the presence of cytosolic snoRNAs shown through the RNA sequencing analysis of the cytosolic fraction **(Figure 11)**. Moreover, we observed a nuclear retention of all investigated snoRNAs in the

mutant strain *mex67-5*, indicating the importance of this protein for the export of snoRNAs **(Figure 13)**.

Another interesting observation comes from the increase in the 3-extended form of snoRNAs in the *mex67-5* mutant strain **(Figure 14)**. The increase in the immature form induced by the *mex67* mutation might be explained by the snoRNAs inability to complete the maturation pathway, making the cytosolic step essential, or by a decrease in snoRNAs degradation that could occur in the cytosol.

In recent years, some research has shown that snoRNAs in humans can accumulate in the cytosol via mechanisms regulated by lipotoxic and oxidative stress **(Holley et al., 2015; Li et al., 2017)**. Furthermore, a recent study in *S. cerevisiae* revealed that some sdRNAs (snoRNA-derived small RNAs) can localize in the cytosol while remaining bound to the ribosome, hypothesizing their function in the inhibition of translation dependent on stress conditions **(Mleczko et al., 2019)**.

However, our results provide the first evidence for a Mex67 export pathway of snoRNAs in yeast and highlight the role of this export factor in the processing of the snoRNAs' 3-extended immature form.

5.2. Cytosolic snoRNAs are mainly composed of the immature form, and the nuclear import is carried out by Cse1 and Mtr10

After showing that snoRNAs can be exported via Mex67, we wondered which form was predominant in the cytosol of the wild type strain. When the *mex67-5* mutant was used, an increase in the 3-extended form was observed **(Figure 14)**, suggesting that it could be the immature form that is exported to the cytosol. To support this hypothesis, we carried out a fluorescent *in situ* hybridization experiment with DIG-labeled RNA probes that targeted both the 3-extended and mature forms of snoRNAs. Again, in order to improve the visualization of cytoplasmic snoRNAs, we used long probes of 200 nucleotides to visualize the cytosolic pool of the 3-extended snoRNAs **(Figure 15B)**. We observed that in wild type, cells with probes for the 3-extended form showed a localization of snoRNAs all over the cell, as opposed to cells with the probe for the mature form, where the localization was mostly nuclear **(Figure 15A)**. This finding supports the hypothesis that in the wild type strain, the snoRNA form exported in the cytosol is most likely immature.

However, if snoRNAs are exported to the cytosol as part of their maturation pathway, this implies that they must be re-imported into the nucleus to fulfill their function **(Kos and Tollervey, 2010)**. Because recent studies have shown that Cse1 and Mtr10 are involved in the re-import of the non-coding RNAs *TLC1* and snRNAs **(Becker et al., 2019; Hirsch et al., 2021)**, we decided to test these two karyopherins as potential snoRNA importers. For this experiment, snoRNAs were labelled with a short 30 nucleotide long DNA-probe that was conjugated with Cy3 at its 3'- and 5'-ends. Because of their size, these probes can more easily enter the nucleus, allowing us to stain the snoRNAs found in the nucleolus and easily identify any cytosolic snoRNA accumulation.

We analyzed the snoRNA localization in three mutant strains of these two karyopherins, *cse1-1*, *mtr10Δ*, and the double mutant *cse1-1 mtr10Δ*, and we observed that some of the tested snoRNAs showed clear import defects. In the capped C/D snR13, the uncapped C/D snR68, and the capped H/ACA snR42, there was a clear cytosolic retention in the mutant strain used **(Figure 17)**. The import defect was stronger in the double mutant than in the single mutants, indicating that these karyopherins collaborate in the nuclear re-import of these three snoRNAs. Curiously, the capped C/D snR13 showed import defects in the single mutant *mtr10Δ*, but not in the single mutant *cse1-1* **(Figure 17)**. It is possible that for this snoRNAs group, the major import factor is Mtr10. However, because the cytosolic retention was stronger in the double mutant, we cannot preclude the possibility that Cse1 activity is involved in the re-import of this snoRNA.

For the intronic snR24 and the capped C/D U3 no import defect was visible in none of the mutant strains used **(Figure 16)**. It was shown that the intronic snoRNAs, even though they are exported via Mex67, undergo a different maturation pathway from the other snoRNAs. It could be that a different karyopherin is used for the re-import or that intronic snoRNAs are exported in order to be degraded. Since the results obtained for the intronic snR24 diverged from those of the other snoRNAs, we decided not to continue the research for this snoRNA group.

The same argument could be valid for U3, where no cytosolic accumulation was visible in the import factor mutants *cse1-1* and *mtr10Δ* **(Figure 16)**. However, given

the importance of this snoRNA, we decided to pursue further research on this snoRNA.

To examine if Cse1 and Mtr10 defects influence snoRNA maturation, we investigated the total and 3-extended snoRNA levels in mutants of both import factors **(Figure 18)**. The results were strikingly similar in the two mutants, but different changes in snoRNA concentration were observed depending on the target and the form analyzed. For the uncapped C/D snR68 and capped H/ACA snR42, there was an enrichment in both total and 3-extended concentration. However, the 3-extended form increased significantly more than the total only in snR42, indicating that the import defect in this snoRNA resulted in a higher accumulation of the immature form **(Figure 18)**. A similar result was also visible for the capped C/D snR13, but in this case, there was no increase in the total pool. The exclusive enrichment of the 3-extended form could result from the relatively short half-life of snR13, approximately 20 min, when compared to other snoRNAs whose half-life largely exceeded 60 min. The short half-life of snR13 could explain the lack of an increase in the total pool of snR13, which is degraded more rapidly. Nevertheless, due to the import block, the newly generated snR13 cannot complete the maturation pathway, resulting in an enrichment of the immature form **(Figure 18)**.

Capped C/D U3 is the only snoRNA tested that shows an increase in the total pool but not in the immature form. Therefore, from this last result, it is reasonable to conclude that defects in CSE1 and MTR10 did not affect the U3 maturation pathway **(Figure 18)**.

To support the results obtained, we isolated RNA from cytoplasmic fractions of the double mutant *cse1-1 mtr10Δ* cells and measured the cytosolic amount of snoRNAs compared to wild type **(Figure 19)**. We showed that all snoRNAs tested accumulate in the cytoplasm upon the re-import block, but the amount varies depending on the snoRNA analyzed. Both the uncapped C/D snR68 and capped H/ACA snR42 accumulate more in their 3-extended form, suggesting that these snoRNAs are exported as immature. Capped C/D snR13 also showed a higher accumulation of the 3-extended form, although to a lesser extent than snR68 and snR42. According to the results obtained with the ratio of the 3-extended form on the total **(Figure 19D)**, it was shown that the fold enrichment for snR13 was only 1.36, a small increase

when compared to snR68 and snR42, both of which had fold enrichments greater than 2. Thus, it is not possible to establish with certainty that for snR13, the 3-extended form is the most abundant in the cytosol. However, based also on previous findings from single mutants *cse1-1* and *mtr10Δ* **(Figure 18)**, it is likely that the snR13 form retained in the cytosol of the double mutant *cse1-1 mtr10Δ* **(Figure 19)** is the 3-extended one.

For U3, the cytoplasmic fraction showed an equal increase in the total and the 3-extended form, making it difficult to distinguish which one is the main form retained in the cytosol of the double mutant **(Figure 19)**.

With these results, we reinforce our hypothesis that snoRNAs move into the cytoplasm as part of their maturation pathway, as defects in the import factors Cse1 and Mtr10 result in an accumulation of immature snoRNAs in the cytosol, probably due to the inability of those snoRNAs to complete their maturation pathway. Moreover, it is probable that Cse1 and Mtr10 cooperate in the re-import of immature snoRNAs because an additive effect was observed when both factors were mutated **(Figure 17)**.

5.3. The Lsm2-8 complex binds snoRNAs and may be involved in nuclear re-import

An important complex that binds *TLC1* and four of the five snRNAs is the Sm-ring, a complex that consists of seven small polypeptides that form a heptameric ring with a small central aperture **(Matera and Wang, 2014; Vasianovich and Wellinger, 2017)**. Furthermore, there is another heptameric protein complex that is known as the Lsm (like Sm) complex because of its similarities to Sm proteins. Two heteroheptameric complexes of Lsm, Lsm1-7 and Lsm2-8, were identified, and the latter was shown to bind to the only member of the snRNA Lsm-class, U6 **(Beggs, 2005; Achsel et al., 1999)**. Recently, it has been shown that Cse1 and Mtr10 are able to re-import *TLC1* and the Sm-class snRNAs into the nucleus by binding to the Sm-ring, a step that takes place in the cytosol **(Becker et al., 2019; Hirsch et al., 2021; Vasianovich et al., 2020)**. The ability of the Sm ring to bind the two import factors, Cse1 and Mtr10, makes this complex critical for completing the maturation pathway of *TLC1* and Sm-class snRNAs.

Interestingly, the Lsm complex has been shown to interact with two snoRNAs, U3 and snR5 **(Fernandez et al., 2004; Kufel et al., 2003b)**. Due to the similarity between the Sm and Lsm rings, it is possible that the two import factors, Cse1 and Mtr10, are able to bind the Lsm2-8 complex as well, making this complex important for the re-import of the RNAs that bind to it, such as U6 and snoRNAs.

There are currently no publications that demonstrate the interaction between the two import factors mentioned above and the Lsm2-8 complex, but this interaction has recently been shown in our laboratory **(Wang and Krebber, personal communication)**. The interaction between Lsm8 and the import factors Cse1 and Mtr10 raises the possibility that the Lsm2-8 complex is essential for the import of the RNAs that bind to it.

Because snoRNAs modify RNA targets in the nucleolus **(Kos and Tollervey, 2010)**, re-import is mandatory after pre-snoRNAs are exported to the cytoplasm, and since the Lsm2-8 complex may be crucial in this step, we decided to investigate whether other snoRNAs, in addition to U3, can bind Lsm8.

Through RNA co-immunoprecipitation experiments, we identified a physical interaction between Lsm8 and eight different immature snoRNAs **(Figure 20)**. It was interesting to note the significant differences in interactions of some snoRNAs. Five of them interacted similarly with Lsm8, but the values obtained with U3 and intronic snoRNAs were significantly higher **(Figure 20B)**. For intronic snoRNAs, it can be explained by the capacity of Lsm2-8 to bind the pre-mRNA containing the intronic snoRNA **(Kufel et al, 2004)**, increasing as a consequence the interaction detected. Therefore, to detect the exclusive binding of Lsm8 with intronic snoRNAs, additional tests must be performed in which the value obtained for the intronic snoRNA is compared to the value obtained by testing the binding of Lsm8 with the pre-mRNA containing the snoRNA. Concerning U3, the large interaction detected in comparison to the other snoRNAs can be explained by its high expression, which turns out to be far superior to all other snoRNAs **(Hughes et al., 1987)**.

With this result, we have shown that not only U3 but also other snoRNAs belonging to different classes can bind the Lsm2-8 complex. This result could be extremely relevant as the karyopherins Cse1 and Mtr10 are able to bind Lsm8 and thus the Lsm2-8 complex could be critical for the re-import of snoRNAs into the nucleus.

Moreover, the Lsm8 binding sequence was found in all snoRNAs tested, even though with small differences from the optimal binding sequence found on the snRNA U6 that is CGUUUU. Depending on the snoRNA tested, the sequence discovered was [C/G][G/C]UUUU, which could further explain why snoRNAs have lower binding than snRNA U6.

To figure out if Lsm8 is critical in snoRNA import, we investigated the influence of the mutant *lsm8-1* on the localization of snoRNAs via a fluorescent *in situ* hybridization experiment using short 30 nucleotide long DNA-probes conjugated with Cy3 at its 3'- and 5'-end. The mutant strain *lsm8-1* is a temperature-sensitive strain that when grown at 37 °C undergoes an Lsm-ring assembly defect **(Pannone et al., 1998)**. It was previously found that in the *lsm8-1* mutant strain, U6 was mislocalized in the cytoplasm, showing that the correct assembly of the Lsm-ring is important for the re-import of U6 into the nucleus **(Becker et al., 2019)**. Therefore, we wondered if this mutant strain would exhibit the same mislocalization effect on snoRNAs. Through this experiment, we were able to detect snoRNA cytosolic accumulation in the mutant strain *lsm8-1*, implying that the correct assembly of the Lsm2-8 complex is important for snoRNA re-import **(Figure 21)**. Interestingly, again the intronic snR24 and the capped C/D U3 did not show a mislocalization as for the other snoRNAs tested.

To support this finding, a cytoplasmic fractionation experiment was carried out in order to test the cytosolic RNA in the *lsm8-1* mutant strain **(Figure 22)**. As for the double mutant *cse1-1 mtr10Δ* **(Figure 19)**, we demonstrated that also in this case, all snoRNAs analyzed were enriched in the cytosol when the correct assembly of the Lsm2-8 complex was impaired. However, with the exception of the capped H/ACA snR42 that accumulated more in its 3-extended form, it was not possible to distinguish which form was predominant in the cytoplasm of the mutant strain **(Figure 22D)**. This result, when combined with the findings obtained with the double mutant *cse1-1 mtr10Δ* **(Figure 19)** and the fluorescent *in situ* hybridization in *lsm8-1* **(Figure 21)**, reinforces the model in which the import factors Cse1 and Mtr10 bind the Lsm2-8 complex to promote snoRNA re-import into the nucleus.

5.4. The Lsm2-8 complex binds snoRNAs either in the nucleus or in the cytosol depending on the snoRNA analysed

The model in which the Sm-ring was thought to bind the *TLC1* and Sm-class snRNAs in the nucleus was modified, showing that this interaction takes place in the cytosol, emphasizing the importance of the cytosolic step for these non-coding RNAs. **(Becker et al., 2019; Hirsch et al., 2021; Vasianovich et al., 2020)**. Because of the similarities found so far between *TLC1*, snRNA and snoRNAs, we wondered if even for snoRNAs, the binding to the Lsm2-8 complex could occur in the cytosol. To investigate where the binding between Lsm2-8 and snoRNAs takes place, we analyzed via RNA co-immunoprecipitation how the physical interaction of Lsm8 and four different snoRNAs changes in import and export factor mutants.

First, we analyzed the binding in the export factor mutant *mex67-5* and found that the interaction with Lsm8 decreased only for the capped C/D U3, while it increased for the capped C/D snR13, uncapped C/D snR68, and capped H/ACA snR42 **(Figure 23)**. This finding suggests that only U3 may bind to the Lsm2-8 complex in the cytosol, whereas for the other snoRNAs tested, the increased interaction with Lsm8 in *mex67-5* supports the hypothesis that the Lsm2-8 complex is loaded in the nucleus prior to export. Then, we tested the binding in the import factor mutant *mtr10Δ* and we have shown that the interaction between Lsm8 and all snoRNAs analyzed, including U3, increased **(Figure 24)**. This result suggests that the Lsm2-8 complex is removed after the re-import step for snR13, snR68, and snR42 because the Lsm2-8 complex is not part of the mature snoRNP and is retained on the snoRNA when the import is blocked. Unlike the other snoRNAs tested, we showed that the interaction between snRU3 and the Lsm2-8 complex may occur in the cytosol because U3 binding to this complex decreases in the export factor mutant *mex67-5* but increases when the import is blocked in *mtr10Δ*.

Because Cse1, like Mtr10, has been shown to be involved in the re-import of snoRNAs **(Figure 17 and 19)** and to bind the Lsm2-8 complex **(Wang and Krebber, personal communication)**, we expected an increased interaction between Lsm8 and snoRNAs in the *cse1-1* mutant as well. However, in the *cse1-1* mutant, the interaction with Lsm8 showed no changes, remaining similar to the wild type strain **(Figure 25)**. It is also important to note that statistically significant results were not

obtained in this mutant strain due to the high disparity of the single results obtained. Therefore, additional tests are required to confirm the obtained result, even though the trend of the single tests has never shown an increase in the interaction as for the *mtr10Δ* mutant **(Figure 24)**. A similar issue was discovered for the non-coding RNA *TLC1*, which showed a decrease in interaction with the Sm-ring in the *cse1-1* strain, in contrast to the result obtained in *mtr10Δ* where this interaction increased **(Hirsch et al., 2021)**. It was hypothesized that this issue arises from Cse1's ability to participate in the stabilization of the Sm-ring, preventing proper ring assembly and, as a result, decreasing the interaction between the Sm-ring and *TLC1* in the *cse1-1* mutant. **(Hirsch et al., 2021)**. Because of the similarities between Sm-ring and Lsm-ring, it is possible that Cse1 also plays a role in the stabilization of the Lsm2-8 complex, which would explain the result obtained in the *cse1-1* mutant.

From the results obtained, we showed that the interaction between the Lsm2-8 complex and the snoRNAs occurs in different ways **(Figure 30)**.
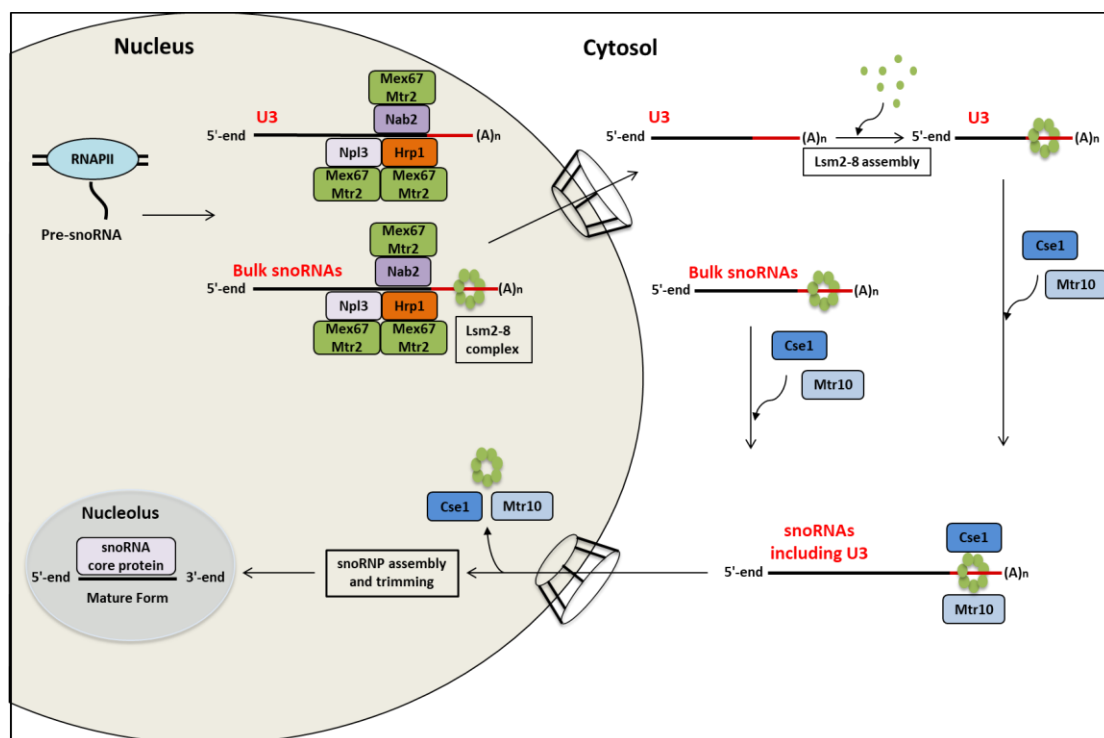
Figure 30: Model of Lsm2-8 binding with snoRNAs. The binding between snoRNAs and the Lsm2-8 complex differs according to the type of snoRNA. For most snoRNAs, binding to the Lsm2-8 complex occurs in the nucleus, and the snoRNA is exported bound to this complex. In the cytosol, the Lsm2-8 complex is important for re-import as it binds the importins Cse1 and Mtr10 and dissociates from the snoRNA once in the nucleus, as it is not part of the mature snoRNP. So far, U3 appears to be the only exception, as it binds the Lsm2-8 complex once exported to the cytosol. Also for U3, the Lsm2-8 complex dissociates after re-import because it is not part of the mature snoRNP. The red line represents the immature portion that is removed before the mature snoRNA is formed.

For the capped C/D snR13, uncapped C/D snR68, and capped H/ACA snR42, the interaction with the Lsm2-8 complex takes place in the nucleus, and it will be removed from the snoRNP once re-imported into the nucleus after the cytosolic step. On the contrary, the capped C/D U3 binds the Lsm2-8 complex in the cytosol after export via Mex67 and will be removed after re-import into the nucleus.

5.5. In *trf4Δ* snoRNAs terminate transcription at the second site and accumulate in the cytosol.

In *S. cerevisiae*, transcription termination of independently transcribed snoRNAs, like for other small non-coding RNAs, occurs via the NNS complex, which is composed of the RNA-binding proteins Nrd1 and Nab3 and the RNA:DNA helicase Sen1 **(Porrua and Libri 2015)**. Then, NNS recruit the TRAMP complex (formed by Trf4/Trf5, Air1/Air2, and Mtr4) that adds a short oligo (A) tail to the 3'-end pre-snoRNA via Trf4, a critical step for the subsequent recruitment of rrp6, which trims the 3'-end pre-snoRNA until the mature extremity is formed **(Tudek et al., 2014)**.

Even though snoRNA transcription termination is carried out mainly in the region where the NNS complex is active (site I), different studies indicate the presence of a second transcription termination region showing a sequence resembling the mRNA cleavage/polyadenylation signal (site II) **(Fatica et al., 2000; Morlando et al., 2001; Steinmetz and Brow 2003; Steinmetz et al., 2006)**. Moreover, it was indicated that in *trf4Δ*, snoRNA transcription is terminated at the second site where the CPF-CFI complex proteins act **(Grzechnik and Kufel 2008)**. Although site II was proposed to represent a "fail safe" mRNA-like signal role, no further research has been conducted to study the function of this second termination site.

Because the results obtained using wild type strains always showed a weak cytosolic signal (FISH) or a low cytosolic concentration (nucleo-cytoplasmic fractionation), we began to suspect that the snoRNAs' localization could be affected by the transcription termination site used. When transcription terminates at site I via the NNS complex, the snoRNAs may remain in the nucleus, whereas when transcription terminates at site II through the CPF-CFI complex, the snoRNAs could perform a cytosolic step. For this reason, we decided to further investigate the role of site II in the maturation of snoRNAs. Therefore, we first wanted to confirm that in *trf4Δ*, the

transcription occurred over the NNS binding site. We extracted the RNA from the *trf4Δ* mutant strain and analyzed the obtained cDNA by comparing it with the wild type strain. In order to understand if the termination had overcome the site I, we used reverse primers that bind to a region beyond the NNS binding site. We tested six snoRNAs from different groups, and for all of them, there was a significant increase in transcripts that bypassed the NNS binding site **(Figure 26)**, confirming that in *trf4Δ*, the majority of the snoRNAs terminated at transcription site II.

After confirming that the NNS binding site is skipped in *trf4Δ*, we wanted to investigate if snoRNAs that terminate transcription at site II are more inclined to be exported into the cytosol. Therefore, a cytoplasmic fractionation experiment was carried out in the mutant strain *trf4Δ* and it was found that all snoRNAs tested were enriched in the cytosol **(Figure 27)**. Only U3 did not show an increase when it was analyzed in the total pool, but as with the other snoRNAs tested, the immature 3-extended form was more abundant in the cytosol **(Figure 27C)**. As a result, we discovered that the majority of the transcripts in the mutant *trf4Δ* cytosol are immature, implying that snoRNAs that terminate transcription at site II are more inclined to be exported to the cytoplasm in their 3-extended form.

Although the results obtained are extremely interesting, indicating that snoRNA export may be dependent on the transcription termination site, the use of the mutant strain *trf4Δ* introduces a problem that must be considered. Because the TRAMP complex is not fully functional in this mutant strain, it is possible that not all the snoRNAs analyzed in *trf4Δ* originate from the second termination site, but some of them may be incorrect snoRNAs that have not been degraded.

5.6. snR65 which cannot terminate transcription via the NNS complex, has a higher cytosolic localization

As previously demonstrated, snoRNAs are more likely to be found in the cytosol if they do not terminate transcription at site I, where the NNS complex is used **(Figure 27)**. Since there are two transcription termination sites **(Fatica et al., 2000; Morlando et al., 2001; Steinmetz and Brow, 2003; Steinmetz et al., 2006)**, it can be assumed that in the *trf4Δ* strain, because the termination via the NNS complex does not function, the snoRNAs should originate from site II, as also shown in the work of

(Grzechnik and Kufel 2008). However, using the *trf4Δ* mutant strain does not allow us to distinguish between correct and incorrect snoRNAs, which cannot be degraded because the TRAMP complex is not fully functional. To overcome this problem, we generated a knockout strain for the uncapped C/D snR65. The *snR65Δ* strain was then transformed with two different plasmids, one containing snR65 with the endogenous termination and the other containing snR65 with mutations in the NNS binding site (NNS*). In both plasmids, snR65 was under the control of the *GAL1* promoter **(Figure 28)**. This allowed us to analyze the localization of snR65 that exclusively terminate transcription at site II without compromising the functionality of the TRAMP complex. The snoRNA localization was carried out via fluorescent *in situ* hybridization where snR65 was labelled with a short 30 nucleotide long DNA-probe that was conjugated with Cy3 at its 3'- and 5'-end. The transcription of snR65 was induced by galactose and localization was tested after 5 and 30 min **(Figure 29)**. In both case we observed a higher cytosolic localization in the NNS* strain, where the transcription terminated at the second site.

Although further analyses need to be carried out to confirm this result, we can conclude from this single experiment that when transcription ends at site II, uncapped C/D snoRNAs are more inclined to be exported to the cytosol.

In order to confirm this result, it will be necessary to test other snoRNAs belonging to different groups and perform further analyses such as cytosolic fractionation in NNS* strain.

5.7. Novel model of snoRNP maturation in *S. cerevisiae*

Based on the findings of this work, we propose the following model for the snoRNAs maturation pathway **(Figure 31)**. The model is based on the study of four distinct snoRNAs: capped C/D snR13, capped C/D U3, uncapped C/D snR68, and capped H/ACA snR42. As a result, we do not consider intronic snoRNAs. Because the model does not take into account the cap, it is not depicted in the figure, which only shows the sign "5'-end."

The snoRNAs are transcribed by RNAP II and, subsequently, with the exception of U3, the pre-snoRNAs are bound by the Lsm2-8 complex. At this step, the pre-

snoRNAs are also bound by non-canonical proteins such as Npl3, Nab2, and Hrp1 **(Chen et al., 20017; Holmes et al., 2015; Kim et al., 2006; Reuter et al., 2015)**, which may also act to prevent pre-snoRNAs degradation. As with mRNAs **(Zander and Krebber, 2017)**, it is possible that Npl3, Nab2, and Hrp1 act as adaptor proteins for the export factor Mex67-Mtr2 which export pre-snoRNAs out of the nucleus. When the snoRNAs reach the cytoplasm, the Lsm2-8 complex assembles on U3 and the karyopherins Cse1 and Mtr10 bind the pre-snoRNAs via the Lsm-ring.
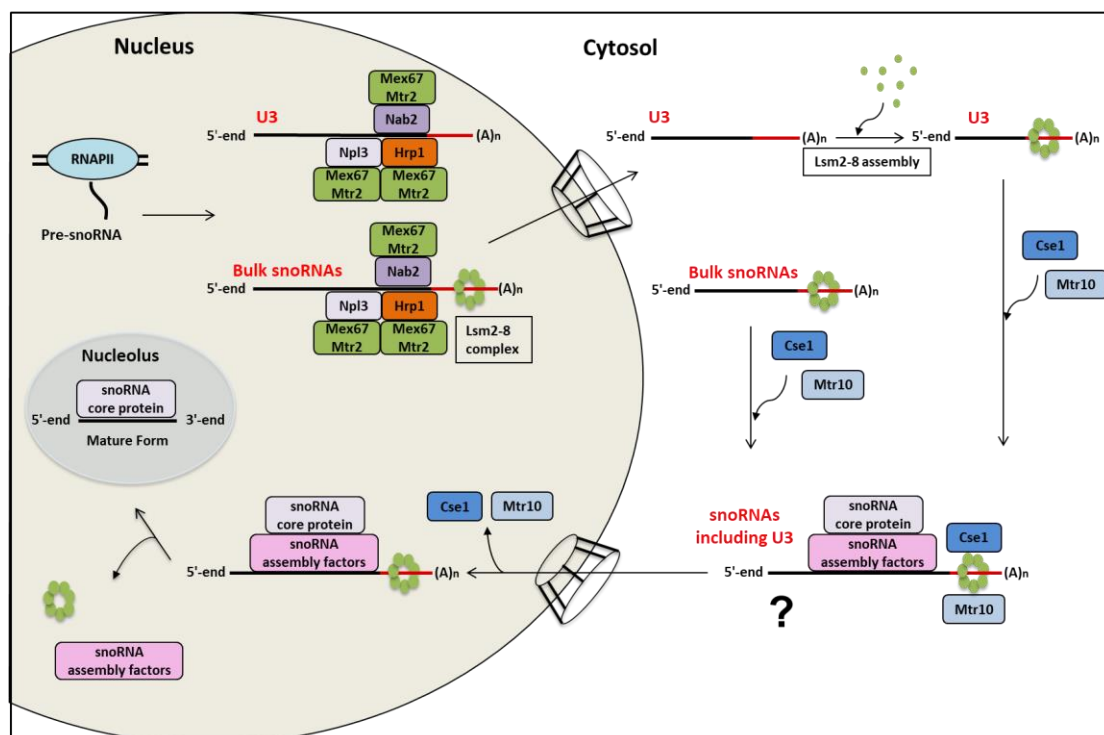
Figure 31: Model for snoRNAs maturation in *S. cerevisiae*. The maturation pathway begins with transcription via RNAP II. Non-canonical proteins such as Npl3, Nab2, and Hrp1 bind snoRNAs and are assumed to act as adaptor proteins for the export factor Mex67-Mtr2. With the exception of U3, the Lsm2-8 complex is loaded on the 3'-end extremity of the pre-snoRNAs. In the cytoplasm, the export receptors Mex67-Mtr2 dissociate from the pre-snoRNA and the Lsm-ring assembles on U3. The pre-snoRNAs are then loaded by the import factors Cse1 and Mtr10 via the Lsm2-8 complex. It is possible that in the cytoplasm there is binding between the pre-snoRNAs and the assembly factors that transport the core proteins. This step has been marked with a question mark because there is no evidence for it. Mtr10 and Cse1 then re-import the pre-snoRNA into the nucleus. Following that, the import factors, the Lsm-ring, and the assembly factors dissociate from the pre-snoRNPs, which undergo extremity trimming until the mature snoRNP is formed and accumulates in the nucleolus as its final destination. The red line represents the immature portion that is removed before the mature snoRNA is formed.

Because it is not fully understood when and where the binding between snoRNAs and assembly factors takes place, it is possible that it occurs during the cytosolic step. Furthermore, the location of the binding between the snoRNAs and the

assembly factors may change depending on the conditions in which the cell is found, as shown in **(Kakihara and Saeki 2014)** where the R2TP complex (an assembly factor for snoRNAs) accumulates in the cytoplasm in a nutrient-limiting condition. However, because we have no evidence as to where this link occurs, we have labeled this step with a question mark.

Both karyopherins, Mtr10 and Cse1, are involved in the re-import of pre-snoRNPs. Indeed, the double mutant *cse1-1 mtr10Δ* showed the highest cytosolic accumulation. Thus, it is possible that the binding between the Lsm-ring and the importins is a quality control step of snoRNP maturation. Following import, the final steps of maturation occur, which include the release of elements such as the Lsm2-8 complex and the assembly factors, as well as the consequent loading of the core proteins and the 3'-end trimming via Rrp6 **(Kufel and Grzechnik 2018)**. Finally, mature snoRNPs localize in the nucleolus where they can act on the modification of pre-rRNAs **(Kos and Tollervey, 2010)**.

In addition to the detection of a cytosolic step for snoRNAs, our work also hypothesized a possible role for the snoRNAs second transcription termination site **(Figure 32)**. We already knew about a second snoRNA transcription termination site, but its function remains cryptic **(Fatica et al., 2000; Grzechnik et al. 2008; Morlando et al., 2001; Steinmetz and Brow, 2003; Steinmetz et al., 2006)**. Based on our findings, we can speculate that the snoRNAs detected in the cytosol are mainly transcribed at site II. Since at the second site acts the CPF-CFI complex, the same complex involved in the termination of the mRNAs, it is possible that the snoRNAs that terminate at site II are more inclined to be exported. On the contrary, snoRNAs that terminate the transcription at site I via the NNS complex could complete the whole maturation pathway in the nucleus and be exported into the cytosol only for degradation. Furthermore, it cannot be excluded that the second transcription site is selected based on specific situations, such as stress conditions, in which the presence of snoRNA in the cytosol could be required. Therefore, it is possible that snoRNAs originating from site II are constantly expressed but at a reduced amount, increasing in concentration only in specific situations.
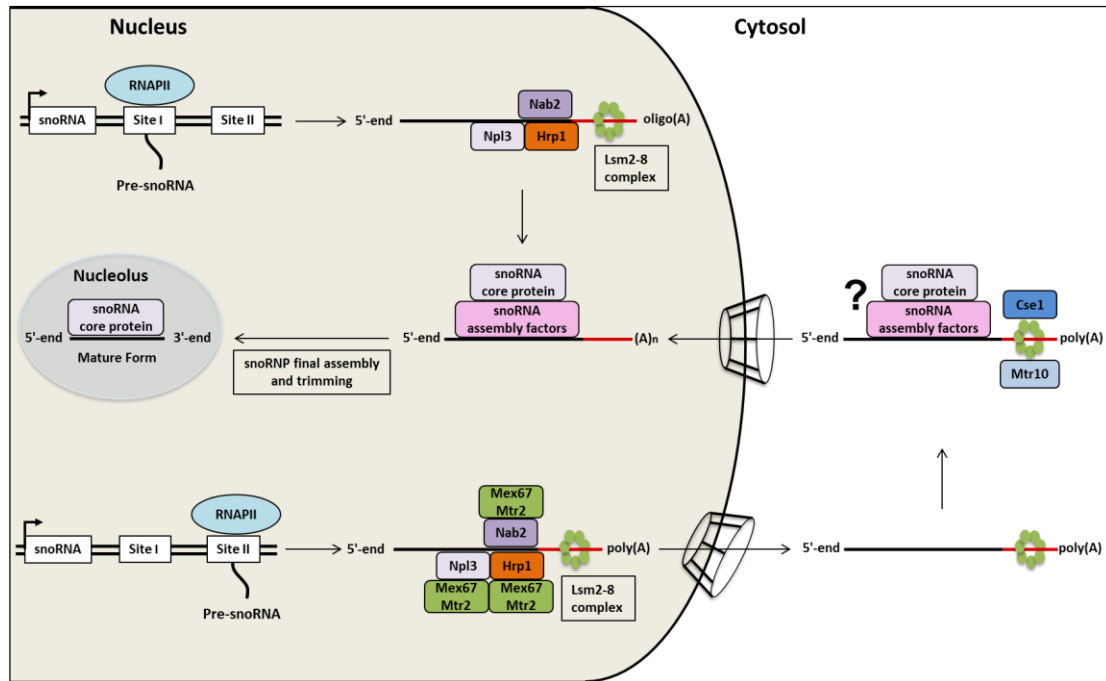
Figure 32: Model for snoRNAs that terminate transcription at the second site. In this model, the NNS complex acts on transcription termination that occurs on the site I. In this case, snoRNAs may not be exported and instead complete the maturation pathway entirely in the nucleus.
The CPF-CFI complex is involved in the transcription termination at site II. This results in a longer pre-snoRNA and involves the same proteins involved in mRNA transcription termination, raising the possibility that snoRNAs terminating at site II are more likely to be exported and have a cytosolic step as part of their maturation pathway.
Site I: site where the binding sequences for Nrd1 and Nab3 are located and where the NNS complex acts for transcription termination.
Site II: site where the sequence resembles the mRNA cleavage/polyadenylation signal and where the CPF-CFI complex acts for transcription termination.

However, other experiments are required to test different snoRNAs and how can change the bind between different proteins, such as the Lsm2-8 complex or the assembly factors, and the snoRNAs when transcription terminates at the second site.

6. References

Achsel T, Brahms H, Kastner B, Bachi A, Wilm M, Lührmann R. A doughnut-shaped heteromer of human Sm-like proteins binds to the 3'-end of U6 snRNA, thereby facilitating U4/U6 duplex formation in vitro. EMBO J. 1999 Oct 15;18(20):5789-802. doi: 10.1093/emboj/18.20.5789. PMID: 10523320; PMCID: PMC1171645.

Aitchison JD, Rout MP. The yeast nuclear pore complex and transport through it. Genetics. 2012 Mar;190(3):855-83. doi: 10.1534/genetics.111.127803. PMID: 22419078; PMCID: PMC3296253.

Alegria-Schaffer A. Western blotting using chemiluminescent substrates. Methods Enzymol. 2014;541:251-9. doi: 10.1016/B978-0-12-420119-4.00019-7. PMID: 24674076.

Aquino GRR, Krogh N, Hackert P, Martin R, Gallesio JD, van Nues RW, Schneider C, Watkins NJ, Nielsen H, Bohnsack KE, Bohnsack MT. RNA helicase-mediated regulation of snoRNP dynamics on pre-ribosomes and rRNA 2'-O-methylation. Nucleic Acids Res. 2021 Apr 19;49(7):4066-4084. doi: 10.1093/nar/gkab159. PMID: 33721027; PMCID: PMC8053091.

Arndt KM, Reines D. Termination of Transcription of Short Noncoding RNAs by RNA Polymerase II. Annu Rev Biochem. 2015;84:381-404. doi: 10.1146/annurev-biochem-060614-034457. Epub 2015 Mar 26. PMID: 25747400; PMCID: PMC5104496.

Becker D, Hirsch AG, Bender L, Lingner T, Salinas G, Krebber H. Nuclear Pre-snRNA Export Is an Essential Quality Assurance Mechanism for Functional Spliceosomes. Cell Rep. 2019 Jun 11;27(11):3199-3214.e3. doi: 10.1016/j.celrep.2019.05.031. PMID: 31189105.

Beggs JD. Lsm proteins and RNA processing. Biochem Soc Trans. 2005 Jun;33(Pt 3):433-8. doi: 10.1042/BST0330433. PMID: 15916535.

Bleichert F, Baserga SJ. The long unwinding road of RNA helicases. Mol Cell. 2007 Aug 3;27(3):339-52. doi: 10.1016/j.molcel.2007.07.014. PMID: 17679086.

Bohnsack MT, Kos M, Tollervey D. Quantitative analysis of snoRNA association with pre-ribosomes and release of snR30 by Rok1 helicase. EMBO Rep. 2008 Dec;9(12):1230-6. doi: 10.1038/embor.2008.184. Epub 2008 Oct 3. PMID: 18833290; PMCID: PMC2570499.

Bouchard-Bourelle P, Desjardins-Henri C, Mathurin-St-Pierre D, Deschamps-Francoeur G, Fafard-Couture É, Garant JM, Elela SA, Scott MS. snoDB: an interactive database of human snoRNA sequences, abundance and interactions. Nucleic Acids Res. 2020 Jan 8;48(D1):D220-D225. doi: 10.1093/nar/gkz884. PMID: 31598696; PMCID: PMC6943035.

Boulon S, Marmier-Gourrier N, Pradet-Balade B, Wurth L, Verheggen C, Jády BE, Rothé B, Pescia C, Robert MC, Kiss T, Bardoni B, Krol A, Branlant C, Allmang C, Bertrand E, Charpentier B. The Hsp90 chaperone controls the biogenesis of L7Ae RNPs through conserved machinery. J Cell Biol. 2008 Feb 11;180(3):579-95. doi: 10.1083/jcb.200708110. PMID: 18268104; PMCID: PMC2234240.

Bouveret E, Rigaut G, Shevchenko A, Wilm M, Séraphin B. A Sm-like protein complex that participates in mRNA degradation. EMBO J. 2000 Apr 3;19(7):1661-71. doi: 10.1093/emboj/19.7.1661. PMID: 10747033; PMCID: PMC310234.

Cavaillé J, Bachellerie JP. SnoRNA-guided ribose methylation of rRNA: structural features of the guide RNA duplex influencing the extent of the reaction. Nucleic Acids Res. 1998 Apr 1;26(7):1576-87. doi: 10.1093/nar/26.7.1576. PMID: 9512526; PMCID: PMC147472.

Chanfreau G, Legrain P, Jacquier A. Yeast RNase III as a key processing enzyme in small nucleolar RNAs metabolism. J Mol Biol. 1998 Dec 11;284(4):975-88. doi: 10.1006/jmbi.1998.2237. PMID: 9837720.

Chanfreau G, Rotondo G, Legrain P, Jacquier A. Processing of a dicistronic small nucleolar RNA precursor by the RNA endonuclease Rnt1. EMBO J. 1998 Jul 1;17(13):3726-37. doi: 10.1093/emboj/17.13.3726. PMID: 9649442; PMCID: PMC1170708.

Chen X, Poorey K, Carver MN, Müller U, Bekiranov S, Auble DT, Brow DA. Transcriptomes of six mutants in the Sen1 pathway reveal combinatorial control of transcription termination across the Saccharomyces cerevisiae genome. PLoS Genet. 2017 Jun 30;13(6):e1006863. doi: 10.1371/journal.pgen.1006863. PMID: 28665995; PMCID: PMC5513554.

Coban I.[1], Hirsch AG.[1], Shomroni O.[2], Giesbrecht O.[1], Salinas G.[2] and Krebber H.[1] Double stranded RNA formation leads to preferential nuclear export and gene expression. Nature, under revision. 2022

Cohen E, Avrahami D, Frid K, Canello T, Levy Lahad E, Zeligson S, Perlberg S, Chapman J, Cohen OS, Kahana E, Lavon I, Gabizon R. Snord 3A: a molecular marker and modulator of prion disease progression. PLoS One. 2013;8(1):e54433. doi: 10.1371/journal.pone.0054433. Epub 2013 Jan 21. PMID: 23349890; PMCID: PMC3549992.

Czekay DP, Kothe U. H/ACA Small Ribonucleoproteins: Structural and Functional Comparison Between Archaea and Eukaryotes. Front Microbiol. 2021 Mar 11;12:654370. doi: 10.3389/fmicb.2021.654370. PMID: 33776984; PMCID: PMC7991803.

Dieci G, Preti M, Montanini B. Eukaryotic snoRNAs: a paradigm for gene expression flexibility. Genomics. 2009 Aug;94(2):83-8. doi: 10.1016/j.ygeno.2009.05.002. Epub 2009 May 13. PMID: 19446021.

Dower WJ, Miller JF, Ragsdale CW. High efficiency transformation of E. coli by high voltage electroporation. Nucleic Acids Res. 1988 Jul 11;16(13):6127-45. doi: 10.1093/nar/16.13.6127. PMID: 3041370; PMCID: PMC336852.

Dupuis-Sandoval F, Poirier M, Scott MS. The emerging landscape of small nucleolar RNAs in cell biology. Wiley Interdiscip Rev RNA. 2015 Jul-Aug;6(4):381-97. doi: 10.1002/wrna.1284. Epub 2015 Apr 16. PMID: 25879954; PMCID: PMC4696412.

Duker AL, Ballif BC, Bawle EV, Person RE, Mahadevan S, Alliman S, Thompson R, Traylor R, Bejjani BA, Shaffer LG, Rosenfeld JA, Lamb AN, Sahoo T. Paternally inherited microdeletion at 15q11.2 confirms a significant role for the SNORD116 C/D box snoRNA cluster in Prader-Willi syndrome. Eur J Hum Genet. 2010 Nov;18(11):1196-201. doi: 10.1038/ejhg.2010.102. Epub 2010 Jun 30. PMID: 20588305; PMCID: PMC2987474.

Fatica A, Morlando M, Bozzoni I. Yeast snoRNA accumulation relies on a cleavage-dependent/polyadenylation-independent 3'-processing apparatus. EMBO J. 2000 Nov 15;19(22):6218-29. doi: 10.1093/emboj/19.22.6218. PMID: 11080167; PMCID: PMC305823.

Fernandez CF, Pannone BK, Chen X, Fuchs G, Wolin SL. An Lsm2-Lsm7 complex in Saccharomyces cerevisiae associates with the small nucleolar RNA snR5. Mol Biol Cell. 2004 Jun;15(6):2842-52. doi: 10.1091/mbc.e04-02-0116. Epub 2004 Apr 9. PMID: 15075370; PMCID: PMC420107.

Fried H, Kutay U. Nucleocytoplasmic transport: taking an inventory. Cell Mol Life Sci. 2003 Aug;60(8):1659-88. doi: 10.1007/s00018-003-3070-3. PMID: 14504656.

Gallardo F, Olivier C, Dandjinou AT, Wellinger RJ, Chartrand P. TLC1 RNA nucleo-cytoplasmic trafficking links telomerase biogenesis to its recruitment to telomeres. EMBO J. 2008 Mar 5;27(5):748-57. doi: 10.1038/emboj.2008.21. Epub 2008 Feb 14. PMID: 18273059; PMCID: PMC2265757.

Ganot P, Caizergues-Ferrer M, Kiss T. The family of box ACA small nucleolar RNAs is defined by an evolutionarily conserved secondary structure and ubiquitous sequence elements essential for RNA accumulation. Genes Dev. 1997 Apr 1;11(7):941-56. doi: 10.1101/gad.11.7.941. PMID: 9106664.

Garfin DE. One-dimensional gel electrophoresis. Methods Enzymol. 2009;463:497-513. doi: 10.1016/S0076-6879(09)63029-9. PMID: 19892189.

Gibson DG, Young L, Chuang RY, Venter JC, Hutchison CA 3rd, Smith HO. Enzymatic assembly of DNA molecules up to several hundred kilobases. Nat Methods. 2009 May;6(5):343-5. doi: 10.1038/nmeth.1318. Epub 2009 Apr 12. PMID: 19363495.

Gietz D, St Jean A, Woods RA, Schiestl RH. Improved method for high efficiency transformation of intact yeast cells. Nucleic Acids Res. 1992 Mar 25;20(6):1425. doi: 10.1093/nar/20.6.1425. PMID: 1561104; PMCID: PMC312198.

Grozdanov PN, Roy S, Kittur N, Meier UT. SHQ1 is required prior to NAF1 for assembly of H/ACA small nucleolar and telomerase RNPs. RNA. 2009 Jun;15(6):1188-97. doi: 10.1261/rna.1532109. Epub 2009 Apr 21. PMID: 19383767; PMCID: PMC2685518.

Grzechnik P, Gdula MR, Proudfoot NJ. Pcf11 orchestrates transcription termination pathways in yeast. Genes Dev. 2015 Apr 15;29(8):849-61. doi: 10.1101/gad.251470.114. Epub 2015 Apr 15. PMID: 25877920; PMCID: PMC4403260.

Grzechnik P, Kufel J. Polyadenylation linked to transcription termination directs the processing of snoRNA precursors in yeast. Mol Cell. 2008 Oct 24;32(2):247-58. doi: 10.1016/j.molcel.2008.10.003. PMID: 18951092; PMCID: PMC2593888.

Grzechnik P, Szczepaniak SA, Dhir S, Pastucha A, Parslow H, Matuszek Z, Mischo HE, Kufel J, Proudfoot NJ. Nuclear fate of yeast snoRNA is determined by co-transcriptional Rnt1 cleavage. Nat Commun. 2018 May 3;9(1):1783. doi: 10.1038/s41467-018-04094-y. PMID: 29725044; PMCID: PMC5934358.

Gueldener U, Heinisch J, Koehler GJ, Voss D, Hegemann JH. A second set of loxP marker cassettes for Cre-mediated multiple gene knockouts in budding yeast. Nucleic Acids Res. 2002 Mar 15;30(6):e23. doi: 10.1093/nar/30.6.e23. PMID: 11884642; PMCID: PMC101367.

Hirsch AG, Becker D, Lamping JP, Krebber H. Unraveling the stepwise maturation of the yeast telomerase including a Cse1 and Mtr10 mediated quality control checkpoint. Sci Rep. 2021 Nov 12;11(1):22174. doi: 10.1038/s41598-021-01599-3. PMID: 34773052; PMCID: PMC8590012.

Holley CL, Li MW, Scruggs BS, Matkovich SJ, Ory DS, Schaffer JE. Cytosolic accumulation of small nucleolar RNAs (snoRNAs) is dynamically regulated by NADPH oxidase. J Biol Chem. 2015 May 1;290(18):11741-8. doi: 10.1074/jbc.M115.637413. Epub 2015 Mar 19. PMID: 25792744; PMCID: PMC4416874.

Holmes RK, Tuck AC, Zhu C, Dunn-Davies HR, Kudla G, Clauder-Munster S, Granneman S, Steinmetz LM, Guthrie C, Tollervey D. Loss of the Yeast SR Protein Npl3 Alters Gene Expression Due to Transcription Readthrough. PLoS Genet. 2015 Dec 22;11(12):e1005735. doi: 10.1371/journal.pgen.1005735. PMID: 26694144; PMCID: PMC4687934.

Huen J, Kakihara Y, Ugwu F, Cheung KL, Ortega J, Houry WA. Rvb1-Rvb2: essential ATP-dependent helicases for critical complexes. Biochem Cell Biol. 2010 Feb;88(1):29-40. doi: 10.1139/o09-122. PMID: 20130677.

Hughes JM, Konings DA, Cesareni G. The yeast homologue of U3 snRNA. EMBO J. 1987 Jul;6(7):2145-55. PMID: 3308452; PMCID: PMC553607.

Kakihara Y, Makhnevych T, Zhao L, Tang W, Houry WA. Nutritional status modulates box C/D snoRNP biogenesis by regulated subcellular relocalization of the R2TP complex. Genome Biol. 2014 Jul 25;15(7):404. doi: 10.1186/s13059-014-0404-4. PMID: 25060708; PMCID: PMC4165372.

Kakihara Y, Saeki M. The R2TP chaperone complex: its involvement in snoRNP assembly and tumorigenesis. Biomol Concepts. 2014 Dec;5(6):513-20. doi: 10.1515/bmc-2014-0028. PMID: 25429602.

Khoshnevis S, Dreggors RE, Hoffmann TFR, Ghalei H. A conserved Bcd1 interaction essential for box C/D snoRNP biogenesis. J Biol Chem. 2019 Nov 29;294(48):18360-18371. doi: 10.1074/jbc.RA119.010222. Epub 2019 Sep 19. PMID: 31537647; PMCID: PMC6885627.

Kim M, Vasiljeva L, Rando OJ, Zhelkovsky A, Moore C, Buratowski S. Distinct pathways for snoRNA and mRNA termination. Mol Cell. 2006 Dec 8;24(5):723-734. doi: 10.1016/j.molcel.2006.11.011. PMID: 17157255.

King TH, Decatur WA, Bertrand E, Maxwell ES, Fournier MJ. A well-connected and conserved nucleoplasmic helicase is required for production of box C/D and H/ACA snoRNAs and localization of snoRNP proteins. Mol Cell Biol. 2001 Nov;21(22):7731-46. doi: 10.1128/MCB.21.22.7731-7746.2001. PMID: 11604509; PMCID: PMC99944.

King TH, Liu B, McCully RR, Fournier MJ. Ribosome structure and activity are altered in cells lacking snoRNPs that form pseudouridines in the peptidyl transferase center. Mol Cell. 2003 Feb;11(2):425-35. doi: 10.1016/s1097-2765(03)00040-6. PMID: 12620230.

Kos M, Tollervey D. The Putative RNA Helicase Dbp4p Is Required for Release of the U14 snoRNA from Preribosomes in Saccharomyces cerevisiae. Mol Cell. 2005 Oct 7;20(1):53-64. doi: 10.1016/j.molcel.2005.08.022. PMID: 16209945.

Kos M, Tollervey D. Yeast pre-rRNA processing and modification occur cotranscriptionally. Mol Cell. 2010 Mar 26;37(6):809-20. doi: 10.1016/j.molcel.2010.02.024. PMID: 20347423; PMCID: PMC2860240.

Kufel J, Allmang C, Petfalski E, Beggs J, Tollervey D. Lsm Proteins are required for normal processing and stability of ribosomal RNAs. J Biol Chem. 2003a Jan

24;278(4):2147-56. doi: 10.1074/jbc.M208856200. Epub 2002 Nov 15. PMID: 12438310.

Kufel J, Allmang C, Verdone L, Beggs J, Tollervey D. A complex pathway for 3' processing of the yeast U3 snoRNA. Nucleic Acids Res. 2003b Dec 1;31(23):6788-97. doi: 10.1093/nar/gkg904. PMID: 14627812; PMCID: PMC290272.

Kufel J, Allmang C, Verdone L, Beggs JD, Tollervey D. Lsm proteins are required for normal processing of pre-tRNAs and their efficient association with La-homologous protein Lhp1p. Mol Cell Biol. 2002 Jul;22(14):5248-56. doi: 10.1128/MCB.22.14.5248-5256.2002. PMID: 12077351; PMCID: PMC139769.

Kufel J, Bousquet-Antonelli C, Beggs JD, Tollervey D. Nuclear pre-mRNA decapping and 5' degradation in yeast require the Lsm2-8p complex. Mol Cell Biol. 2004 Nov;24(21):9646-57. doi: 10.1128/MCB.24.21.9646-9657.2004. PMID: 15485930; PMCID: PMC522261.

Kufel J, Grzechnik P. Small Nucleolar RNAs Tell a Different Tale. Trends Genet. 2019 Feb;35(2):104-117. doi: 10.1016/j.tig.2018.11.005. Epub 2018 Dec 16. PMID: 30563726.

Lai YH, Choudhary K, Cloutier SC, Xing Z, Aviran S, Tran EJ. Genome-Wide Discovery of DEAD-Box RNA Helicase Targets Reveals RNA Structural Remodeling in Transcription Termination. Genetics. 2019 May;212(1):153-174. doi: 10.1534/genetics.119.302058. Epub 2019 Mar 22. PMID: 30902808; PMCID: PMC6499532.

Larochelle M, Lemay JF, Bachand F. The THO complex cooperates with the nuclear RNA surveillance machinery to control small nucleolar RNA expression. Nucleic Acids Res. 2012 Nov 1;40(20):10240-53. doi: 10.1093/nar/gks838. Epub 2012 Sep 10. PMID: 22965128; PMCID: PMC3488260.

Laurent JM, Young JH, Kachroo AH, Marcotte EM. Efforts to make and apply humanized yeast. Brief Funct Genomics. 2016 Mar;15(2):155-63. doi: 10.1093/bfgp/elv041. Epub 2015 Oct 13. PMID: 26462863; PMCID: PMC4803062.

Li MW, Sletten AC, Lee J, Pyles KD, Matkovich SJ, Ory DS, Schaffer JE. Nuclear export factor 3 regulates localization of small nucleolar RNAs. J Biol Chem. 2017 Dec 8;292(49):20228-20239. doi: 10.1074/jbc.M117.818146. Epub 2017 Oct 11. PMID: 29021253; PMCID: PMC5724009.

Li S, Duan J, Li D, Ma S, Ye K. Structure of the Shq1-Cbf5-Nop10-Gar1 complex and implications for H/ACA RNP biogenesis and dyskeratosis congenita. EMBO J. 2011 Nov 25;30(24):5010-20. doi: 10.1038/emboj.2011.427. PMID: 22117216; PMCID: PMC3242979.

Liang XH, Fournier MJ. The helicase Has1p is required for snoRNA release from pre-rRNA. Mol Cell Biol. 2006 Oct;26(20):7437-50. doi: 10.1128/MCB.00664-06. Epub 2006 Aug 14. PMID: 16908538; PMCID: PMC1636851.

Liang XH, Liu Q, Fournier MJ. rRNA modifications in an intersubunit bridge of the ribosome strongly affect both ribosome biogenesis and activity. Mol Cell. 2007 Dec 28;28(6):965-77. doi: 10.1016/j.molcel.2007.10.012. PMID: 18158895.

Lidschreiber M, Easter AD, Battaglia S, Rodríguez-Molina JB, Casañal A, Carminati M, Baejen C, Grzechnik P, Maier KC, Cramer P, Passmore LA. The APT complex is involved in non-coding RNA transcription and is distinct from CPF. Nucleic Acids Res. 2018 Nov 30;46(21):11528-11538. doi: 10.1093/nar/gky845. PMID: 30247719; PMCID: PMC6265451.

Lui L, Lowe T. Small nucleolar RNAs and RNA-guided post-transcriptional modification. Essays Biochem. 2013;54:53-77. doi: 10.1042/bse0540053. PMID: 23829527.

Marnef A, Richard P, Pinzón N, Kiss T. Targeting vertebrate intron-encoded box C/D 2'-O-methylation guide RNAs into the Cajal body. Nucleic Acids Res. 2014 Jun;42(10):6616-29. doi: 10.1093/nar/gku287. Epub 2014 Apr 20. PMID: 24753405; PMCID: PMC4041459.

Massenet S, Bertrand E, Verheggen C. Assembly and trafficking of box C/D and H/ACA snoRNPs. RNA Biol. 2017 Jun 3;14(6):680-692. doi: 10.1080/15476286.2016.1243646. Epub 2016 Oct 7. PMID: 27715451; PMCID: PMC5519232.

Matera AG, Wang Z. A day in the life of the spliceosome. Nat Rev Mol Cell Biol. 2014 Feb;15(2):108-21. doi: 10.1038/nrm3742. Erratum in: Nat Rev Mol Cell Biol. 2014 Apr;15(4):294. PMID: 24452469; PMCID: PMC4060434.

Matera AG, Terns RM, Terns MP. Non-coding RNAs: lessons from the small nuclear and small nucleolar RNAs. Nat Rev Mol Cell Biol. 2007 Mar;8(3):209-20. doi: 10.1038/nrm2124. PMID: 17318225.

Meinel DM, Burkert-Kautzsch C, Kieser A, O'Duibhir E, Siebert M, Mayer A, Cramer P, Söding J, Holstege FC, Sträßer K. Recruitment of TREX to the transcription machinery by its direct binding to the phospho-CTD of RNA polymerase II. PLoS Genet. 2013 Nov;9(11):e1003914. doi: 10.1371/journal.pgen.1003914. Epub 2013 Nov 14. PMID: 24244187; PMCID: PMC3828145.

Mleczko AM, Machtel P, Walkowiak M, Wasilewska A, Pietras PJ, Bąkowska-Żywicka K. Levels of sdRNAs in cytoplasm and their association with ribosomes are dependent upon stress conditions but independent from snoRNA expression. Sci Rep. 2019 Dec 5;9(1):18397. doi: 10.1038/s41598-019-54924-2. PMID: 31804585; PMCID: PMC6895083.

Moqtaderi Z, Struhl K. Genome-wide occupancy profile of the RNA polymerase III machinery in Saccharomyces cerevisiae reveals loci with incomplete transcription complexes. Mol Cell Biol. 2004 May;24(10):4118-27. doi: 10.1128/mcb.24.10.4118-4127.2004. PMID: 15121834; PMCID: PMC400477.

Morlando M, Greco P, Dichtl B, Fatica A, Keller W, Bozzoni I. Functional analysis of yeast snoRNA and snRNA 3'-end formation mediated by uncoupling of cleavage and polyadenylation. Mol Cell Biol. 2002 Mar;22(5):1379-89. doi: 10.1128/MCB.22.5.1379-1389.2002. PMID: 11839805; PMCID: PMC134709.

Mouaikel J, Verheggen C, Bertrand E, Tazi J, Bordonné R. Hypermethylation of the cap structure of both yeast snRNAs and snoRNAs requires a conserved methyltransferase that is localized to the nucleolus. Mol Cell. 2002 Apr;9(4):891-901. doi: 10.1016/s1097-2765(02)00484-7. PMID: 11983179.

Olson BL, Siliciano PG. A diverse set of nuclear RNAs transfer between nuclei of yeast heterokaryons. Yeast. 2003 Jul 30;20(10):893-903. doi: 10.1002/yea.1015. PMID: 12868058.

Ooi SL, Samarsky DA, Fournier MJ, Boeke JD. Intronic snoRNA biosynthesis in Saccharomyces cerevisiae depends on the lariat-debranching enzyme: intron length effects and activity of a precursor snoRNA. RNA. 1998 Sep;4(9):1096-110. doi: 10.1017/s1355838298980785. PMID: 9740128; PMCID: PMC1369685.

Paci A, Liu XH, Huang H, Lim A, Houry WA, Zhao R. The stability of the small nucleolar ribonucleoprotein (snoRNP) assembly protein Pih1 in Saccharomyces cerevisiae is modulated by its C terminus. J Biol Chem. 2012 Dec 21;287(52):43205-14. doi: 10.1074/jbc.M112.408849. Epub 2012 Nov 8. PMID: 23139418; PMCID: PMC3527908.

Pannone BK, Xue D, Wolin SL. A role for the yeast La protein in U6 snRNP assembly: evidence that the La protein is a molecular chaperone for RNA polymerase III transcripts. EMBO J. 1998 Dec 15;17(24):7442-53. doi: 10.1093/emboj/17.24.7442. PMID: 9857199; PMCID: PMC1171088.

Paul A, Tiotiu D, Bragantini B, Marty H, Charpentier B, Massenet S, Labialle S. Bcd1p controls RNA loading of the core protein Nop58 during C/D box snoRNP biogenesis. RNA. 2019 Apr;25(4):496-506. doi: 10.1261/rna.067967.118. Epub 2019 Jan 30. PMID: 30700579; PMCID: PMC6426285.

Peng WT, Robinson MD, Mnaimneh S, Krogan NJ, Cagney G, Morris Q, Davierwala AP, Grigull J, Yang X, Zhang W, Mitsakakis N, Ryan OW, Datta N, Jojic V, Pal C, Canadien V, Richards D, Beattie B, Wu LF, Altschuler SJ, Roweis S, Frey BJ, Emili A, Greenblatt JF, Hughes TR. A panoramic view of yeast noncoding RNA processing. Cell. 2003 Jun 27;113(7):919-33. doi: 10.1016/s0092-8674(03)00466-5. PMID: 12837249.

Porrua O, Hobor F, Boulay J, Kubicek K, D'Aubenton-Carafa Y, Gudipati RK, Stefl R, Libri D. In vivo SELEX reveals novel sequence and structural determinants of Nrd1-Nab3-Sen1-dependent transcription termination. EMBO J. 2012 Oct 3;31(19):3935-48. doi: 10.1038/emboj.2012.237. Epub 2012 Aug 28. PMID: 23032188; PMCID: PMC3463846.

Porrua O, Libri D. Transcription termination and the control of the transcriptome: why, where and how to stop. Nat Rev Mol Cell Biol. 2015 Mar;16(3):190-202. doi: 10.1038/nrm3943. Epub 2015 Feb 4. PMID: 25650800.

Reuter LM, Meinel DM, Sträßer K. The poly(A)-binding protein Nab2 functions in RNA polymerase III transcription. Genes Dev. 2015 Jul 15;29(14):1565-75. doi: 10.1101/gad.266205.115. PMID: 26220998; PMCID: PMC4526739.

Rose, M.D., Winston, F., and Hieter, P. (1990). Methods in Yeast Genetics, A Laboratory Course Manual. Cold Spring Harbor Laboratory. In Biochemistry and Molecular Biology Education, (NY: Cold Spring Harbor), pp. 101–102.

Rothé B, Saliou JM, Quinternet M, Back R, Tiotiu D, Jacquemin C, Loegler C, Schlotter F, Peña V, Eckert K, Moréra S, Dorsselaer AV, Branlant C, Massenet S, Sanglier-Cianférani S, Manival X, Charpentier B. Protein Hit1, a novel box C/D snoRNP assembly factor, controls cellular concentration of the scaffolding protein Rsa1 by direct interaction. Nucleic Acids Res. 2014;42(16):10731-47. doi: 10.1093/nar/gku612. Epub 2014 Aug 28. PMID: 25170085; PMCID: PMC4176330.

Sambrook, J., Fritsch, E.F., and Maniatis, T. (1989). Molecular cloning: a laboratory manual. Mol. Cloning a Lab. Manual.

Schulz D, Schwalb B, Kiesel A, Baejen C, Torkler P, Gagneur J, Soeding J, Cramer P. Transcriptome surveillance by selective termination of noncoding RNA synthesis. Cell. 2013 Nov 21;155(5):1075-87. doi: 10.1016/j.cell.2013.10.024. Epub 2013 Nov 7. PMID: 24210918.

Steinmetz EJ, Brow DA. Ssu72 protein mediates both poly(A)-coupled and poly(A)-independent termination of RNA polymerase II transcription. Mol Cell Biol. 2003 Sep;23(18):6339-49. doi: 10.1128/MCB.23.18.6339-6349.2003. PMID: 12944462; PMCID: PMC193702.

Steinmetz EJ, Ng SB, Cloute JP, Brow DA. cis- and trans-Acting determinants of transcription termination by yeast RNA polymerase II. Mol Cell Biol. 2006 Apr;26(7):2688-96. doi: 10.1128/MCB.26.7.2688-2696.2006. PMID: 16537912; PMCID: PMC1430333.

Segref A, Sharma K, Doye V, Hellwig A, Huber J, Lührmann R, Hurt E. Mex67p, a novel factor for nuclear mRNA export, binds to both poly(A)+ RNA and nuclear pores.

EMBO J. 1997 Jun 2;16(11):3256-71. doi: 10.1093/emboj/16.11.3256. PMID: 9214641; PMCID: PMC1169942.

Senger B, Simos G, Bischoff FR, Podtelejnikov A, Mann M, Hurt E. Mtr10p functions as a nuclear import receptor for the mRNA-binding protein Npl3p. EMBO J. 1998 Apr 15;17(8):2196-207. doi: 10.1093/emboj/17.8.2196. PMID: 9545233; PMCID: PMC1170564.

Sherman F. Getting started with yeast. Methods Enzymol. 2002;350:3-41. doi: 10.1016/s0076-6879(02)50954-x. PMID: 12073320.

Sherman F, Hicks J. Micromanipulation and dissection of asci. Methods Enzymol. 1991;194:21-37. doi: 10.1016/0076-6879(91)94005-w. PMID: 2005789.

Siprashvili Z, Webster DE, Johnston D, Shenoy RM, Ungewickell AJ, Bhaduri A, Flockhart R, Zarnegar BJ, Che Y, Meschi F, Puglisi JD, Khavari PA. The noncoding RNAs SNORD50A and SNORD50B bind K-Ras and are recurrently deleted in human cancer. Nat Genet. 2016 Jan;48(1):53-8. doi: 10.1038/ng.3452. Epub 2015 Nov 23. PMID: 26595770; PMCID: PMC5324971.

Sikorski RS, Hieter P. A system of shuttle vectors and yeast host strains designed for efficient manipulation of DNA in Saccharomyces cerevisiae. Genetics. 1989 May;122(1):19-27. doi: 10.1093/genetics/122.1.19. PMID: 2659436; PMCID: PMC1203683.

Sklenar AR, Parthun MR. Characterization of yeast histone H3-specific type B histone acetyltransferases identifies an ADA2-independent Gcn5p activity. BMC Biochem. 2004 Jul 26;5:11. doi: 10.1186/1471-2091-5-11. PMID: 15274751; PMCID: PMC509278.

Sloan KE, Gleizes PE, Bohnsack MT. Nucleocytoplasmic Transport of RNAs and RNA-Protein Complexes. J Mol Biol. 2016 May 22;428(10 Pt A):2040-59. doi: 10.1016/j.jmb.2015.09.023. Epub 2015 Oct 3. PMID: 26434509.

Spiller MP, Boon KL, Reijns MA, Beggs JD. The Lsm2-8 complex determines nuclear localization of the spliceosomal U6 snRNA. Nucleic Acids Res. 2007;35(3):923-9. doi: 10.1093/nar/gkl1130. Epub 2007 Jan 23. PMID: 17251193; PMCID: PMC1807951.

Sprague GF Jr. Assay of yeast mating reaction. Methods Enzymol. 1991;194:77-93. doi: 10.1016/0076-6879(91)94008-z. PMID: 2005823.

Stewart M. Nuclear export of mRNA. Trends Biochem Sci. 2010 Nov;35(11):609-17. doi: 10.1016/j.tibs.2010.07.001. Epub 2010 Aug 16. PMID: 20719516.

Tieg B, Krebber H. Dbp5 - from nuclear export to translation. Biochim Biophys Acta. 2013 Aug;1829(8):791-8. doi: 10.1016/j.bbagrm.2012.10.010. Epub 2012 Nov 2. PMID: 23128325.

Tollervey D. A yeast small nuclear RNA is required for normal processing of pre-ribosomal RNA. EMBO J. 1987 Dec 20;6(13):4169-75. PMID: 3327689; PMCID: PMC553900.

Tollervey D, Guthrie C. Deletion of a yeast small nuclear RNA gene impairs growth. EMBO J. 1985 Dec 30;4(13B):3873-8. PMID: 3004976; PMCID: PMC554743.

Tollervey D, Lehtonen H, Carmo-Fonseca M, Hurt EC. The small nucleolar RNP protein NOP1 (fibrillarin) is required for pre-rRNA processing in yeast. EMBO J. 1991 Mar;10(3):573-83. PMID: 1825809; PMCID: PMC452687.

Torchet C, Badis G, Devaux F, Costanzo G, Werner M, Jacquier A. The complete set of H/ACA snoRNAs that guide rRNA pseudouridylations in Saccharomyces cerevisiae. RNA. 2005 Jun;11(6):928-38. doi: 10.1261/rna.2100905. PMID: 15923376; PMCID: PMC1370777.

Tuck AC, Tollervey D. A transcriptome-wide atlas of RNP composition reveals diverse classes of mRNAs and lncRNAs. Cell. 2013 Aug 29;154(5):996-1009. doi: 10.1016/j.cell.2013.07.047. PMID: 23993093; PMCID: PMC3778888

Turowski TW, Tollervey D. Cotranscriptional events in eukaryotic ribosome synthesis. Wiley Interdiscip Rev RNA. 2015 Jan-Feb;6(1):129-39. doi: 10.1002/wrna.1263. Epub 2014 Aug 29. PMID: 25176256.

Tudek A, Porrua O, Kabzinski T, Lidschreiber M, Kubicek K, Fortova A, Lacroute F, Vanacova S, Cramer P, Stefl R, Libri D. Molecular basis for coordinating transcription termination with noncoding RNA degradation. Mol Cell. 2014 Aug 7;55(3):467-81. doi: 10.1016/j.molcel.2014.05.031. Epub 2014 Jul 24. PMID: 25066235; PMCID: PMC4186968.

van der Werf J, Chin CV, Fleming NI. SnoRNA in Cancer Progression, Metastasis and Immunotherapy Response. Biology (Basel). 2021 Aug 20;10(8):809. doi: 10.3390/biology10080809. PMID: 34440039; PMCID: PMC8389557.

van Nues RW, Granneman S, Kudla G, Sloan KE, Chicken M, Tollervey D, Watkins NJ. Box C/D snoRNP catalysed methylation is aided by additional pre-rRNA base-pairing. EMBO J. 2011 May 10;30(12):2420-30. doi: 10.1038/emboj.2011.148. PMID: 21556049; PMCID: PMC3116282.

Vasianovich Y, Bajon E, Wellinger RJ. Telomerase biogenesis requires a novel Mex67 function and a cytoplasmic association with the Sm_7 complex. Elife. 2020 Oct 23;9:e60000. doi: 10.7554/eLife.60000. PMID: 33095156; PMCID: PMC7644208.

Vasianovich Y, Wellinger RJ. Life and Death of Yeast Telomerase RNA. J Mol Biol. 2017 Oct 27;429(21):3242-3254. doi: 10.1016/j.jmb.2017.01.013. Epub 2017 Jan 20. PMID: 28115201.

Watkins NJ, Bohnsack MT. The box C/D and H/ACA snoRNPs: key players in the modification, processing and the dynamic folding of ribosomal RNA. Wiley Interdiscip Rev RNA. 2012 May-Jun;3(3):397-414. doi: 10.1002/wrna.117. Epub 2011 Nov 7. PMID: 22065625.

Watkins NJ, Gottschalk A, Neubauer G, Kastner B, Fabrizio P, Mann M, Lührmann R. Cbf5p, a potential pseudouridine synthase, and Nhp2p, a putative RNA-binding protein, are present together with Gar1p in all H BOX/ACA-motif snoRNPs and constitute a common bipartite structure. RNA. 1998 Dec;4(12):1549-68. doi: 10.1017/s1355838298980761. PMID: 9848653; PMCID: PMC1369725.

Wilusz CJ, Wilusz J. Lsm proteins and Hfq: Life at the 3' end. RNA Biol. 2013 Apr;10(4):592-601. doi: 10.4161/rna.23695. Epub 2013 Feb 7. PMID: 23392247; PMCID: PMC3710366.

Winston F, Dollard C, Ricupero-Hovasse SL. Construction of a set of convenient Saccharomyces cerevisiae strains that are isogenic to S288C. Yeast. 1995 Jan;11(1):53-5. doi: 10.1002/yea.320110107. PMID: 7762301.

Woolford JL Jr, Baserga SJ. Ribosome biogenesis in the yeast Saccharomyces cerevisiae. Genetics. 2013 Nov;195(3):643-81. doi: 10.1534/genetics.113.153197. PMID: 24190922; PMCID: PMC3813855.

Wu H, Becker D, Krebber H. Telomerase RNA TLC1 shuttling to the cytoplasm requires mRNA export factors and is important for telomere maintenance. Cell Rep. 2014 Sep 25;8(6):1630-1638. doi: 10.1016/j.celrep.2014.08.021. Epub 2014 Sep 15. PMID: 25220466.

Xiao Z, McGrew JT, Schroeder AJ, Fitzgerald-Hayes M. CSE1 and CSE2, two new genes required for accurate mitotic chromosome segregation in Saccharomyces cerevisiae. Mol Cell Biol. 1993 Aug;13(8):4691-702. doi: 10.1128/mcb.13.8.4691-4702.1993. PMID: 8336709; PMCID: PMC360095.

Yang PK, Hoareau C, Froment C, Monsarrat B, Henry Y, Chanfreau G. Cotranscriptional recruitment of the pseudouridylsynthetase Cbf5p and of the RNA binding protein Naf1p during H/ACA snoRNP assembly. Mol Cell Biol. 2005 Apr;25(8):3295-304. doi: 10.1128/MCB.25.8.3295-3304.2005. PMID: 15798213; PMCID: PMC1069627.

Yang PK, Rotondo G, Porras T, Legrain P, Chanfreau G. The Shq1p.Naf1p complex is required for box H/ACA small nucleolar ribonucleoprotein particle biogenesis. J Biol Chem. 2002 Nov 22;277(47):45235-42. doi: 10.1074/jbc.M207669200. Epub 2002 Sep 11. PMID: 12228251.

Zander G, Krebber H. Quick or quality? How mRNA escapes nuclear quality control during stress. RNA Biol. 2017 Dec 2;14(12):1642-1648. doi:

10.1080/15476286.2017.1345835. Epub 2017 Jul 31. PMID: 28708448; PMCID: PMC5731798.

Zeng F, Hao Z, Li P, Meng Y, Dong J, Lin Y. A restriction-free method for gene reconstitution using two single-primer PCRs in parallel to generate compatible cohesive ends. BMC Biotechnol. 2017 Mar 17;17(1):32. doi: 10.1186/s12896-017-0346-5. PMID: 28302113; PMCID: PMC5356277.

Zhou L, Hang J, Zhou Y, Wan R, Lu G, Yin P, Yan C, Shi Y. Crystal structures of the Lsm complex bound to the 3' end sequence of U6 small nuclear RNA. Nature. 2014 Feb 6;506(7486):116-20. doi: 10.1038/nature12803. Epub 2013 Nov 17. PMID: 24240276.

Zhao R, Kakihara Y, Gribun A, Huen J, Yang G, Khanna M, Costanzo M, Brost RL, Boone C, Hughes TR, Yip CM, Houry WA. Molecular chaperone Hsp90 stabilizes Pih1/Nop17 to maintain R2TP complex activity that regulates snoRNA accumulation. J Cell Biol. 2008 Feb 11;180(3):563-78. doi: 10.1083/jcb.200709061. PMID: 18268103; PMCID: PMC2234237.

Zimta AA, Tigu AB, Braicu C, Stefan C, Ionescu C, Berindan-Neagoe I. An Emerging Class of Long Non-coding RNA With Oncogenic Role Arises From the snoRNA Host Genes. Front Oncol. 2020 Apr 7;10:389. doi: 10.3389/fonc.2020.00389. PMID: 32318335; PMCID: PMC7154078.

7. Acknowledgement

I would like to express my appreciation to everyone who supported me during my work. In particular, I wish to extend my gratitude to Prof. Dr. Heike Krebber for giving me the opportunity to work in this field as well as for her great supervision over the course of these years.

I would also like to thank the members of my thesis committee, PD Dr. Wilfred Kramer and Dr. Oliver Valerius, for the assistance and the advice provided, which proved valuable and was greatly appreciated.

I would also like to thank all the other members of my examination board, Prof. Dr. Kai Heimel, Prof. Dr. Stefanie Pöggeler, and Prof. Dr. Jörg Stülke.

I would like to thank the former and current members of the departments for their great teamwork and valuable advice. A special thanks goes to Dr. Ivo Coban, who supervised me in the early phase of my work and helped me start this project. Furthermore, I am particularly grateful to Fei Yu, who has become part of the snoRNA project in the course of her lab rotations, master thesis, and now PhD.

Finally, I would like to thank my parents, brothers, girlfriend, and friends, who supported me in every situation, motivated me, and believed in me. Thank you very much for that.

8. Curriculum Vitae

Gianluca Zaccagnini

Date of birth: 26.11.1988

Place of birth: Rome, Italy

2018 – Present	Georg-August-Universität Göttingen, Germany
	PhD student in the group of Prof. Dr. Heike Krebber, department of Molecular Genetics, Institute for Microbiology and Genetics.
2017 – 2017	IRBM-ADVENT company, Pomezia, Italy.
	Work internship
2014 – 2016	Roma Tre University, Italy.
	Master of Science (M.Sc.) in Biology for Molecular, Cellular and Physiopathologic Research, Biology Faculty.
	Master Thesis in the group of Dr. Luigi Chiarini, research center ENEA, National Agency for New Technologies, Energy and Sustainable Economic Development, "Valorization of an effluent of the dairy industry: production of hydrogen and 2,3-butanediol from scotta"
	Supervisor from Roma Tre University: Prof. Dr. Livia Leoni
2009 – 2014	Roma Tre University, Italy.
	Bachelor of Science (B.Sc.) in Biological Science, Biology Faculty
	Bachelor Thesis in the group of Prof. Dr. Manuela Cervelli, Department of Sciences, "Molecular mechanisms at the base of primary open-angle glaucoma"
2002 – 2008	Liceo scientifico Ilaria Alpi (Scientific high school)

9. Appendix
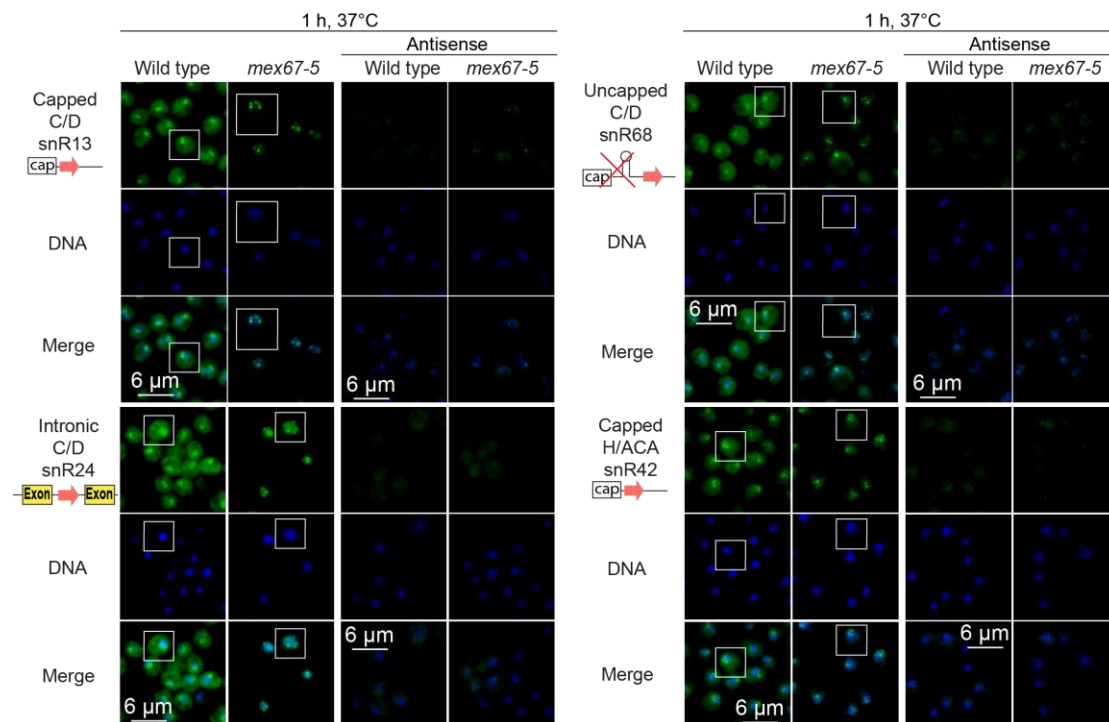
Figure 33: FISH analysis of the mex67-5 mutant strain. The indicated strains were incubated for 1 h at 37 °C prior to fixation. Cells were fixed with 4 % formaldehyde and snoRNAs were hybridized with 100-300 nucleotide long, DIG-labeled RNA probes and detected via FITC conjugated α-DIG-antibody (green). The DNA was stained with DAPI (blue). As a negative control, DIG-labeled RNA probes for antisense snoRNAs were used.